

GEOLOGY AND GEOCHEMISTRY OF THE HERMOSA MINING DISTRICT
SIERRA COUNTY, NEW MEXICO

BY
KHOSROW BAZRAFSHAN

New Mexico Bureau
of
Geology and Mineral Resources

A Dissertation
submitted to
Department of Geoscience,
New Mexico Institute of Mining and Technology

In partial fulfilment of the
requirements for the degree
of Doctor of Philosophy

May 1989

This thesis is accepted on behalf of the faculty
of the Institute by the following committee:

Advisor

Date

ABSTRACT

The Hermosa mining district is located in the eastern foothills of the northern Black Range of southwestern New Mexico. Exposed Ordovician to Permian sedimentary rocks are the predominant rock types in the Hermosa district. These Paleozoic sediments are flanked on the west and southwest by Tertiary volcanic and volcanoclastic rocks and on the east by late Tertiary well consolidated conglomerate and gravel of the Palomas Gravels. Tertiary intrusives occur in the form of flow banded rhyolite plugs and dikes in the district. The emplacement of the intrusives in the district was controlled by major faults.

The Hermosa mining district is situated in the Basin and Range province of southwestern New Mexico. The structural fabric of the district is the result of integration of Laramide compressional tectonic activities, Emory Cauldron formation of early Oligocene, Rio Grande rift opening of mid-Oligocene and Basin and Range development in the early Miocene. Two major structures flank the mining district: (1) the Emory Caldera to the west and southwest, and (2) the Winston Graben, the westernmost part of the Rio Grande rift, to the east. The exposed and mineralized Paleozoic sedimentary rocks are uplifted between these two major structures. The uplifted block is well-dissected by regional and local scale faults. North-to-northwest and northeast-to-east trending faults have sliced the district into long narrow blocks in a general north-south direction. Transverse faults, with general east-west strikes, divide the long and narrow north-south slices into smaller blocks. The Bull Frog fault, a north-northwest trending fault, runs through the center of the mining district. This fault and related fractures have controlled igneous intrusions, ore mineralization, and fluid flow in the district.

The Palomas Camp, Antelope-Ocean Waves mines, and Flagstaff-American Flag mines are the known and exploited mineralized zones in the mining district. Ore deposits occur as small pockets, pods, and pipe-like bodies in fissure veins. Low grade disseminated ore is also present in the district. Most of the ore is concentrated at the intersections of major faults and small, local-scale faults and fractures. Argentiferous galena, sphalerite, and chalcopyrite are the main ore minerals. Acanthite, pyrargyrite, polybasite, native silver, silver halides and extremely fine-grained gold have contributed to district production. Talc, calcite, and quartz are the main gangue minerals; talc formation, silicification (jasperoid) and decalcification are the principal types of alteration.

Approximately 7000 fluid inclusions in 450 quartz, calcite, sphalerite, and barite samples were analyzed, using a heating-freezing stage. The results of the thermometric analyses indicate that ore-mineralization temperature for silver-base metal deposits ranged from 220 to 270 C with the fluid salinity of 2-9 eq. wt.% NaCl. For silver-gold deposits, the

mineralization temperature ranged from 240 to 290 C with fluid salinity of 0 to 2.5 eq. wt.% NaCl. Temperature distribution maps were constructed based on thermometric data, and the maps indicate several high-temperature centers in the district. These high-temperature centers are upwelling zones concentrated along the Bull Frog fault and related fractures. Gold and silver assay values from the district were plotted. Strong correlations are noted between shallow depth high-temperature upwelling zones and high gold assay values. Silver and base metals were deposited in deeper and cooler zones with fluids of high-salinity. These correlations suggest similarities between the Hermosa fossil geothermal system and present-day active geothermal systems which deposit precious and base metals.

The composition of the volatile phase of the fluid inclusions was determined by thermal decrepitation of 75 samples from the district, using mass spectrometry apparatus. The gas species in the volatile phase are CO₂, N₂, CH₄, H₂S, CO, SO₂, H₂, He, Ar and C_nH_n. The results of the volatile analyses indicate that gold occurrences in the district are associated with fluids with high (>0.01 mole %) H₂S concentration. The high values of CO₂, H₂S, and H₂ in the gas phase of the fluid system, and gas-rich inclusions (Type II), in samples from the Wolford, Flagstaff-American Flag, and Antelope-Ocean Wave mines indicate that boiling of the fluid system was the main mechanism of ore deposition. The microthermometric and gas analyses indicate that mixing of two or more fluids (F I, F II, F III, F IV, F V, and F VI) was responsible for ore deposition in the Antelope-Ocean Wave mines and the southern area in the district.

Limited stable isotope analyses indicate that meteoric waters were the dominant type of fluid in the hydrothermal system in the district. A few oxygen isotope data suggest a magmatic fluid contribution to the hydrothermal system. Helium isotope analysis also suggests the presence of magmatic components in the gas phase of the fluid system of the district.

Using data from volatile and microthermometric analyses the solubility of metals present in the deposits was calculated. A computer program (GEOMOD) and the geochemical data were used to construct boiling and mixing models for metal transportation and deposition by the ore-forming fluids in the district. Based on the results of this study, new targets for gold and silver mineralization have been identified.

ACKNOWLEDGEMENTS

This study has benefited from the technical advice of my adviser Dr. Dave Norman and I wish to thank him. I thank Dr. Andrew Campbell for his valuable help in the analyses of data. The helium isotope analysis by Dr. Norman and stable isotope analyses by Dr. Campbell are greatly appreciated. Thanks also go to the other members of my thesis committee, Dr. Antonius J. Budding, Dr. Gerardo W. Gross, and Dr. Clay T. Smith for their reviewing and editing of the manuscript.

The New Mexico Bureau of Mines and Mineral Resources, Dr. Frank Kottowski, Director, partially supported this work in form of a grant. This Bureau assistance is greatly appreciated. I also wish to thank Dale Carlson and Joe Glines of Triple S Development Corporation for field assistance and Pan and Paul Eimon who edited the first draft of this work.

I am grateful for the moral support and understanding of my mother, my family, and my friend Dr. A. Birjandi which sustained me during several years of study in this country.

TABLE OF CONTENTS

Chapter 1. Geology of the Hermosa mining district.....	
Introduction.....	
Previous work.....	
Objectives of this study.....	
Historical development.....	
Stratigraphy.....	
Precambrian basement.....	
Cambro-Ordovician system.....	
Bliss Sandstone.....	
Ordovician system.....	
El Paso Group.....	
Montoya Group.....	
Silurian system.....	
Fusselman Dolomite.....	
Devonian system.....	
Mississippian system.....	
Lake Valley Formation.....	
Kelly Limestone.....	
Pennsylvanian system.....	
Magdalena Group.....	
Permian system.....	
Abo Formation.....	
Tertiary Rocks.....	
Rubio Peak Formation.....	
Sandstone of the Hermosa Area.....	
Latite and Quartz Latite Ash-Flow Tuff.....	
Tertiary Intrusives.....	
Andesite dikes.....	
Tertiary sedimentary rocks.....	
Palomas Gravels.....	
Structural geology.....	
Tectonic setting of the region.....	
Northeast to east-northeast trending faults.....	
North-northwest trending faults.....	
Structures in the Hermosa mining district.....	
Structural control of the mineralization and intrusives.....	
Chapter 2. Ore deposits of the Hermosa mining district.....	
General characteristics of carbonate hosted veins and disseminated deposits.....	
Introduction to ore deposits in the Hermosa district.....	
Ore type, shape, and character.....	
Mineralogy.....	
Gangue minerals.....	
Sulfide minerals.....	
Other accessory minerals.....	
Paragenesis.....	
Alteration.....	
Talc formation.....	

Jasperoid formation.....
Limestone alteration.....
Oxidation.....
Age of mineralization.....
Mineral zonation.....
Comparison of the Hermosa deposits with other Pb-Zn-Ag-Au.....
deposits.....
Chapter 3. Geochemistry of the Hermosa mining district.....
Part I Microthermometry analysis.....
Introduction.....
Method of study.....
Sample selection.....
Methods.....
Calibration.....
Boiling of a fluid system and related fluid inclusions.....
Density of fluids in fluid inclusions.....
Pressure correction.....
Compositional types of fluid inclusion.....
Cooling and heating observations.....
Freezing behaviors.....
Freezing data.....
Heating Behaviors.....
Homogenization data.....
Pressure correction for Th data from the Hermosa district..
Results of Heating-freezing experiments of mineralized zones..
Wolford mines.....
Antelope-Ocean Wave mines.....
Flagstaff-American Flag mines.....
Southern area.....
Palomas Camp.....
Interpretation of the heating and freezing data.....
Wolford mines.....
Antelope-Ocean Wave mines.....
Flagstaff-American Flag mines.....
Southern area.....
Palomas Camp.....
Part II Gas analysis of the fluid inclusions.....
Introduction.....
Sample preparation.....
Instrumentation.....
Results of gas analysis.....
Stable isotope analyses.....
Helium isotope analyses.....
Part III Discussion.....
Modeling for metal transportation and deposition by the
hydrothermal fluids in the Hermosa mining district.....
Depositional mechanisms (models).....
Boiling model.....
Mixing.....
Summary and conclusions.....

Suggestions for future investigations.....

Appendix I: detail description of rocks in the Hermosa district..

Appendix II: Results of heating and freezing analyses.....

Appendix III: Resulte of assay analyses.....

Appendix IV: Results of gas analyses.....

Appendix V: Recalculated values of gas concentration in Appendix IV.....

References.....

LIST OF FIGURES

1. Location map.....
2. Distribution of rhyolite domes, plugs, and dikes.....
3. Structural setting of the region.....
4. Rhyolite dome disturbs the Paleozoic rocks.....
5. Paleozoic rocks in the Paloma Camp.....
6. Regional geologic map of southwestern New Mexico.....
7. Tectonic sketch map of southwestern New Mexico.....
8. Regional Paleothermal anomaly.....
9. Calcite and ore mineralization.....
10. layered and disseminated hypogene pyrite.....
11. Early pyrite replaces sphalerite.....
12. Chalcopyrite exsolutions in sphalerite.....
13. Veins of chalcopyrite and covellite in sphalerite.....
14. Ore sample from the Day mine.....
15. Deformed galena cleavages.....
16. Chalcopyrite replaces sphalerite.....
17. Acanthite replaces covellite.....
19. Paragenetic sequences of minerals in the Hermosa district....
20. Experimentally determined curve for breakdown of dolomite....
21. T-X (CO₂) diagram metamorphism of carbonate rocks.....
22. Altered Tertiary volcanoclastics.....
23. Schematic cross section through the Linkham TH 600 stage.....
24. Layout of Linkham stage.....
25. Calibration curve.....
26. Relationships between degree of fill and density.....
27. Type I fluid inclusions.....
28. Type II fluid inclusions.....
29. Type II (gas-rich) fluid inclusions.....
30. Type II (gas-rich) irregular fluid inclusions.....
31. Type III fluid inclusion.....
32. T-X plot for the low-temperature part of the NaCl system.....
33. Secondary fluid inclusion in calcite.....
34. Histogram of temperature of homogenization the Wolford mines.
35. Histograms of Th of the Antelope-Ocean Wave mines.....
36. Histogram of Th of the Flagstaff-American Flag mines.....
37. Histograms of Th of the southern area.....
38. Histogram of Th of the Palomas Camp.....
39. Different types of fluids in a hydrothermal system.....
40. Th vs. salinity for the Wolford mines.....
41. Th vs. salinity for the Antelope-Ocean Wave mines.....
42. Th vs. salinity for the Flagstaff-American Flag mines.....
43. Th vs. salinity for the southern area.....
44. Th vs. salinity for the Palomas Camp area.....
45. Schematic diagram of the gas analyses apparatus.....
46. Decrepitation curves for calcite and quartz.....
47. Plot of $d D$ vs. $d O$
48. Log FO₂-ph diagram.....
49. Log FO₂-FS₂ diagram.....
50. Mean Th distribution map.....
51. The Th of the first stage of ore mineralization.....
52. Salinity distribution map.....
53. Gold assay value distribution map.....

54.	Silver assay value distribution map.....
55.	H ₂ S concentration map.....
56.	Gold solubility map.....
57.	CO ₂ concentration map.....
58.	Diagrammatic presentation of different fluids.....
59.	Map of different types of fluids in the district.....
60.	Boiling model for Zn, Pb, Cu, Fe, Ag and Au.....
61.	Mixing model for concentration of ore-metals.....
62.	Generalized cross section of the mineralized area.....

LIST OF PLATES

Plate I. Geologic of the Hermosa mining district

(In the back pocket)

Plate II. Location of different mines in the district

LIST OF TABLES

1. Production from the Hermosa mining district.....
2. Generalized stratigraphic section.....
3. Mineral occurrences.....
4. Oxygen and hydrogen stable isotope data.....
5. Helium isotope data.....
6. Results of the boiling calculations.....
7. Results of the mixing calculations.....

GEOLOGY OF THE HERMOSA MINING DISTRICT

INTRODUCTION

The Hermosa mining district is located in the eastern foothills of the Black Range, 45 km (28 mi) west of Truth or Consequences and 24 km (15 mi) south-southeast of Winston, in western Sierra County, New Mexico (Fig.1).

After the early discoveries of bonanza type ores in 1879, the town of Hermosa was established and became the support center for mining activities in the district. This community with several hundred population flourished until about 1893, when the demonetization of silver affected most mining activities in the western United States.

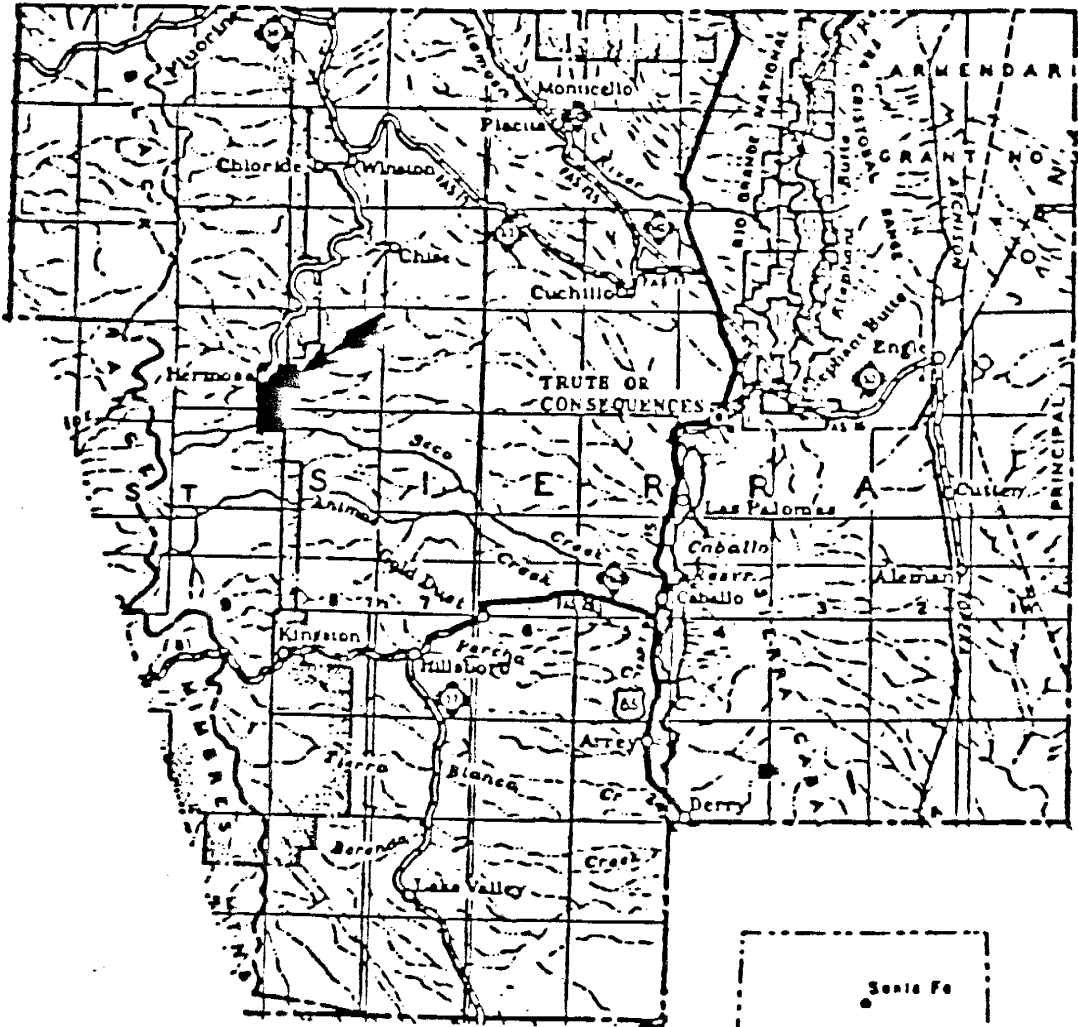
Mines in the district produced about \$1.5 million in silver from high grade ores, concentrated in faults and fractures in Paleozoic carbonates. Small amounts of lead, zinc, copper, and gold also were produced. Early miners quickly recognized the character of the deposits and were often rewarded if they persistently followed thin stringers of ore "leads" from one ore pocket to the next (Shepard, 1984). Hand-sorted ore often contained more than 100 ounces of silver per ton.

The area mapped in this study is about 15 km (9 mi) long in the north-south direction and 8 km (5 mi) wide in the east-west direction (Plate I). The southwestern corner of the Sugarloaf Peak and northwestern corner of the Apache Peak 7-1/2 minute quadrangle sheets were used as the base map.

The mineralized areas in Plate 1 include the Palomas Camp, the Antelope-Ocean Wave area, the Wolford mines, the

Figure 1.

Location map of the Hermosa Mining District in Sierra County, New Mexico. Physiographic features are also shown. Arrow indicates the study area.



Flagstaff-American Flag mines, the Silver-Queen area, the Southern area by Seco Canyon, and numbers of smaller workings and prospects throughout the district. The locations of different mines are shown in Plate II.

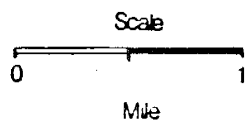
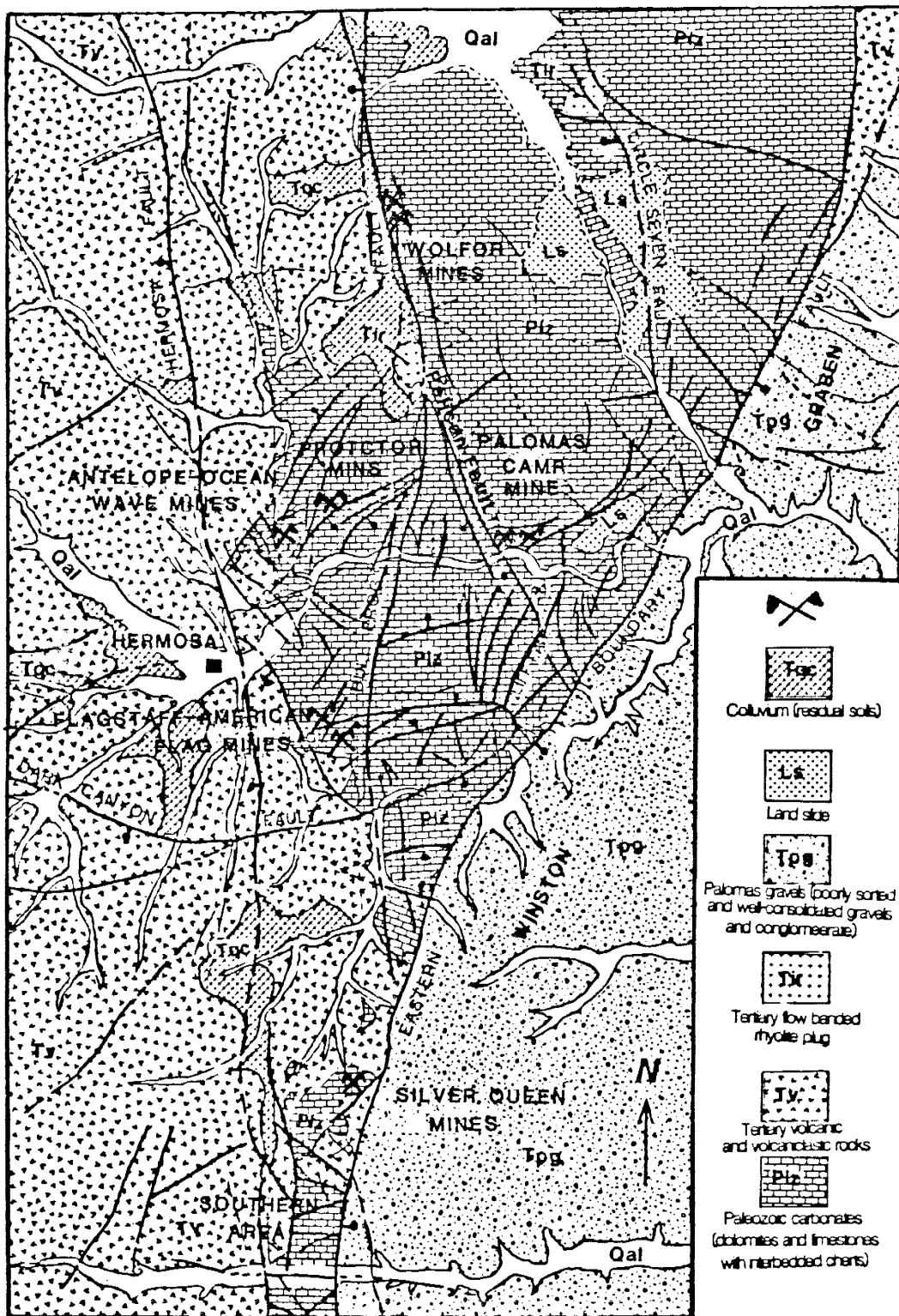
New Mexico State Highway 52 provides access from Truth or Consequences to Winston, and from Winston Forest Service Road 157 leads to the Hermosa district. Several dirt roads in the district lead to the Wolford, Antelope-Ocean Wave, and Palomas Camp areas. Road 157 continues to the south and provides access to the North Seco Canyon which is the southernmost part of the district. Physiographically, the district reflects a complex history of sedimentation, erosion, igneous and tectonic activities.

PREVIOUS WORK

Gordon et al, (1910) described the general geology and ore deposits of the Hermosa mining district. Jones (1922) in a report for the Hermosa Silver Mines Company outlined a plan of development for the company's claims. Harley (1934) in, *The Geology and Ore Deposits of Sierra County*, describes geology and ore deposits of the Hermosa district, and attributes most of the ore deposits to the occurrences of andesite and rhyolite dikes in the district. Jicha (1954b) studied the paragenesis of the ores in the Palomas Camp. Jahns (1955b, 1957) published detailed maps of the Palomas Camp area and briefly discusses the geology, ore deposits and

Plate II. Location of different mines in the district

PLATE II



possibilities for additional discoveries. Ericksen et al. (1970) in an appraisal of the mineral deposits of the Black Range Primitive Area, described the sedimentary and volcanic rocks of the Hermosa district. Maxwell and Heyl (1975) briefly described geology and mineralogy of the Hermosa and surrounding mining districts. Shepard (1984) completed a Masters thesis and described geology and ore deposits of the district. In his study Shepard relates the ore occurrences to the development of the Emory Cauldron in the region.

OBJECTIVES OF THIS STUDY

Since the beginning of this study the objectives of the investigation has been the followings: 1) To define a detailed geologic history of the district and the spatial and temporal relationships of mineralization to rock type, structure (local and regional scale), igneous activities, tectonic setting of the district, and develop a map at 1:3000 scale that shows these relationships. 2) To describe in detail rock units and ore occurrences in the district. 3) To define the physicochemical conditions of the ore mineralization using microthermometric and gas analyses data from the district. 4) To develop fluid composition, fluid flow pattern, temperature distribution and metal distribution maps of the district based on geologic and geochemical data. 6) To develop geochemical models for ore deposition in the district. 7) Based on the findings suggest exploration targets for further developments

of known deposits and unexplored area in the district.

HISTORICAL DEVELOPMENT

During the late part of the last century, western New Mexico was the scene of intense mining activity. Harry W. Elliott, a native of Arkansas, was one of the first people to prospect the Palomas Creek (Rio Palomas) region (Jones, 1922). In 1879, Elliott made the first discovery in the Flagstaff-American Flag area. Later he gave his discovery claims to two prospectors, and they mined about \$ 60,000 worth of silver from these two claims.

Elliott's discovery encouraged other prospectors and miners, and the Hermosa townsite was established to support the mining activity. Hermosa is a Spanish word, meaning beautiful, fine, fair. The first discovery in Palomas Camp was made by a prospector from Leadville, Colorado, by the name of Miller and he called it "Palomas Chief". Other claims and discoveries in this area were made shortly after Miller's find. The new finding shifted mining activity from the Flagstaff-American Flag area to Palomas Camp, but most of the population continued to stay at Hermosa (Jones, 1922). Later during this period (1880s and 1890s) the Antelope-Ocean Wave deposits were discovered. Ore pockets in the district were generally very rich in silver. It was not uncommon, following careful hand sorting, for ores to average more than 500 oz Ag/ton. During this period of activity at the Palomas Camp,

ore production was coming from a number of mines including the Day, Foster-Nourse, Eagle, St. Charles, Mooney-Adams, Mexican, Bishop, Palomas Chief, and Berlow-Roberts on the north side of the canyon, and Cliff, Nana, Atlantic Cable, and Hummingbird mines on the south side. G. W. Wolford developed the Wolford workings in the northern part of the district along the Bull Frog fault but oxidation of the deposits and removal of silver resulted in little high-grade silver in these workings.

By the summer of 1885, the Hermosa mining district had a small adobe smelter with a one-ton daily capacity and a concentrator capable of processing between 17 and 20 tons per day of the lower-grade ores (Shepard, 1984). In 1893, the government's silver demonetization program adversely affected the mining activities in the Hermosa district which was reduced to sporadic mining and exploration. For the next 40 years limited production continued and mining development was restricted to the Stephens crosscut in Hickland Canyon and sinking the Pelican Shaft drift in Palomas Camp. In 1932, C. S. Ross undertook some mining development at the intersection of the Kendall and Pelican faults (Harley, 1934). Several tons of high-grade ore (50-100 oz Ag/ton) were mined. In 1952, Messrs George Koepke and H. B. Jones briefly mined the Nana mine (Jicha, 1954b) and several tons of ore were removed.

Brass Ring Resources, Ltd., of Canada started an exploration program consisting of field and underground mapping and sampling, geophysical surveys (induced

polarization and resistivity) and both diamond and percussion drilling during the summers of 1980 and 1981. The field operations were managed by Triple S Development Corporation of Albuquerque. This operation ended in October 1981 but Triple S Development continued some work in the district until Fall 1983. During this period the Lewandowski (H-15) shaft (E1/4, Sec. 14, T13S, R9W) was sunk. Low-grade silver and high-grade lead-zinc were discovered in this shaft. In late 1982 and early 1983, exploration activities were concentrated on the Slater crosscut in the Antelope-Ocean Wave mines. Percussion long-holes were drilled and a winze was sunk to intersect ore beneath the main drift level. A small rich ore pocket was encountered which contained up to 800 oz Ag/ton. Later (1987) analysis of a hand-picked sample from this pocket by this investigator indicated that this same ore pocket also contains about 37 ppm gold. Triple S Development claims that some of the ores from this working contain up to 3 ounces of gold.

Harley (1934) estimated that the total value of ores produced from the Hermosa district was about \$1,500,000. Table 1 shows production from mines in the district (Harley, 1934). Since 1934, less than \$50,000 of ore has been produced.

Table 1. Production from variou Mines in the Hermosa mining district through 1932 (from Harley, 1934)

Property	Value
Pelican - Albatrose	
Vulture - Eagle	\$1,000,000
Palomas Chief	200,000
Antelope-Ocean Wave	200,000
Flagstaff-American Flag	
Wolford	
Argonaut	100,000
Cliff - L - Embolite	
Miscellaneous	
Total	\$1,500,000

STRATIGRAPHY

A composite stratigraphic section of exposed and unexposed rocks in the Hermosa mining district is shown in Table 2. The section consists of Paleozoic sediments and Tertiary volcanic and volcanoclastic rocks. The exposed Paleozoic formations include (from oldest to youngest): the El Paso Group, Montoya Group, Fusselman Dolomite, Ocate Formation, Percha Shale, Lake Valley Formation, Kelly Limestone, Magdalena Group, and Abo Formation. The Bliss Sandstone of Cambro-Ordovician age and the Precambrian basement do not outcrop in the Hermosa district, however they have been penetrated by diamond drill holes.

The Tertiary volcanic and volcanoclastic rocks are well exposed in the western part of the district. These rocks include the Rubio Peak Formation, the Sandstone of the Hermosa Area, and Latite and Quartz Latite Ash-Flow Tuffs. Tertiary intrusives consist of a few rhyolite and andesite plugs and dikes. On the eastern edge of the district, the Paleozoic and Tertiary rocks are cut off by the Eastern Boundary fault, which places these rocks against the late-Tertiary Palomas Gravels (Plate I).

Because of the intense faulting, the Paleozoic rocks do not outcrop in a continuous section. However, good exposures of these rocks form the steep south-facing slopes of canyon walls such as Palomas, Circle Seven, Hickland, and Dark canyons (Plate I).

Table 2.

Generalized stratigraphic section of the Hermosa mining district.
(After Jahns, 1957 and Shepard, 1984)

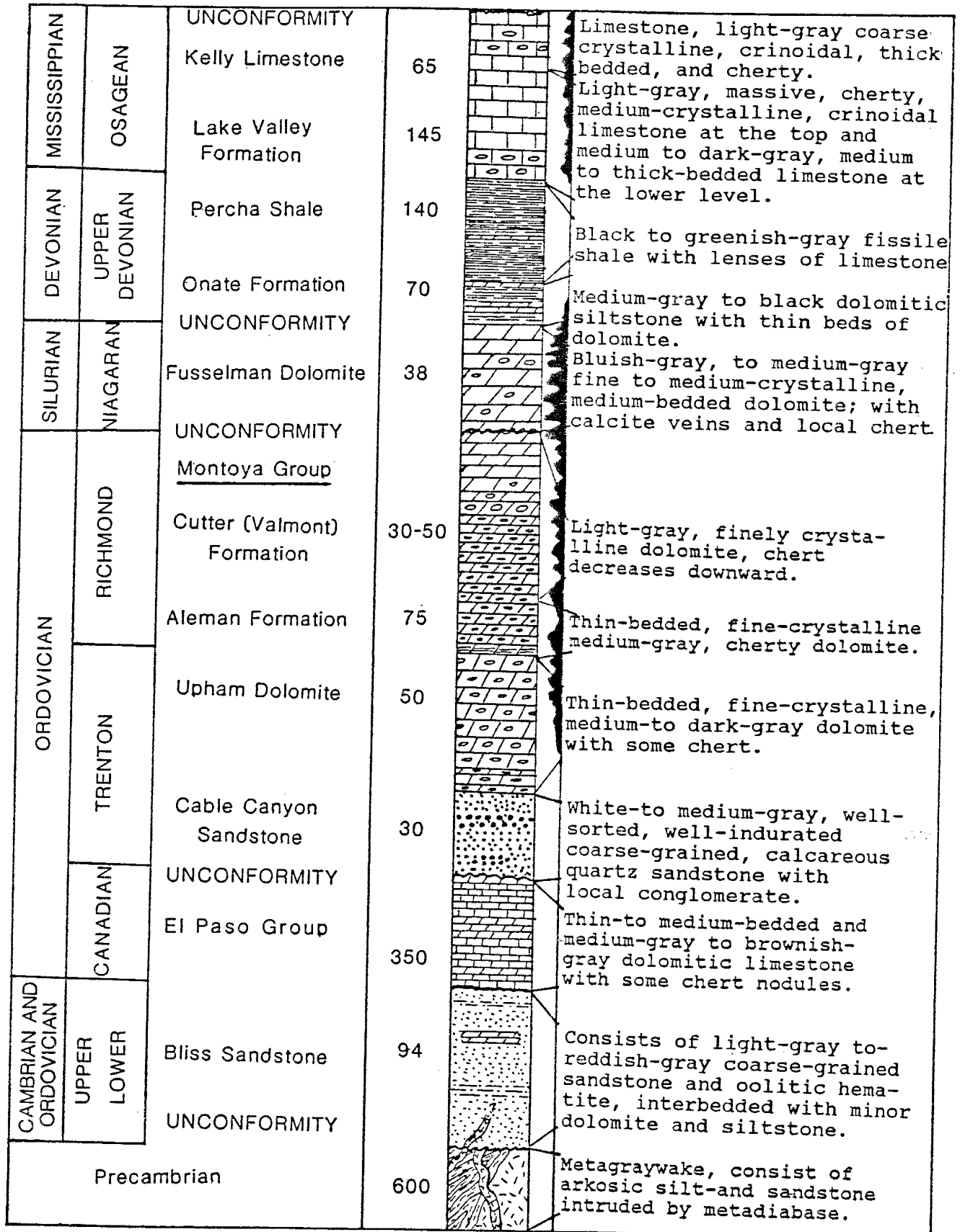


Table 2. (continued)

	SERIES	FORMATTION	THICK-NESS ft	LITHO-LOGY	ORE SHOW	DESCRIPIYON OF ROCK TYPES
QUATERNARY	PLEISTOCENE TO HOLOCENE	Alluvium	70		ORE SHOW	Clay, silt, sand, and gravel in stream beds.
		Landslide deposits	40			Dislocated and brecciated blocks of Paleozoic rocks.
Colluvium	5-20		Residal solis with some talus and gravel.			
TERTIARY	MIOCENE	Palomas Gravels	850			Poorly sorted, well indurated, and heterolithic gravele and sands.
		Intrusive rocks Rhyolite plugs and dikes Andesite dikes	?			Yellowish to reddish-brown, porphyriyic to aphanitic flow-banded rhyolite plugs. Altered grayish-green andesite with phenocrysts of feldspars and hornblende.
	OLIGOCENE	Latite and quartz latite ash-flow tuff	320			Light gray to greenish-gray to pinkish-gray crystal-poor to crystal-rich ash-flow tuffs Interbedded wit sndstone.
		Sandstone of the Hermosa area	890			Light yellowish-gray to light purple-gray volcanioclastic sandstone, siltstone, and shale interbedded with ash-flow tuffs, baslt and basaltic andesite.
		Rubio Peak Formation	350 400			Upper: massive aphanitic and porphyritic lava flow and latite ash-flow tuff. Lower: andesitic breccia mud flows. Massive to poorly-bedded and heterolithic.
	PERMIAN	WOLF-CAMPPIAN	UNCONFORMITY			
Abo Fqrmation			variable			
PENNSYLVANIAN	MORROWAN-VIRGILIAN	UNCONFORMIY				
		Magdalena Group				
		Madera Formation	970		Gray-to brownish-gray thin-to thich-bedded cherty limestone with shale layers in the upper part.	
		Sandia Formation	152		Fine-crystalline, medium-to dark-gray, cherty limestone, siltstone, and sandstone with lenses of conglomerate.	

The Paleozoic rocks in the Hermosa district are uplifted and exposed as a horst, because of the intense tectonic activities of mid-to-late Tertiary time. This horst is flanked by late-Tertiary sediments on the east and mid-to-late Tertiary extrusives on the west.

In the following paragraphs rock types present in the district are described. Detailed description of rock type, subdivision of formations, distribution, and other characteristics of rocks are discussed in Appendix I.

PRECAMBRIAN BASEMENT

Diamond drill cores indicate Precambrian rocks are predominantly metagrawacke, that consists mainly of moderately to well-sorted fine-grained arkosic sandstones and siltstones. The clasts show variation in color from yellowish-gray to greenish-gray that give them a laminated appearance. Shepard (1984) noted that the siltstones are composed of discrete grains of quartz, K-feldspar, and plagioclase. Drilling has also intercepted metadiabase dikes that principally consist of hornblende and plagioclase. Condie (1982) indicates an age of 1.65-1.72 b.y., and suggests that the Precambrian rocks in southwestern New Mexico are a part of a crustal province extending from Central New Mexico to Illinois.

CAMBRO-ORDOVICIAN SYSTEMS

BLISS SANDSTONE

The Bliss Sandstone is not exposed in the Hermosa district. However, cores from drill holes show that this formation is about 29 m (95 ft) thick. Except for a few basal medium to thick-bedded horizons of coarse-grained sandstone and oolitic hematite, this formation is thin-bedded. The lower part of the formation consists of white conglomeratic sandstone, feldspathic sandstone and oolitic hematite. Thin horizons of dolomitic limestone are present just above the Precambrian basement and the oolitic hematite. The upper section consists of reddish-brown to greenish-gray fine-grained sandstones and siltstones rich in hematite and glauconite.

ORDOVICIAN SYSTEM

EL PASO GROUP

The El Paso Group consists of two formations, the Sierrite Limestone (lower) and the Bat Cave Dolomitic limestone (upper). The Sierrite formation is about 30-50 m (98-164 ft) thick in the Hermosa district. This formation is thin to medium bedded, and consists of medium-gray and micritic dolomitic limestone. The Bat Cave formation forms the bulk of the El Paso Group. This formation mainly consists of medium-

to-thick beds with alternating dark-gray to medium-gray limestone, dolomitic limestone, and dolomite.

MONTOYA GROUP

The Montoya Group consists of four units. From the base upward these units are the Cable Canyon Formation, Upham Dolomite, Aleman Formation, and Cutter (Valmont) Formation. The Cutter Formation is a light-gray, coarse-grained, massive, friable to well indurated and calcareous quartz sandstone. The texture ranges from well-sorted, medium-grained sand to unsorted pebbles and conglomerate. This formation is about 10 m (33 ft) thick.

The Upham Dolomite is about 15 m (49 ft) thick, and it is massive-bedded, micro-to-coarse-crystalline, medium-gray to dark-gray dolomite. In some locations, this formation appears intensely brecciated and calcite fills the fractures and joints.

The Aleman Formation is about 23 m (75 ft) thick, and consists of thin-bedded, medium-gray, fine-to-medium-crystalline dolomite and chert ribbons and nodules. The alternate dolomite and chert beds gives a banded appearance to this formation. Because of the color variation of these bands, local miners call this formation "Zebra Beds".

The Cutter Formation is about 10-15 m (33-49 ft) thick and consists of light-gray to yellowish-gray, fine-crystalline dolomite. The chert content decreases upward. In several

locations, this formation contains breccia clasts of presumably sedimentary origin. It seems that these clasts represent collapse features resulting from the development of karst topography.

SILURIAN SYSTEM

FUSSELMAN DOLOMITE

The Fusselman Dolomite is about 12 m (39 ft) thick and consists of dark-gray to bluish-gray, thick-bedded, micritic, and cherty dolomite. Tectonic deformations have fractured this formation more than any other rocks in the district. Most of these fractures are filled with calcite. The Fusselman Dolomite is the most productive formation in the district with most of the known ore-grade mineralization filling in its fractures.

DEVONIAN SYSTEM

The Devonian system in the Hermosa district consists of Onate and Percha Shale formations. The Onate Formation is composed of dark to medium-gray dolomitic siltstone with thin beds of dolomite in the lower parts. This formation is about 21 m (69 ft) thick.

The Percha Shale is about 43 m (141 ft) thick. The lower part is black fissile shale and the upper part ranges from

green to greenish-gray calcareous shale. Some black micritic limestone lenses are present in the upper part.

MISSISSIPPIAN SYSTEM

LAKE VALLEY FORMATION

The Lake Valley Formation is about 44 m (144 ft) thick. The basal portion of this formation consists of thin-to-thick-bedded, medium to dark brownish-gray, fossiliferous, and micritic limestone with dark-gray chert nodules. The upper section consists of gray to pinkish-gray, fossiliferous, massive, and micritic to coarse-crystalline limestone. Where silicified the Lake Valley Formation crops out as rough, flinty and porous jasperoid.

KELLY LIMESTONE

The Kelly Limestone is a medium to coarse-grained thick-bedded crinoidal limestone. Silicified outcrops of this formation are common in the district.

PENNSYLVANIAN SYSTEM

MAGDALENA GROUP

The Magdalena Group composes two formations: the Sandia

(lower) and Madera (upper). The Sandia Formation consists of dark to gray, fine-grained interbedded cherty limestone, siltstone, and fine to coarse-grained sandstone with local lenses of conglomerates. This formation is about 46 m (151 ft) thick. Green, red, and white chert nodules and lenses are abundant in the basal units.

Shepard (1984) described and divided the Madera Formation into five members (from oldest to youngest) Madera No.1, Big Cliff, Madera No.2, Double Cliff, and Upper Undifferentiated member. This study uses the same subdivision for consistency in mapping and description. The Madera Formation is about 230 m (755 ft) thick and consists of thin to thick-bedded, light to dark brownish-gray micritic to medium-crystalline, fossiliferous limestone. Chert nodules are common but their size and amount vary in different members. For detailed description of each member see Appendix I.

PERMIAN SYSTEM

ABO FORMATION

The Abo Formation consists of reddish-brown to dark-red or purplish-brown shale, siltstone, and sandstone. In the Hermosa district, this formation occurs as exotic allochthonous blocks of tens to hundreds of meters in dimension, which have been rafted to their present-day position by the flow of Tertiary andesite, lahars, and breccias.

TERTIARY ROCKS

RUBIO PEAK FORMATION

Throughout the Black Range, the Rubio Peak Formation is divisible into distinct lower and upper units. The aggregate thickness of these two units is about 320 m (755 ft) and increases westward. The lower unit dominantly consists of subrounded, heterolithic clasts of aphanitic to porphyritic intermediate volcanic rocks and Paleozoic limestone, siltstone, and sandstone. The upper unit contains exotic blocks of Abo Formation. Poorly-sorted, clast-supported, boulder to cobble conglomerates with some sandstone occur at the base of this unit. Various shades of colors from dark-purple to dark-green are common in this formation. Radiometric dates of 37.3 ± 2.3 m.y. (Murvin and Cole, 1978) and 36.7 ± 1.4 m.y. (Loring and Loring, 1980) are reported for these rocks.

SANDSTONE OF THE HERMOSA AREA

The Sandstone of the Hermosa Area consists of light yellowish-gray to light purple-gray volcanoclastic sediments. Detrital grain sizes range from silt to conglomerate, but fine to coarse-grained sandstone is the predominant lithology. Interbedded with this formation are basaltic andesite and tuff units, which have erupted from local sources.

LATITE AND QUARTZ LATITE ASH-FLOW TUFFS

The Latite and Quartz Latite Ash-Flow Tuffs consist of two units. The basal ash-flow tuffs are a light greenish-gray color and contain abundant pumice fragments. Scattered phenocrysts of quartz, sanidine, and plagioclase give a fragmental texture to this unit. The upper unit is pinkish-gray in color and consists of quartz, sanidine, and plagioclase phenocrysts with a groundmass of sericite, epidote, and pumice.

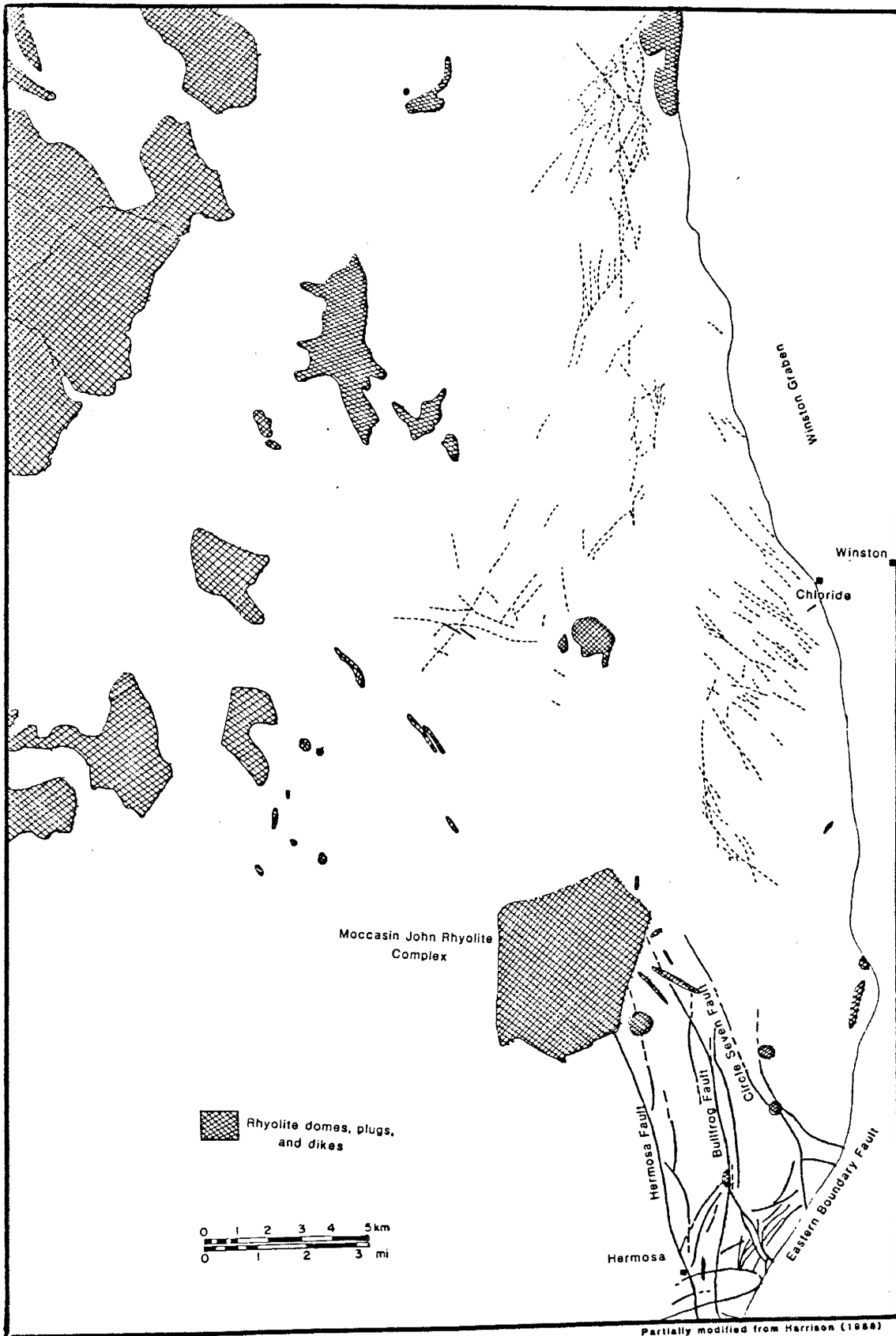
INTRUSIVE ROCKS

A few rhyolite plugs and andesite dikes occur along or close to the surface expression of major faults and fractures in the Hermosa mining district. The Moccasin John rhyolite dome complex (Ericksen et al., 1970) occurs about 8 km (5 mi) northwest of the study area. Many of the rhyolite plugs and dikes in the region appear to be related to this complex. Thermal effects from these plugs and dikes are probably the main source of heat for the hydrothermal system in the region.

Two large rhyolite plugs occur along the Bull Frog and Circle Seven faults in the Hermosa district (Plate I). All rhyolite domes, plugs and dikes in the region (Fig.2) show similar lithology and structural control. These flow-banded rhyolites are yellowish-brown to reddish-brown in color. Near vertical, well-defined flow foliation can be seen in these

Figure 2.

Distribution of rhyolite domes, plugs, and dikes in Taylor Creek, Chloride, and Hermosa mining districts. The Moccasin John complex is the possible heat source for hydrothermal activities in the region.



Partially modified from Harrison (1988)

intrusives. A typical rhyolite plug exhibits planar to contorted banding appearance (Ericksen et al., 1970).

The flow-banded rhyolites consist of phenocrysts of quartz, sanidine, and biotite with a fine-grained matrix of sanidine, plagioclase, and quartz. Hematite is the only opaque mineral present in these rocks. In the southwestern part of the study area, flow-banded rhyolite dikes intrude rocks as young as the Sandstone of the Hermosa Area, which is older than 29 m.y. Lithological similarities, structural control similarities, and geographical distribution of these intrusives suggest that they all belong to the same period of igneous activity in the region.

ANDESITE DIKES

Dikes of andesitic composition have penetrated the Paleozoic and Tertiary rocks in the district. Most of these dikes occur in and along east-northeast trending faults. These rocks consist of phenocrysts of plagioclase, K-feldspar, and hornblende. The groundmass consists of the same minerals but is fine-grained.

TERTIARY SEDIMENTARY ROCKS

PALOMAS GRAVELS

The Palomas Gravels form the hills and valleys east and

southeast of the Hermosa mining district. The Eastern Boundary fault (Plate I) is a structural contact between the Palomas Gravels and the Paleozoic sedimentary and Tertiary volcanic rocks. The Palomas Gravels consist of a variety of volcanic rocks. Silt and fine sand compose the matrix. The fragments are poorly-sorted and well-rounded. The formation is light brownish-gray to light pinkish-gray in color and about 260 m (853 ft) thick.

STRUCTURAL GEOLOGY

REGIONAL TCTONIC SETTING

The Hermosa mining district is situated in the Basin and Range province of southwestern New Mexico. The structural fabric of this area is the result of complex interaction of Laramide compression tectonic activities, Emory Cauldron formation of late-Eocene age, Rio Grande rift opening of mid-Oligocene age, and the basin and range development of early-Miocene age continuing to the present. Figure 3 shows the position of the Hermosa district in relation to the Winston graben (a part of the Rio Grande rift) and the Emory Cauldron.

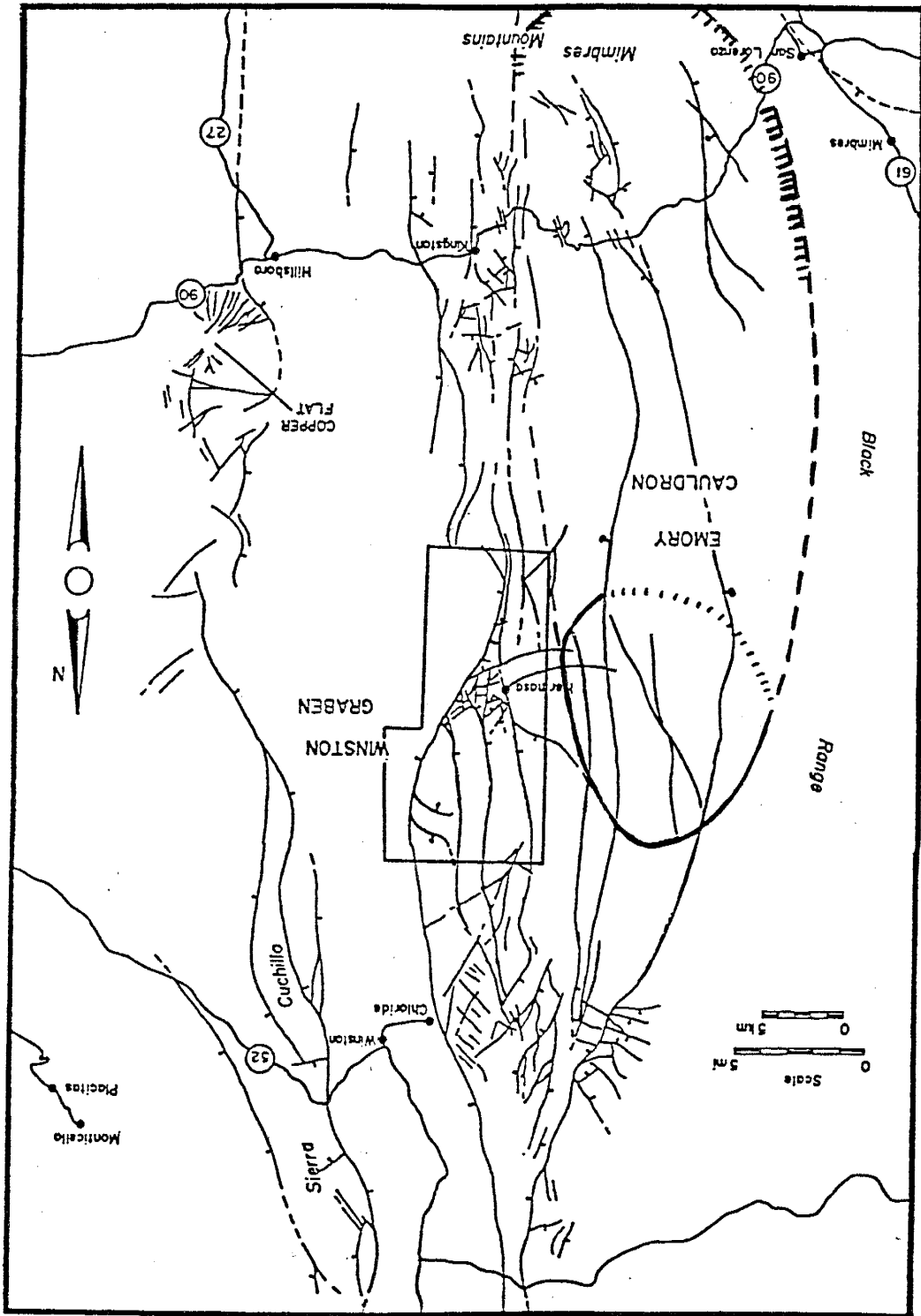
Laramide compressional tectonic activities in the region are characterized by strike-slip faulting (Seager, 1983; Seager et al., 1986) with west-northwest to northwest trending and north-northeast to north trending dextral-strike-slip faulting (Chapin and Cather, 1982; Seager, 1975; Kelley and McCleary, 1960). In the Hermosa district, most of the Laramide structures have been modified and deformed by the Rio Grande rift opening and basin and range faulting.

The Emory Cauldron is a north-south elongated cauldron, which formed about 35 m.y. ago (Elston et al., 1975; McIntosh 1986) and occurs to the west of the Hermosa mining district (Fig.3).

Elston et al., (1975) considered the Emory Cauldron the

Figure 3.

Structural setting of the Hermosa, Chloride, and Kingston mining districts. Emory Cauldron and Winston graben are the two major structures in the region (partially modified from compiled work of Shepard, 1984).



source of the rather extensive and thick Kneeling Nun ash-flow tuff of Oligocene age (33.4 ± 1.0 m.y., McDowell, 1971; and 35.28 m.y., McIntosh, 1986) in southwestern New Mexico.

Because southwestern New Mexico has undergone several periods of tectonic deformation, it is difficult to recognize faults and fractures related to the Emory Cauldron formation, or those of earlier deformations. Reactivation of pre-existing Paleozoic and Laramide age structures, due to pre-and post-Emory Cauldron structural deformations in the region, is very common (Chapin and Seager, 1975; Elston et al, 1975). Regardless of the age of the structures, the formation of the Emory Cauldron and related structures had a profound effect on the structural setting of the region and probably prepared the ground condition for later mineralization.

Cenozoic evolution of the modern plate boundary along the western United States from a compressional to a predominantly transform boundary coincided with changes from compressional to extensional deformations in the interior of the western United States. These changes of tectonic regime from compressional to extensional deformations about 36 my ago (Chapin et al., 1987) were accompanied by volcanic changes from intermediate calc-alkali to bimodal basaltic andesite and silicic volcanism (Christiansen and Lipman, 1972). Combinations of two or more of planar, listric, and low-angle faults are associated with extensional terrains.

The Rio Grande rift and Basin and Range environment in south western New Mexico are parts of the Cenozoic extensional

deformations in western North America. The Winston graben is the most prominent extensional feature close to the study area, and the Moccasin John Rhyolite dome is the largest extensional related intrusion in the region. These two features show the profound effects of the Cenozoic extensional deformation on the Hermosa district and vicinity.

STRUCTURES IN THE HERMOSA MINING DISTRICT

The Hermosa Mining District is bounded by the Eastern Boundary fault on the east and the Hermosa fault on the west (Plate 1). The Paleozoic rocks of the district are uplifted as a block between these two faults. The displacements vary from 90 m (295 ft) to 300 m (984 ft). The 3.2 km (2 mi) wide (east-west) and 9.5 km (6 mi) long (north-south) uplifted block is intensely broken and fractured. The width of this block and its related mineralized zones decreases southward. Groups of North-to-northwest-and northeast-to-east trending faults have broken the uplifted Paleozoic rocks into discrete and smaller blocks. Each block, in turn, is deformed by numerous smaller faults and fractures. The intersections of two or more of these smaller faults and fractures, near a major fault or faults, are favored by mineralizing fluids.

Folding has played a minor role in the structural fabric of the district. Most of the dip and strike changes of formations are attributed to the tilting of the faulted blocks. In general, the Paleozoic rocks dip to the north-

northeast at low angles (5 to 20 degrees) with some local variations.

In the Palomas Camp the Paleozoic strata tend to dip radially away from the center of the camp area. Harley (1934) attributed this doming to a possible intrusive in the area which is not exposed or encountered during mining and drilling. This doming could also be the effect of a large number of faults with radiating strikes, which affect local dips of Paleozoic rocks. Drag folds are observed along the Pelican and Circle Seven faults in the Palomas Camp. Just south of the Wolford mines (Plate I) doming of Paleozoic rocks due to intrusion of a rhyolite plug is clearly evident (Fig.4). Along the western edge of the mapped area, the volcanic rocks overlap the Paleozoic rocks at a low angle of from 5 to 15 degrees. The attitudes of the volcanic rocks conform a regional westward-dipping homocline which is the prevailing structure of the Black Range (Shepard, 1984).

North-northwest trending and northeast to east-northeast ← trending faults are the dominant patterns in the Hermosa mining district.

NORTHEAST TO EAST-NORTHEAST TRENDING FAULTS

Eastern Boundary, Emerick Mountain, and Dark Canyon faults are typical examples of northeast to east-northeast trending faults (Plate I). Mexican, Kendall, and Cliff faults are representatives of minor faults with similar strikes in the

Figure 4.

Light-yellowish brown rhyolite dome deforms the Paleozoic strata (Magdalena Group). Note on both sides of the dome the sedimentary rocks are horizontal.

study area. The three major faults are downdropped from a few tens to a few hundreds of meters to the southeast. The smaller faults and fractures have little or no displacement, but they contain most of the ore mineralization in the district.

The western margin of the Winston graben is the Eastern Boundary fault and it marks the eastern limit of mineralization in the mining district. Silicification, in the form of jasperoid and quartz, is common along this, as is hematization which stains fault gouge in carbonate rocks. This fault is a major late-Tertiary regional fault and it extends well beyond the northern and southern limits of the Hermosa mining district.

The Dark Canyon fault offsets both Paleozoic and Tertiary strata in the central part of the mapped area and strikes east-west to east-northeast; it is downthrown to the south. It cuts the Bull Frog as well as other faults in the central part of the district. It has displaced the 35 m.y. old Rubio Peak Formation in Sec. 25, T13S, R9W and the younger olivine basalt, interbedded with the Sandstone of the Hermosa Area (29-26 m.y.). The Dark Canyon fault has been active during much of the Tertiary and postdates many other faults in the district (Shepard, 1984).

A well exposed portion of Dark Canyon fault can be seen in the NE1/4 Sec.25, T13S, R9W which places the Sandia Formation against the Fusselman Dolomite. A stratigraphic throw of approximately 150 m (492 ft) has been inferred from this displacement. A jasperoid ridge about 10 m (33 ft) wide with

reddish-brown silicified breccia marks the location and width of the fault zone in the slopes on the northern side of Dark Canyon Creek.

The Emerick Mountain Fault lies in Emerick Mountain and in Hickland Canyon in the central to north-central part of the district (Plate I). The fault zone is marked by silicified fault breccia and lack of drag or tilt in the adjacent beds. Two or three more faults with the same northeast strike are present in the Emerick Mountain fault zone and they all terminate against the Bull Frog fault. Behind the Protector mine, the Emerick fault offsets the Paleozoic rocks about 110 m (361 ft). In Hickland Canyon, the Emerick Mountain fault bifurcates and continues southwest where it displaces Paleozoic rocks and is buried by Tertiary breccia of the Rubio Peak Formation (Shepard, 1984). The Emerick Mountain fault zone has been penetrated by an andesitic dike which is well exposed on the northeast side of Hickland Canyon. The dike is intensely altered. The Emerick Mountain fault and associated fractures were the main conduits for hydrothermal fluids in the Protector and Antelope-Ocean Wave mines.

The Palomas Camp area is intensely deformed and exhibits an oval or dome-shaped structure, about 550 m (1804 ft) long. Kendall, Mexican, and Cliff faults are the most prominent faults in this strongly fractured zone. These and many smaller structures exhibit a northeast trend with a N 45-50 E strike. Offsets of the Paleozoic rocks in the camp area are exposed in cliffs on the north side of Palomas Creek (Fig.5). These

Figure 5.

Paleozoic rocks on the north side of the Palomas Camp have been deformed by Pelican fault. The amount of displacement is about 60 m (197 ft).

faults and fractures, have caused intense brecciation of the sedimentary rocks. Intersections of these faults with north-trending faults have prepared a favorable structural control for ore deposition. Deformed mineralized veins suggest continued tectonic and structural deformation in the region. Offsets along these faults range from 10 m (33 ft) to 45 m (148 ft) with dips ranging from 60 to 85 degrees.

NORTH-NORTHWEST TRENDING FAULTS

The Hermosa, Bull Frog, and Circle Seven faults are the most prominent fractures in this group. They all show a down-to-the-west drop of 85 m (275 ft) or greater. Two smaller but important faults, with similar orientation, are present in the Palomas Camp area. The Pelican fault on the west and Palomas Chief fault on the east make the western and eastern limits of Palomas Camp mineralization. Many other north to northwest trending faults and fractures are not described here (Plate I). Most of these structures are related to major faults in the region and they are usually the zones for ore mineralization.

The Hermosa fault runs through the entire mining district in a north-south direction. Displacement along this fault increases northward. To the north, the Hermosa fault has a stratigraphic separation of about 210 m (689 ft) between juxtaposed Rubio Peak and Latite and Quartz Latite formations. The best exposures are on the east side of the South Fork of

Palomas Creek, a short (200 m) distance north of the old townsite of Hermosa. At this location, the fault's outcrop is about 5 m (16 ft) wide; the fault zone is intensely brecciated, silicified, and stained with hematite. The width of the fault zone is extremely variable along strike.

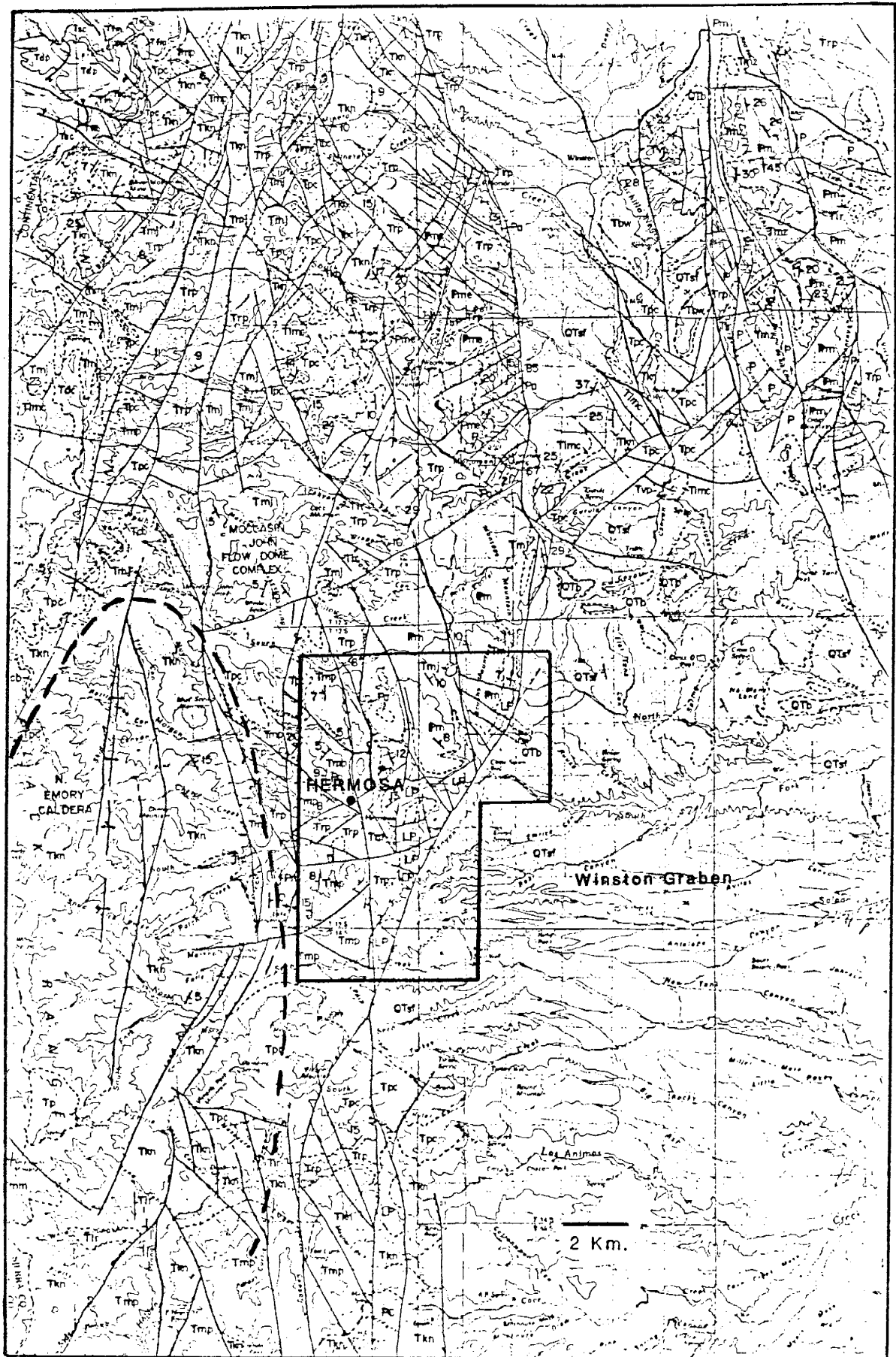
The Hermosa fault is a major regional structure that continues beyond the northern limit of the mapped area. Figure 6 (from Harrison, 1988) includes this and other structural relationships in the region. It is the belief of this investigator that the Hermosa fault also continues to the south with similarly large displacement. However, at the southern end of the mapped area, relatively thick Tertiary deposits make it difficult to trace a single continuous break. At the extreme south end of mapped area, two faults with strikes similar to that of the Hermosa fault, have stratigraphic displacements of up to 60 m (197 ft). One of these faults continues beyond the southern limit of the mapped area crossing Seco Canyon (Plate I).

The distance between the Hermosa fault and the Eastern Boundary fault in the northern part of the study area is about 7 km (4.4 mi) but the southward convergence of the fault zones reduces this to about 400 m (1312 ft). At the southern boundary of the map area, these two major regional faults are parallel to each other.

The convergence of the Hermosa and Eastern Boundary faults to the south has contributed to the uplift of the Paleozoic strata exposed between them. Numbers of smaller faults, with

Figure 6.

Regional geologic map of southwestern New Mexico compiled by Harrison (1988). The map shows major faults in the Hermosa and adjacent mining districts. Eastern Boundary, Bull Frog, and Hermosa faults are extended well beyond of the northern and southern limits of the mapped area. Winston graben (Las Animas) on the east and Emory caldera on the west are also shown. The effects of each structure on the region are well shown.



parallel, diagonal and perpendicular strikes to the major faults have separated the uplifted block into smaller tilted blocks. Each smaller block in turn has been cut by other faults and fractures. The intense faulting and fracturing in such a narrow zone, has provided an excellent environment for ore mineralization. Brecciation and silicification (jasperoid formation) is intense. Cross cutting faults between two larger structures have juxtaposed younger Paleozoic (Mississippian) and Tertiary volcanic rocks with older Paleozoic (Ordovician) rocks. Thirty to sixty meters (98 to 197 ft) of displacement in both strike-slip and vertical directions are common. The step-like topography of this part of the mining district is the result of such block faulting.

The Bull Frog fault is another regional north-south to north-northwest trending fault, extending through the central part of the district and continuing beyond the northern limit of the mapped area, and southward. The Bull Frog fault is cut by the Dark Canyon fault, and it joins with the Eastern Boundary fault. Displacement along this fault increases to the north; near the Wolford mines, the stratigraphic displacement across the fault is up to 110 m (361 ft).

The Bull Frog fault is well exposed where it crosses the South Fork of Palomas Creek in the NE1/4 Sec.24, T13S, R9W. Stratigraphic displacement at this locality is about 150 m (492 ft), and, like the Hermosa fault, it is down to the west; the upper part of the Lake Valley Limestone is faulted against the Double Cliff member of the Madera Formation. In

the central part of the mapped area, the Bull Frog fault lies east of the Flagstaff-American Flag mines. At this location younger Paleozoic carbonates such as Sandia, Kelly, and Lake Valley formations have been silicified extensively. Some disseminated sulfide mineralization is associated with this jasperoid formation.

The Bull Frog fault zone is about 3 m (10 ft) wide and is marked by silicification and brecciation. In the northern part of the mining district, the Bull Frog fault and smaller related structures have prepared the upthrown part of the Madera Limestone for mineralization.

The third major fault of the north-northwest trending group of faults is the Circle Seven fault which is exposed in the northeastern part of the mapped area. Shepard (1984) named the fault because it partially controls the Circle Seven Creek drainage. The best exposure of this fault is in Circle Seven Canyon where Kelly Limestone is faulted against Aleman Formation with a down-to-the-west stratigraphic throw of about 140 m (459 ft).

Near the northern boundary area the Circle Seven fault exhibits brecciation, silicification, and oxidation of iron sulfides. No ore mineralization has been found in the jasperoids or anywhere else along this fault. In the very northern part of the study area, this fault displaces a rhyolite plug. From the field evidence and composition of the rhyolite, it is inferred that this plug is related to the Moccasin John rhyolite dome which is about 28 m.y. old. Thus

the Circle Seven fault is younger than 28 m.y. By analogy, other faults with similar strikes are younger than 28 m.y. This conclusion supports the idea that the formation of these faults is genetically related to the development of the Rio Grande rift and the Basin and Range province in southwestern New Mexico. In addition to this structural evidence, the bimodal igneous activities in the region also support the extensional nature of structural deformation in this area.

The Pelican fault marks the western limit of the Palomas Camp area and strikes northwest. This fault merges with Bull Frog fault north of Palomas Canyon and, to the south, it joins the Eastern Boundary fault. At the junctions and in their vicinities at both ends, extensive shattering of the rocks occurs providing favorable areas for ore mineralization and prospecting. These areas are marked with iron-stained siliceous rocks of the Madera Formation. The Pelican fault and related parallel structures are an important control on ore mineralization in the Day mine, one of the major ore producing mines in Palomas Camp. Stratigraphic throw of about 67 m (220 ft) down-to-the-west puts the Lake Valley Formation against Percha Shale just above the Day Mine.

The Palomas Chief fault is another relatively important north-south trending fault in Palomas Camp. This fault forms eastern limit of Palomas Camp and it intersects Mexican fault to the north. It is well exposed in the north and south sides of Palomas Creek. Stratigraphic throw along this fault is about 60 m (197 ft) down to the east.

STRUCTURAL CONTROL OF MINERALIZATION AND INTRUSIVES

Faulting is the main ore controlling structure in the Hermosa mining district. Most of the ore occurrences in the district are formed along faults with small (0.1-15 m) displacements. Faults with large displacements contain little or no ore. In areas with good ore concentrations, such as Palomas Camp and the Antelope-Ocean Wave mines, major faults intersect with smaller faults. Intertwining, slitting, and branching structures result from this fabric. Bedding plane control of ore occurrences is limited to the Palomas Camp area where the Percha Shale has controlled fault continuations and upward fluid movement. Ore occurrences whether controlled by faulting or bedding planes form as masses, tabular to pod-like bodies, and fissure veins. Different forms of ore concentration are associated with different formations. For example, fissure veins are most common in faulted and fractured Aleman, Cutter, and Fusselman dolomites.

Deformation, in the form of drag-folding, is associated with faults that contain mineralization and is restricted to thin-bedded dolomite intervals such as lower Cutter and Aleman formations (Shepard, 1984). Jahns (1957) noted that, between closely spaced faults, the dolomites are warped and dislocated in irregular zones and accompanied by talc alteration.

In the Antelope-Ocean Wave mine area two groups of mineralized faults with north-northeast and north-northwest

strikes respectively intersect and form an extensive shattered zone. Open spaces and cavities which resulted from such deformation were used by hydrothermal fluids for silicification of the fractured rocks and deposition of ore and gangue minerals. The shattering in this area covers about 2 square km (0.8 square mi), but only in a small area does mineralization occur. Mineralization is restricted to the Cutter and Fusselman formations (Plate 1, NE1/4 Sec.26, T13S, R9W). The overlying Rubio Peak Formation also has been deformed and altered by hydrothermal fluids but no ore mineralization has been encountered. In the Chloride mining district to the north, which shows similar structural deformation, the Rubio Peak Formation is the main host rock for ore mineralization.

Intrusive rocks, in the form of domes, plugs, and dikes, show a close association with major structures not only in the study area but throughout the region. Rocks of different compositions, are controlled by faults of different trends. Andesite dikes follow northeast and east-northeast trending faults whereas rhyolite plugs and dikes are controlled by north-northwest trending faults.

Narrow plugs and dikes of aphanitic to porphyritic andesites occur along northeast to east-northeast trending faults at the portal of the Bishop workings in Palomas Camp. A similar dike occurs along the Emerick Mountain fault. This dike is exposed in Emeric Mountain and the bottom of Hickland Canyon.

Rhyolite domes and plugs are relatively abundant in the northern part of the study area and farther north in the Chloride mining district. Along the Bull Frog fault, just south of the Wolford mines, a plug about 300 m (984 ft) in diameter has intruded and domed the Madera Formation (Fig.4). About 2.5 km (1.5 mi) northeast of this plug, another plug about 460 m (1509 ft) in diameter has intruded the Circle Seven fault (Fig.2). Further north, just north of Circle Seven Creek, numbers of flow-banded rhyolite plugs and dikes have intruded major structures including the Circle Seven fault. Along northward continuations of the Hermosa and Circle Seven faults, a large rhyolite dome, which makes up Sugarloaf Peak (Ericksen et al., 1970) has intruded the Paleozoic and Tertiary rocks. Further north to northwest, the major flow banded rhyolite dome of the Moccasin John Complex is exposed (Ericksen et al., 1970, and Harrison, 1987). This complex was apparently the main source of most (if not all) of the rhyolite domes, plugs, and dikes in the region (Fig.2).

Along Bull Frog fault near Dark Canyon, a similar rhyolitic dike intrudes Paleozoic and Tertiary volcanic rocks. From the intrusion of this dike into the Sandstone of the Hermosa Area, Shepard (1984) assigned a mid-Oligocene age to the rhyolite intrusions in the district. Isotopic dating (Harrison, 1988) of the Moccasin John Complex indicates about 28 m.y. of age for this complex, which confirms Shepard's conclusion. In the Pelican fault zone a similar rhyolite dike is present.

Based on these observations, it could be concluded that

major structures in the region have controlled intrusive occurrences. It is also possible to conclude that, because two different compositions of intrusives occur in two different groups of structures with different trends, these intrusives have occurred in two different periods.

TECTONIC INTERPRETATION OF THE STRUCTURES IN THE DISTRICT

Almost all the epithermal vein deposits in the Western United States and Mexico were developed during Eocene to Miocene time. Tertiary structures whether mineralized or unmineralized show a similar sense of displacement, orientation, and form. Such similarities and the time interval suggest that the formation of structures and, much of the mineralization were in responses to large-scale regional deformation and hydrothermal activities rather than the formation of cauldrons and related structures.

During late Mesozoic and early Tertiary, deformation resulted from east-west compression (Coney, 1981). In the Western United States, this compressional deformation occurred during late Cretaceous to early Eocene and has been renamed the Laramide orogeny. Associated with the Laramide orogeny was widespread volcanism and intrusion; the Mogollon-Datil volcanic field in southwestern New Mexico is a typical complex. The volcanics and intrusives are cut by a series of north-to-northeast dextral wrench faults of probable late Eocene age (Harrison, 1987). A number of intermediate intrusions in this region host some of the precious-base metal and porphyry copper deposits (Copper Flat, Kingston and Hillsboro) are attributed to these intrusives in these districts (Elston, 1976; Harley, 1934). Similar structures, intrusives, and ore deposits are known in Nevada, Utah, Idaho and Sierra Madre Occidental of Mexico. Evidence from

epithermal veins, and their associated structures and dikes in the Western United States, suggests that the Laramide compressive deformation continued until about 35 m.y. ago, but that the mountain-building phase was terminated about 50 m.y. ago (Tweto, 1975). If this conclusion is justified then the compression was very weak in late Eocene, and the transitional period from compressional to extensional deformation had already started. Such a transition from compressive to extensional deformation correlates well with tectonic activity and related changes between the Western North American plate and the Pacific plate (Coney, 1981).

In the Hermosa mining district, evidence for Laramide deformation is not recognized. Insufficient erosion of thick volcanic rocks may conceal possible Laramide deformation, or younger structures associated with the Rio Grande rift opening or Basin and Range block faulting, may have distorted Laramide patterns in the district beyond recognition. However, evidence from areas north and south of the district suggest that Laramide deformation is widespread in the region.

East-west compression in the North American plate ended about 35 m.y. ago and extensional deformation began about 29 m.y. ago (Chapin and Seager, 1975); by 25 m.y. ago the region was experiencing widespread extension (Christiansen and Lipman, 1972). In the Western United States inconclusive dating indicates that very few mineral deposits developed in the 5 to 6 m.y. interval of stress and tectonic transition (Dreier, 1984). Extensional deformation may have started

earlier (35-30 m.y. ago) in Mexico and moved northward. Chapin and Seager (1975) have asserted that the opening of the Rio Grande rift started about 29 m.y. ago in southern New Mexico and gradually moved northward into Colorado. In southwest New Mexico Emory and several other cauldrons represent the major structural deformation during this transitional period (Elston, 1976).

In the western United States, epithermal vein deposits dating from late Oligocene to Miocene are abundant. These veins occur in variety of structures such as normal faults, listric faults, tension fractures, strike-slip faults and regional detachment zones. Most of the epithermal veins are parallel to basin and range structures with stratigraphic offsets of more than 200 to 300 m (656 to 984 ft). These epithermal deposits are important because of their economic value and regional tectonic significance.

A district by district study of the structural control of vein deposits in the Western United States reveals that they occur in faults related in trend, type, and age to non-mineralized structures of the region (Dreier, 1984). This observation suggests that the regional tectonism rather than local deformation determines the vein patterns. In southwestern New Mexico, including the Hermosa mining district, high-angle normal and oblique-slip faults are later filled by epithermal quartz-calcite-sulfide mineralization. K-Ar radiometric dates (Bauman, 1984) from nearby vein deposits in the Chloride district range from 26 to 29 m.y. The

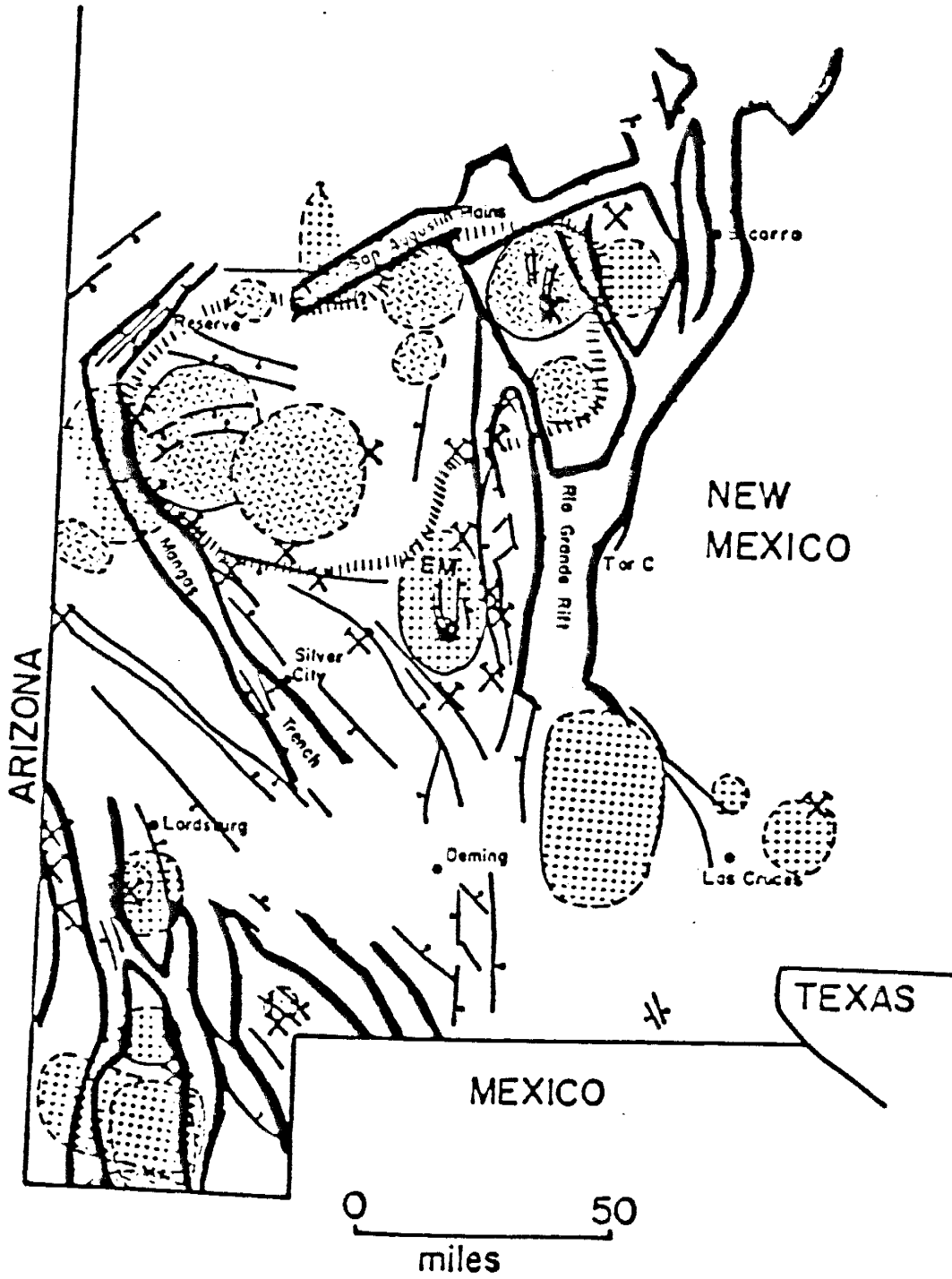
general north-south to northwest-southeast fault trends and the timing of the faulting and related veins are consistent with the timing of the Rio Grande rift opening, about 29 m.y. ago (Chapin and Seager, 1975).

In southwestern New Mexico, Elston et al., (1976) attribute most epithermal deposits to cauldron formation in the Mogollon-Datil volcanic field during Oligocene to Miocene time (Fig.8). Among Calc-alkalic volcanic centers in this volcanic field, the Emory Cauldron is the largest and is also associated with the a number of mineral deposits (Fig.7). However, principal veins at Mogollon, which account for majority of production, trend north and west-northwest and are associated with normal faults of regional extent. Therefore, evidence for the association of any ore deposits with the Emory Cauldron is not particularly convincing.

Shepard (1984) asserts that the collapse of the Emory Cauldron about 35 m.y. ago developed a ring fracture zone that extends through the Hermosa Mining District. He suggests that Hermosa, Bull Frog, and Circle Seven faults are part of a ring fracture zone because they dip to the west and are downthrown towards the interior of the cauldron. However, these structures extend well beyond the zone of influence of the Emory Cauldron; in addition the timing of mineralization in the Hermosa district and other districts away from the Emory cauldron, in southwestern New Mexico, suggests that both mineralized and unmineralized structures in the region have formed in response to larger regional tectonic deformation.

Figure 7.

Tectonic sketch map of southwestern New Mexico. The map shows caldera occurrences, Rio Grande rift, and Basin and Range province in this region. EM=Emory Cauldron (from Elston et al., 1976).



Such a tectonic deformation and its timing is consistent with the relaxation of the compressive stresses and the scope of underthrusting at the western plate boundary.

In the Hermosa mining district, younger (late Miocene to present) structures have been dominant in the district and whatever structural influence could be attributed to the Emory Cauldron has been obliterated by later overprinting. Many of these younger structures are non-mineralized normal and oblique-slip faults with north-south to north-northeast and northwest-southeast trends. The Eastern Boundary fault is apparently the major structure related to this young phase of deformation.

The Pelican and Palomas Chief faults are closely associated with mineralizing events in the Palomas Camp. These two faults were active channelways for hydrothermal fluids. Later movements along these two faults downdropped the Paleozoic rocks on either side of a mineralized horst and the deposits might never have been discovered had this block not retained its elevation (Shepard, 1984).

In the Palomas Camp and Antelope-Ocean Wave mines, displacement along structural zones in Ordovician and Silurian formations occurred before the main stage of mineralization. The trends of these smaller faults and their dislocation directions correspond with those of major regional faults. The deformed zones consist of closely spaced, sub-parallel, small displacement faults and their related small joints and fractures. At Palomas Camp, movement occurred mainly beneath

incompetent layers of Devonian dolomitic siltstone and Percha Shale. In the Antelope-Ocean Wave structural zone, mid-Tertiary Rubio Peak Formation is displaced by smaller faults and fractures. Propylitic alteration along these faults in the Rubio Peak Formation is common.

In conclusion, based on the regional nature of the major faults in the the study area, emplacement of rhyolite dikes, plugs, and domes in the region, structural and ore deposition similarities with other ore deposits in the western United States and the age of ore mineralization, ore deposition in the Hermosa mining district is mainly controlled by structures resulting from initial stages of Rio Grande rift opening, about 29 m.y. ago; formation of the Emory Cauldron dose not appear to be a major influence.

ORE DEPOSITS OF THE HERMOSA MINING DISTRICT

GENERAL CHARACTERISTICS OF CARBONATE HOSTED VEIN AND DISSEMINATED DEPOSITS

Carbonate-hosted vein and disseminated sulfide (base and precious metals) deposits occur throughout the western United States and northern Mexico. Most of these deposits in the Western United States are concentrated within the Basin and Range province. Many of the sediment-hosted precious metal deposits in Nevada are aligned along well-defined, northwest-striking regional trends that are characterized by an alignment of igneous rocks and magnetic anomalies along structural trends (Percival et al, 1987). These deposits are commonly irregular in shape and, in the case of massive sulfides, are elongate in form. Most of these deposits are strata-bound but rarely stratiform. Carbonate host rocks are not metamorphosed or metamorphism is not recognized. For the most part, the ores are complex and represent an assemblage of base and precious metal, sulfide and sulfosalt minerals in gangue minerals of quartz, calcite, fluorite, and pyrite. The ores have been deposited at temperatures ranging from about 200 to 400 C and at depths of 500 to 3000 m (1640-9843 ft).

The host rocks are silty dolomite and limestone, siltstone, sandstone, conglomerate, argillite, and interbedded chert and shale (Percival et al, 1987). Carbonate host rocks are the predominant host lithology, but any lithology may serve as host if the permeability is favorable for the introduction of

hydrothermal solutions. Carbonate host compositions are not consistent for these deposits as a whole. Both limestones and dolomites may be hosts at scales ranging from mines to districts to regions (Titley and Megaw, 1985). At mine or district scale, there tend to be one or two lithologies that are preferred hosts. For example, in the Hermosa district the host lithology in the Palomas Camp and Antelope-Ocean Wave mines is dolomite but in the Wolford and Flagstaff-American Flag mines the host lithology is limestone. McKinstry (1948) suggests that the occurrence of ore in a particular sedimentary bed is not a habit that precludes the occurrence of ore in another. Any particular depositional environment, such as marine or platform is not necessarily a preferred for ore deposition, although in many of the Great Basin deposits in Nevada the shelf environment is preferred.

Carbonate-hosted ores are associated with intermediate to felsic intrusions in the form of dikes, sills, plugs, and domes, but in many districts the genetic relationship of intrusion to ore mineralization is not clear. The ages of these deposits are often have been determined from associated intrusives, ranging from Cretaceous to mid-Tertiary. The Getchell mine in northern Nevada has been dated by radiometric techniques as Cretaceous (Bagby and Berger, 1985).

High-angle (normal) to locally low-angle and/or strike-slip faults are important structures for concentration of ore where fractured and brecciated zones allow hydrothermal fluids to penetrate favorable host rocks. In the case of massive sulfide

deposits, confinement of to carbonate host is the most fundamental control on ore deposition; basement structure may also be the ultimate control for localizing deeper intrusions and guiding or channeling hydrothermal solutions. Properties (temperature, salinity, metal content...etc) of ore solutions, the shape and distribution of solution channels, permeability contrast within sections (shale, volcanic rock, and carbonates), and properties of a carbonate section (presence of organic materials) have important control on ore deposition in this type of deposits (Titley and Megaw, 1985).

Hydrothermal alteration in this type of deposit includes decalcification, silicification, argillization, and calcite and quartz veining (Percival, 1987). Jasperoid formation as a form of silica replacement of carbonate rocks is an important part of the mineralization process. However, not all jasperoids are associated with ore mineralization. Argillic alteration is associated with variable amounts of hydrous silicate minerals such as chlorite, talc, and various clay minerals. In the Hermosa district at Palomas Camp, talc is the predominant alteration mineral. Commonly, altered zones and ore occurrences close to the main hydrothermal conduits are silicified while away from these faults, alteration occurs as decalcification, hydrous mineral formation and calcite veining. Most of these deposits are oxidized to some extent. Oxidized ores are usually altered to oxides and sulfates, and may be acid leached with residual enrichment by silver, gold, lead, and zinc.

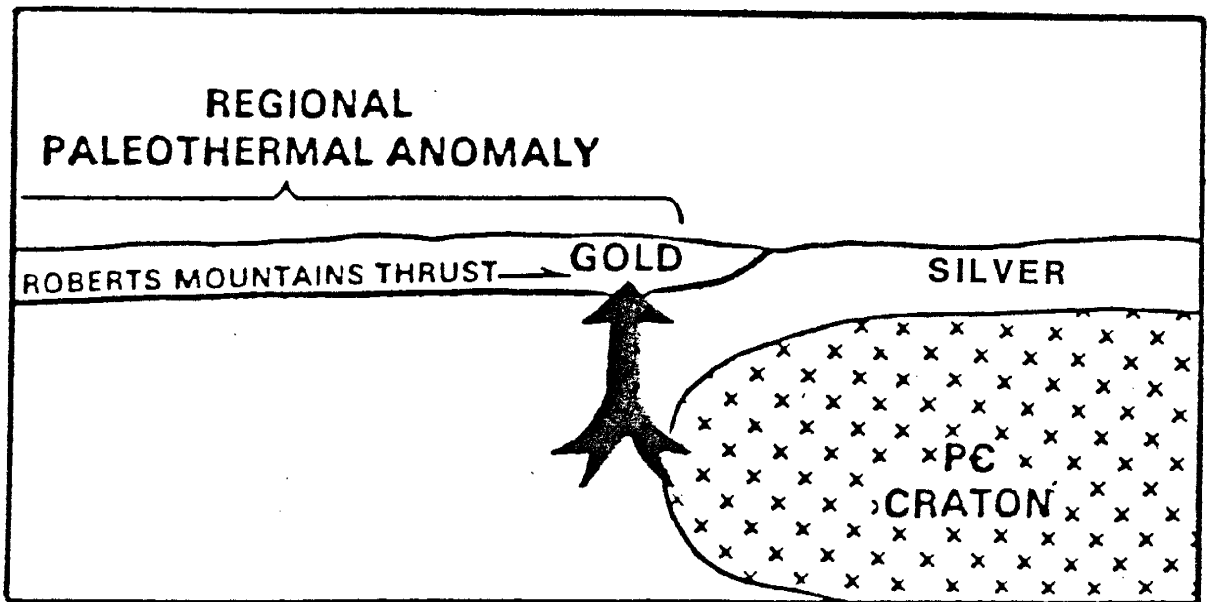
Silicified carbonates generally have ore restricted to faulted and fractured zones (quartz veinlets). Away from the shattered zones, pod-like and disseminated ores are present. In the Hermosa mining district veins are more abundant and their relationship to precious metal occurrences is clear. The dominant mineralogy includes pyrite, cinnabar, stibnite, arsenopyrite, fluorite, barite, calcite, silver minerals, gold, and various thallium and arsenic sulfides and sulfosalts. Gold is usually associated with iron sulfides.

Stable isotope data from the Cortez, Carlin, and Mercur mines suggests the importance of meteoric waters in the formation of these deposits; sediments were the source of sulfur for the formation of sulfide minerals.

A genetic model was proposed by Cunningham (1988) for the origin of precious metal deposits hosted by sedimentary rocks. His model suggests that this type of deposit formed near the top of hydrothermal systems located at the upwelling limbs of convection cells. Some of these cells are clearly associated with igneous centers whereas some are not, and there may be a continuum between them with shallow stocks localizing gold deposits related to volcanic rocks and deeper stocks underlying sedimentary-rock-hosted deposits. In his model, Cunningham (1988) relates most of the sedimentary-rock-hosted gold deposits in Nevada to the western margin of the buried Precambrian granitic craton. He believes the Precambrian granitic craton has a profound influence on geologic events throughout the Phanerozoic in Nevada. Figure 8 shows the

Figure 8.

Cross section illustrating the spatial relationship between the regional paleothermal anomaly, locations of the gold and silver deposits and the buried western margin of the Precambrian craton. (From Cunningham, 1988)



spatial relationships of sedimentary-rock-hosted gold deposits in Nevada. Cunningham explains that: "The spatial coincidence of the eastern edge of the regional paleothermal anomaly with the western margin of the continental crust and many of the major disseminated gold deposits suggests that deep crustal rifting along a reactivated zone of weakness at the old cratonic boundary may have supplied the heat that localized large convection systems during the southward sweep of igneous activity between 34 and 20 Ma or the incipient of Basin and Range faulting 18-14 Ma. Increase in the geothermal gradient could also develop hydrothermal circulation cells in permeable rocks leading to the formation of disseminated gold deposits without any requirements for igneous activity (Romberger, 1986)."

Tectonostratigraphic terrain studies by Albers (1983) indicate that base metal deposits in the United States hosted by high-temperature carbonates are confined to terrains underlain by Precambrian crust. Studies by Campa and Coney (1983) showed a significant restriction of silver-base metal deposits to terrains floored by Paleozoic or older age (Fig.8). Considering all of the geological, geochemical, and tectonic setting similarities and geographic position, it is appropriate to include the Hermosa deposits in the group of deposits described by Albers (1983) and Campa and Coney (1983).

A review of sedimentary-hosted precious-base metal deposits in the western United States and Mexico shows that most of

these deposits occur in carbonate rocks, in particular in dolomitic limestones and dolomites, with similar structural controls for each geological period. But mineralogy and the amounts of gold, silver, and base metals differ in different terrains. The idea of high gold occurrences in terrains at the margin of the Precambrian craton and high silver-base metal occurrences in terrains floored by the Precambrian craton explains this continental metal zoning in carbonate-hosted metal deposits. Low gold and high silver and base metal mineralization in the Hermosa mining district and other similar districts in the region are explained with this model. Considering the similarities in lithology of the host rocks, igneous association, structural control, mineralogy, temperature of mineralization, fluid composition, and isotopic composition of most of the epithermal deposits in the western United States and Mexico, this model explains the differences between gold-rich and silver-base metal-rich deposits in the region. It is the opinion of this investigator that, besides the local variations of geological and geochemical characteristics, the type of underlying Precambrian rocks in southwestern New Mexico may have influenced the variation of silver and base metal grades in different locations in the region.

INTRODUCTION TO ORE DEPOSITS IN THE HERMOSA DISTRICT

In comparison to other ore deposits in New Mexico and the southwestern United States, ore deposits in the Hermosa mining district were small in size and tonnage (ten tons to several hundred tons). However, in many cases, these deposits were high-grade ore pockets in faults and fractures. The Palomas Camp, Antelope-Ocean Wave mines, Flagstaff-American Flag mines and Silver-Queen prospects (Plate II) were the major producers in the mining district. Numerous other showings occur throughout the district. There is a close relationship between ore occurrences and intense structural deformation and this remains to be exploited to the south. In the Palomas Camp and Antelope-Ocean Wave mines, Ordovician and Silurian rocks are the ore hosts. In the Flagstaff-American Flag mines, the Upper Mississippian Lake Valley limestone is the host rock, and in the Wolford and Protector mines, ore occurs in Madera limestone of Pennsylvanian age.

The Palomas Camp area is located in the east-central part of the study area in the South Fork of Palomas Canyon. Many mines and prospects are on both (north and south) sides of Palomas Creek. Most of the production from this area came from mines on the north side of the canyon.

North to north-northwest trending structures were the main producers in this highly mineralized area bounded by the Palomas Chief fault on the east and the Pelican fault on the west. Intersections between these two faults with other major

breaks, such as Kendall and Mexican, created favorable structural zones for ore deposition. Numerous smaller faults and fractures completed the brecciation.

The Antelope-Ocean Wave mines are located in the east-central (NE1/4, Sec. 23, T13S, R9W) part of the study area. North to north-east trending faults dominate the structure in this area. Intersections of these faults and smaller north-to-northwest trending faults, have created an intensely fractured area amenable to the movement of hydrothermal fluids. The Rubio Peak Formation has been penetrated and altered by hydrothermal fluids suggesting that ore was deposited after the eruption of this formation about 35 m.y. ago. The Antelope mines and Slater adit are the principal workings in this area. Although numbers of shallow prospects and shafts (15-60 m deep) are present, the Slater tunnel was the only accessible underground working in this group and it was studied and sampled in detail. The tunnel is driven in Fusselman dolomite and most of the mineralization occurred in a silicified-brecciated zone. A new shaft was sunk in 1981-1982 to explore an ore body which was discovered by diamond drilling about 360 m (1181 ft) northeast of the Slater workings. In this location, fractures contained ore, with grades averaging 25 to 30 oz Ag/ton.

The Flagstaff-American Flag mines are located about 1.2 km (0.75 mi) southwest of the Hermosa town site (Sec. 25, T13S, R9W). All of the production (about 120,000 ounces of silver) came from a small prospect (12 m shaft) in silicified and

brecciated Lake Valley limestone (Jones, 1922; Harley, 1934). Larger disseminated ore bodies exist to the north and east of the old workings and these may contain substantial amounts of low-grade ore. In this area dolomites below the Lake Valley Limestone have not been explored. Both Ordovician and Silurian dolomites may contain high-grade ores similar to those in Palomas Camp. Conditions are favorable since (1) the area has undergone several periods of deformation and it has been brecciated rather intensely; and (2) mineralization and silicification in a younger formation (Lake Valley Limestone) suggest that the hydrostatic pressure of hydrothermal fluids was sufficiently high to break through the impermeable Percha Shale which is a controlling factor in Palomas Camp and Antelope-Ocean Wave mines.

The Protector mine is located between Palomas Camp and the Antelope-Ocean Wave mines. Mineralization in the Protector mine occurs in Madera Limestone as replacements and small veins. Two north-northeast trending drifts have been mined out. Mineralization is associated with calcite, talc and some quartz. Silicification of the brecciated host increases upward. On the surface above these workings jasperoid is relatively abundant with some disseminated sulfides. Weathering appears to have leached out most of the sulfide minerals in both silicified and unsilicified host rocks. Strong hematite staining of the host rocks, in particular in the upper level drift, often accompanies such leaching and oxidation. The possibility of an enriched ore zone at a lower

level of this mine is good. Dolomitic rocks below the fractured and mineralized Madera Limestone at this location could be hosts for high-grade ore similar to that found in Palomas Camp and Antelope-Ocean Wave mines. In addition, the Protector mine is closer to the Bull Frog fault, the main conduit for hydrothermal fluids in the district. Fluid inclusion analyses indicate high temperature (290-320 C) hydrothermal fluids were active here.

The Wolford mines are located in the north-central part of the study area (S1/2, Sec. 12, T13S, R9W). In these mines, the association of ore mineralization with the Bull Frog fault and related fractures and with the rhyolite intrusion about 300 m (984 ft) south of the mines is clear (Plate 1). The Madera limestone, with interbedded sandstone, is the host for ore occurrences. Two stages of hydrothermal activity are recognized, and mineralization is associated with the first stage of alteration. Quartz, calcite, talc, and siderite are the common gangue minerals. Chalcopyrite is more abundant here than in other mines in the district. The second stage of the alteration is associated with little or no ore mineralization. Weathering has leached out most of the sulfide in the silicified host. Supergene Supergene enriched zones at lower levels is very possible in this area. As is the case in the Protector and Flagstaff-American Flag mines, dolomites of older formations have not been explored in this locality. The combination of favorable structures, favorable host, and high temperature fluids make the Wolford mines area one of the most

interesting exploration targets in the mining district.

The Big Tree workings which include a shaft and several adits are located in the southern part of the study area in NE1/4, Sec. 36 T13S, R9W, near the Eastern Boundary fault. The host rock is brecciated Fusselman dolomite. Large amounts of talc are associated with mineralization and silicification. Mineralization follows a well defined but small north-to-northeast trending fault and fracture zone. Very little Fusselman Dolomite is exposed because it has been cut off to the east by the Eastern Boundary fault, covered to the north by younger Paleozoic rocks, and covered to south and west by Tertiary volcanic rocks. About 1 km (0.6 mi) southwest of the Big Tree area (S1/2 Sec. 36, T13S, R9W) a silicified breccia zone dolomite is exposed. A shaft and few shallow pits indicate limited mining activities. Most of these prospect pits are in well exposed silicified outcrops. The mineralization is associated with silicification and talc in the Montoya Group and Fusselman dolomites. Silicified zones are strongly weathered and sulfides in these zones are oxidized. Occasional grains of sulfides are seen in the jasperoid outcrops.

Farther south, at the very end of the mapped area (1/2E, Sec. 1, T14S, R9W) Paleozoic rocks from the Montoya Group to Kelly Limestone are exposed. These rocks are badly fractured by north to northeast-trending, north-northwest trending and transverse east-west trending faults. Several scattered prospects in silicified dolomites of the Montoya Group are

called the Silver- Queen Group mines. Except for small prospects mentioned, no serious exploration has been carried out in this intensely fractured, silicified, and uplifted block. The few prospects show mineralization fissure veins, mainly in Silurian and Ordovician dolomites. In some cases erosion has removed all favorable dolomites, and Cable Canyon and El Paso rocks are exposed. In addition to quartz, calcite, and talc as gangue minerals, the ore mineralization in this area is also associated with barite which may indicate a different type of fluid or a different stage of mineralization. Structure, rock type, brecciation, and alteration of the rocks, including large areas of silicification in this locality, make this unexplored part of the mining district a very desirable target for further ore exploration.

ORE TYPE, SHAPE, AND CHARACTER

In the Hermosa mining district form, size, and mineralogy of the ore deposits reflect the complex structure, physicochemical condition of mineralization, and fluid flow pattern of the district. The ores of the district occur as thin shoots, stringers, pockets, pod-like masses, and disseminated sulfide minerals along steep to near-vertical faults and fractures with small displacements associated with major regional faults, in particular with the Bull Frog fault. Some mineralization occurs at the intersection of major faults and bedding planes and slips. In most cases, the replacement ores occur along bedding planes of Fusselman Dolomite which underlies the non-reactive and impermeable Percha Shale. Shepard (1984) noted that small concentrations of sulfides occurring in what early miners referred to as "sags" at the Fusselman-Onate contact. In the mining district, ore deposition is confined to three main stratigraphic intervals: (1) the Upper Ordovician and Silurian units (Upham, Aleman, Cutter and Fusselman Dolomites); (2) the Lake Valley and Kelly Limestones; and (3) a massive limestone bed in the Madera Formation (Shepard, 1984). The largest part of mineralization occurs in Ordovician and Silurian dolomites. The favorable horizon for mineralization in the Palomas Camp and Antelope-Ocean Wave mines is about 50 m (160 ft) of Ordovician and Silurian dolomites below the Devonian Percha Shale. Mineralization in this horizon extends for hundreds of meters

(200-300 m in Palomas Camp) laterally. It is clear that the vertical extent of mineralization, in addition to the physicochemical conditions, is mainly controlled by faults and associated brecciation. Lateral extension of mineralization is mainly controlled by bedding planes between the Percha Shale and Fusselman Dolomite. Early miners concentrated their mining activities on this favorable horizon in Palomas Camp and Antelope-Ocean Wave areas.

One of the main characteristics of these deposits is that the ore bodies are small in size; a few hundred tons of high-grade ore is often accompanied by 2 to 10 times as much low-grade ore (Jicha, 1954b).

Jicha (1954b) noted many high-grade ore bodies enclosed in talc, commonly mixed with calcite. The thickness of this "skin" of talc ordinarily ranges from 4 mm to 8 cm (0.16-3.2 in), but locally this thickness may reach 0.75 m (2.4 ft). Disseminated ores consist of sulfides scattered through large masses of talc and partially altered dolomite. The amount of talc is much higher in the Palomas Camp mines than in other deposits in the district. Commonly, a large amount of talc is a good indicator of nearby ore mineralization. With few exceptions talc is present where there is high-grade ore mineralization. Talc skins or envelopes stretch out along fault or fracture zones with very thin stringers of ore in them. Talc is present only in faults and fractures in dolomite. Mineralization is also associated with quartz and calcite. In the Flagstaff-American Flag mines, the ore is

accompanied by quartz and calcite. In the Wolford mines, most of the ores occur in quartz veins or in highly silicified limestone. In the Lewandowski (H-15) shaft (Hickland Canyon), galena and sphalerite replace calcite which indicates that calcite concentrated sulfide minerals in this location. In the Day mine (Palomas Camp), high-grade ores are associated with calcite and/or talc. In many places where ore and talc are present calcite is mixed with talc and also fills the openings along many of the larger pre-mineralization faults. There are locations where calcite and ore occur together and no talc is present. Jicha (1954b) noted that, where calcite occurs along bedding-plane slips, it commonly forms the locus of deposition for sulfides. Many of the high-grade ores occur as pod-like forms or "pillows" up to 1 m (3.3 ft) long and 0.3 m (1 ft) wide in the Antelope-Ocean Wave mines and 0.6 m (2 ft) long and 0.25 m (10 in) wide in the Palomas Camp area. In the Day mine, large amounts of disseminated ore were encountered. Ore petrography and assays of this disseminated ore show relatively high amounts of copper and silver (3-10 oz Ag/ton) content. To date no disseminated ore has been mined. The disseminated ores have the same mineralogy as fissure vein ores. Throughout the district, the high-grade ores consist mainly of galena, sphalerite, chalcopryrite, and acanthite. Relatively large amounts of accessory minerals, such as tetrahedrite, pyrargyrite, polybasite, covellite, digenite, and native silver, are present. Galena, sphalerite, chalcopurite, and early pyrite are commonly coarse-grained (up

to 25 mm). The silver bearing minerals, covellite and digenite are fine-grained. Gold has not been seen in ore petrographic analysis but it has been detected in assays. Gold grains are probably very fine (less than one micron) and associated with chalcopyrite, galena, or pyrite.

Talc, calcite, and quartz are the main gangue minerals. Smaller amounts of barite and clay minerals are present in some of the mineralized areas. Talc is the result of interaction between hydrothermal fluids and wall rocks and fault gouge in dolomite with chert nodules. Commonly, small (1-4 mm) crystals of calcite are associated with such talc formation. In the Silver-Queen prospects the main gangue mineral is barite. In the Flagstaff-American Flag, Protector, and Wolford mines the ores are associated with quartz or silicified hosts. The gangue mineral distribution (in particular quartz) is controlled by structures in the district. Bull Frog fault trends north-south through the center of the mining district. Mines on or close to this fault commonly have greater amounts of silicification and little or no talc formation. Temperature of hydrothermal fluids decreases away from this fault. Quartz is deposited in higher temperature zones next to the fault and talc and calcite were deposited farther away from it in a cooler environment. Another possible explanation for this kind of gangue mineral distribution is that gangue minerals formed at different stages of mineralization or were formed by different hydrothermal fluids.

The hypogene ores of the mining district have been subject

to sporadic but extensive supergene alteration and oxidation. Shepard (1984) noted that the majority of the fault zones are tight and talc has tended to seal out meteoric waters. However, in areas where later faulting and solution have exposed primary ores to meteoric waters, extensive oxidation of ore minerals has been observed. Intense oxidation both surface and underground is present in the Wolford and Protector mines along the Bull Frog fault, and in the Day mine along the Pelican fault. These faults appear to have been reactivated after ore mineralization and meteoric waters have penetrated the mineralized zones. Offset ore shoots indicate tectonic activity after ore mineralization. Cellular box works of residual silica indicate dissolution of sulfide minerals.

MINERALOGY

Mineralogy of the ore deposits of the Hermosa mining district is rather simple and includes both primary and secondary minerals. The main ore minerals are galena, sphalerite, and chalcopyrite. Lesser amounts of acanthite (argentite?), tetrahedrite, pyrargyrite, polybasite, miargyrite, and stephinite are present. Cerargyrite, and covellite occur as minor replacement species. Shepard (1984) believes that these secondary minerals may have been responsible for some of the rich ores discovered in the mining district. Jicha (1954b) identified thirty-eight mineral species of both primary and secondary origin. Talc, calcite, quartz, and barite are the gangue minerals identified in the district. A list of mineral species of the Hermosa mining district is given in Table 3.

GANGUE MINERALS

TALC

Talc is the most abundant gangue mineral in the district. The amount of talc varies from mine to mine but it is present in all mineralized dolomite. Ores usually occur as small pockets with talc skin or as disseminated fine-grained minerals throughout talc fissure veins. Talc occurs before, during, and after ore mineralization in yellowish-white,

Table 3. Mineral occurrences in the Hermosa mining district
(from Jicha, 1954b)

Mineral	Chemical formula	Mineral	Chemical formula
Anglesite	Pb CO ₃	Hematite	Fe ₂ O ₃
Acanthite	Ag ₂ S	Lepidocrocite	Fe(OH)
barite	BaSO ₄	Limonite	Hydrated Fe oxides
Bornite	Cu ₅ FeS ₄	Malachite	Cu ₂ CO ₃ (OH) ₂
Brochantite ?	Cu ₄ SO ₄ (OH) ₄	Manganite	MnO(OH) ₂
Bromyrite	AgBr	Marcasite	FeS ₂
Calcite	CaCO ₃	Miargyrite	Ag ₂ Sb ₂ S ₄
Cerargyrite	AgCl	Mimetite	Pb ₅ (As ₄ , PO ₄) ₃ Cl
Cerussite	PbCO ₃	Polybasite	Ag ₁₆ Sb ₂ S ₁₁
Chalcocite	Cu ₂ S	pyrargyrite	Ag ₃ SbS ₃
Chrysocolla	CuSiO ₃ .2H ₂ O	Pyrite	FeS ₂
Chalcopyrite	CuFeS ₂	Pyromorhite	Pb ₅ (PO ₄ , AsO ₄) ₃ Cl
Covellite	CuS	Quartz	SiO ₂
Cuprite	Cu ₂ O	Silver	Ag
Embolite	Ag(Cl, Br)	Smithsonite	ZnCO ₃
Galena	Pbs	Sphalerite	ZnS
Gold	Au	Talc	Mg ₃ (Si ₂ O ₅) ₂ (OH) ₂
Goethite	HFeO ₂	Tetrahedrite	Cu ₁₂ Sb ₄ S ₁₃
Gypsum	CaSO ₄ .2H ₂ O	Vanadinite	Pb ₅ (VO ₄) ₃ Cl

light-green, dark-green and black.

CALCITE

Calcite occurs in three forms and three stages of mineralization: (1) Fine to medium, rhombohedral crystals of pre-ore mineralization. This type is white to colorless and occurs in cavities and veins within dolomite and limestone hosts. (2) Large to medium, milky white, rhombohedral crystals associated with ore mineralization stages. Calcite of this stage is associated with sulfide minerals such as galena, sphalerite, and chalcopyrite (Fig.9). In many localities this calcite is the byproduct of dolomite alteration. Large milky crystals of calcite associated with mineralization without talc are observed in the H-15 shaft in Hickland Canyon (Fig.9) and Flagstaff-American Flag mines. This type of calcite is also found in barren fault and fracture planes. In the Antelope-Ocean Wave and the Flagstaff-American Flag mines some of the calcite of this stage is completely or partially replaced by silica. Disseminated chalcopyrite sphalerite, and galena are common in calcite. And (3) late stage, coarse-crystalline cloudy to glassy calcite crystals have a complex rhombohedral/scalenohedral form. These crystals occur with no ore or talc and fill fractures and openings. Their paragenetic position and low temperature of formation indicate that they are late stage crystals.

Figure 9.

Milky calcite associated with ore mineralization. The calcite localizes sulfide minerals such as sphalerite, chalcopyrite, argentiferous galena, and acanthite. The large ore and gangue mineral of this sample (H-15), suggest they have grown in open spaces.

QUARTZ

Quartz occurs before and during the ore mineralization period, as vuggy crystalline aggregates and large open space filling crystals. Quartz occurrences in the Antelope-Ocean Wave mines are micro and crypto-crystalline replacement silica. In the siliceous ore zone of these mines, the host rock has been completely replaced by silica. In the Wolford and the Flagstaff-American Flag mines most of the ores are associated with large euhedral to subhedral quartz crystals in open spaces. Sulfide minerals commonly coat vuggy early quartz crystals and are disseminated within quartz crystals which formed during ore deposition. Post-ore quartz crystallization occurs in the Antelope-Ocean Wave and the Flagstaff-American Flag mines. In both areas, coarse quartz crystals are associated with coarse calcite crystals. Quartz occurs in cloudy, milky white, and clear crystals in mineralized zones. In the Flagstaff-American Flag mines some of the quartz crystals are partially or completely replaced by calcite.

BARITE

Barite occurs as yellowish, translucent, tabular crystals with oxidized ores in the Day mine and Silver-Queen prospects. Paragenetic and fluid inclusion analysis indicate that barite mineralization took place late. Three types of barite have

been observed in the district: (1) Tabular to blade crystals and crystalline masses, (2) Euhedral tabular crystals of golden color, (3) A fine-grained massive type. The first type is the most abundant and the second and third types are locally abundant in the district.

SULFIDE MINERALS

PYRITE

Pyrite is an ubiquitous but not abundant mineral in the district and it occurs as euhedral to subhedral fine-grained (0.5-2 mm) crystals. It is syngenetic in the sedimentary rocks, and occurs as epigenetic crystals during the early period of mineralization. In most cases pyrite occurrences are as disseminated grains, but in the Slater working, pyrite occurs in mixed layers with silver minerals and disseminated throughout quartz and calcite veins (Fig.10). Throughout the district both types of pyrite have been replaced by galena, sphalerite, and chalcopyrite (Fig.11) indicating it is one of the earliest sulfide minerals. The epigenetic pyrite is associated with other sulfides and talc. Marcasite was not seen in this study but Jicha (1954b) reports marcasite incrustation on galena.

Figure 10.

Hypogene layered and disseminated pyrite in quartz vein (slt-9).
The dark-blue and large (5-10 mm) crystals are pyrargyrite.
The sample is from Slater working of the Antelope-Ocean Wave mines.

Figure 11.

Early pyrite is replaced by sphalerite (Dy-56). Note the disseminated pyrite remnants in sphalerite. The sample is from the Day mine in Palomas Camp.

SPHALERITE

Sphalerite is one of the most abundant sulfide minerals in the district. It occurs as coarse-grained aggregates of euhedral crystals. The color ranges from light to dark amber to yellowish-green, which indicate the variation of iron and manganese content. Large crystal sizes of this mineral in many localities such as the Day and Nana mines and H-15 shaft suggest that sphalerite has formed in open spaces (Fig.9). Microscopic study of sphalerites indicate numerous chalcopyrite exsolutions (chalcopyrite disease) in this mineral (Fig.12). Yellowish-green, subhedral-to anhedral and dodecahedral grains of sphalerite intergrow with galena crystals in the H-15 shaft (Fig.9). Although sphalerite is relatively abundant in the study area, its association with high-grade ores is less than that of galena and chalcopyrite. Paragenetic studies suggest that sphalerite is slightly earlier than galena. Inclusions of galena and tetrahedrite are not uncommon in sphalerite crystals. In ore samples from the Day mine, replacement of sphalerite by galena is observed (Fig.15)¹³. Small veins of galena, chalcopyrite, acantite, and calcite are seen in sphalerite crystals throughout the district (Fig.16)¹⁴.

GALENA

Galena is the most abundant sulfide mineral in the district

Figure 12.

Chalcopyrite exsolution blebs in sphalerite (this is known as chalcopyrite disease). These blebs occur in sphalerite throughout the district.

13
Figure 14.

Ore sample from the Day (Dy-9) mine shows the replacement of sphalerite by galena. Sphalerite forms rings around the galena core.

Figure ¹⁴~~13~~.

Small veins (0.2-2 mm) of chalcopyrite and covellite in sphalerite (Dy-31). The covellite is replacing chalcopyrite. These veins also suggest the presence of tectonic activities during the ore mineralization period. The sample is from thd Day mine in Palomas Camp.

exhibiting various ratios with sphalerite. It occurs mostly as coarse-grained aggregates of euhedral crystals in open spaces. The galena cubes have been modified by exsolution of an high silver content. A sample of galena from the Slater working of the Antelope-Ocean Wave mines assayed 200 oz Ag/ton. Shepard (1984) and Jicha (1954b) noted that galena occurs in three different forms within the district: (1) cubic crystals modified by octahedrons and occasionally as dodecahedrons; (2) as very fine-grained "sugary" textured pods; and (3) as coarse, bladed or feathery crystals (Fig.9). Post-mineralization tectonic activity have fractured and deformed the galena crystals (Fig.15-A). During later hydrothermal activity, small veins of chalcopyrite and calcite have formed in the fractured galena. Throughout the district, galena has been replaced partially by chalcopyrite, acanthite, and covevellite. Cleavage faces of galena cubes are curved in high silver ores. Such curvature has been ascribed to a high silver content (Fig.15-B).

CHALCOPYRITE

Chalcopyrite is not abundant in the district, but it is present in form of coarse anhedral grains associated with other sulfide minerals. It is abundant as exsolution blebs (chalcopyrite disease) in sphalerite crystals. In a few localities, such as the Antelope-Ocean Wave and the Wolford mines, chalcopyrite occurs as disseminated fine grains and

Figure 15.

A: Galena cleavages are deformed due to the post-ore deformation.

B: Argentiferous galena. The cleavages are curved due to silver exsolution. Samples from the Antelope-Ocean Wave mines (slt-11).

hair-like veins. Oxidation of these disseminated grains in quartz veins of the Wolford mines has resulted in the formation of malachite and azurite. Chalcopyrite is common in the high-grade silver ores. In the Slater working and the Wolford mines, chalcopyrite is also associated with relatively high gold values, up to 37 ppm in the Slater working and 1-3 ppm in the Wolford mines. Paragenetically, chalcopyrite occurs after galena and replaces pyrite, sphalerite, and galena, in turn is replaced by covellite and acanthite (Fig.16). Chalcopyrite is the dominant copper mineral in the district but its amount decreases southward and eastward away from major faults. Veinlets of chalcopyrite in sphalerite, galena, quartz, and calcite have been observed in these deposits (Fig.14). Jicha (1954b) noted that some bornite is associated with chalcopyrite in samples from the Nana mine.

TETRAHEDRITE

Tetrahedrite occurs in small blebs and masses mainly associated with sphalerite. It also occurs as exsolution blebs in chalcopyrite and acanthite. It has been seen mainly in ores from the Palomas Camp, and it is not abundant. In hand specimen tetrahedrite occurs as steel-gray fine-grained compact aggregates. In reflected light, tetrahedrite is seen to form irregular masses in or near contacts with other sulfides. Its color is highly variable, possibly because of the wide range of Ag, Zn, and Fe content replacing Cu.

Figure 16.

Chalcopyrite replaces sphalerite and is being replaced by covellite. The sample is from the Antelope Ocea Wave mines (slt-20).

COVELLITE

Covellite mainly occurs as replacement rims around chalcopyrite pyrite grains and as small microscopic veinlets and blebs in acanthite. Most of the covellite in the district is an alteration product of chalcopyrite (Fig.16). Most of the covellite blebs, replacement rims, and microscopic veinlets are associated closely with chalcopyrite grains. A few microscopic veinlets of covellite have been seen in quartz and acanthite. Covellite in turn has been replaced by acanthite (Fig.19). Jicha (1954b) reports some chalcocite closely associated with covellite in ores from the Palomas Camp area.

SILVER-BEARING MINERALS

Most of the silver in the district is in argentiferous galena, but some fine-grained masses and disseminated grains of silver minerals are scattered throughout the high-grade ores. Native silver, acanthite, and polybasite (a sulfo-salt) were identified in the ores from the district. These minerals commonly replace earlier sulfides.

NATIVE SILVER

Native silver occurs as a minor mineral in ore samples studied from the district. It occurs as small and irregular grains either alone in talc or enclosed in acanthite and

Figure 17.

Medium-bluish-gray acanthite replaces blue to dark blue covellite.
B is the enlargement of the indicated portion of A

covellite. Only in high-grade ores is native silver observed. Native silver grains have a creamy white color. In polished sections this soft mineral has abundant polishing scratches, and is rather quickly tarnished.

ACANTHITE

Somewhat spongy cavity-fillings acanthite grains are most abundant in high-grade ores from the Antelope-Ocean Wave and Palomas Camp mines. They occur as small blebs, veinlets and small aggregates associated with chalcopyrite, galena, sphalerite, and tetrahedrite. The mineral is very soft and takes a poor polish in the porous aggregates. Textural evidence suggests that acanthite has embayed or replaced chalcopyrite and covellite and in turn it has been replaced by polybasite (Fig.17). Acanthite occurs in vugs in some places in association with native silver (Jicha, 1954b). Individual veinlets of acanthite also have been seen in quartz veins in the district.

Jicha (1954b) noted that acanthite is also closely associated with pyrargyrite and miargyrite. In the Slater working, a high-grade ore was sampled in Fusselman dolomite. This ore is composed of deformed galena, sphalerite with chalcopyrite disease, chalcopyrite with partial replacement by covellite, and acanthite. Assay of this ore indicates about 800 oz Ag and 37 ppm Au per ton of ore.

POLYBASITE

Polybasite occurs as gray with greenish tint, platy grains in vuggy siliceous ores. It usually replaces covellite, acanthite and tetrahedrite. Shepard (1984) noted that color in polybasite varies from yellowish-green through bluish-gray with a pronounced reddish contrast that may be due to internal reflections. This mineral is most abundant in siliceous ores of the Slater working.

PYRARGYRITE

Pyrargyrite occurs in rich siliceous ores in small aggregates in open spaces. In hand specimens, pyrargyrite crystals have dark bluish gray color and, in polished sections, are more bluish than gray. Pyrargyrite takes good polish with the hardness of H. When there is enough space, pyrargyrite crystals are as large as 7 mm (Fig.10). Pyrargyrite is closely associated with polybasite occurrences.

OTHER ACCESSORY MINERALS

Miargyrite and silver halides such as cerargyrite, embolite, and bromyrite have been reported from the district, but Jicha (1954b), Shepard (1984), and this study were unable to find any of these minerals.

Malachite and azurite are found as films, stains, and

crusts on most oxidized ores that contained copper sulfides, in particular in the Wolford and Antelope-Ocean Wave mines. Cerussite and limonite are very common products of oxidation of the ore in the district. Hematite is found in the Palomas Camp and Wolford mines as fine dark brown coatings.

PARAGENESIS

Jicha (1954b) described the paragenesis of mineralization in the Palomas Camp mines. Paragenetic study in this paper covers the entire Hermosa mining district and develops a slightly different paragenetic sequence than that of Jicha. The following paragraphs summarize the work by Jicha (1954b) with modifications resulting from this study.

Except for some acanthite and all covellite and chalcocite, the sulfide minerals are of hypogene origin. Supergene calcite and quartz are also present.

Small fractures filled with supergene ores and gangue minerals including late calcite and quartz, suggest tectonic activity during and after ore mineralization in the district. Mineralization occurred with apparent continuity, but Jicha (1954b) divided the mineral deposition in the Nana mine into several phases for convenience in reference and description. Figure 18 shows the paragenetic sequences for the whole mining district.

Figure 18.

Paragenetic sequences of ore and gangue minerals in the Hermosa mining district. The dashed lines indicate fracturing

PHASE	1	2	3	4	5	6
TALC						
CALCITE						
QUARTZ						
PYRITE						
SPHALERITE						
GALENA						
CHALCOPYRITE						
ACANTHITE						
TETRAHEDRITE						
Ag-SULFIDES						
BARITE						

ALTERATION

In the Hermosa mining district, hydrothermal alteration of host rocks occurs as : (1) talc formation associated with calcite and quartz in dolomites; (2) silicification of carbonate hosts; (3) alteration of limestones to powdery white clay-like minerals; and (4) sericitization of Tertiary volcanic rocks overlying Paleozoic strata. Shepard (1984), suggests that different types of alteration may be the manifestation of different levels within the same hydrothermal system.

TALC FORMATION

Talc with associated calcite is the most abundant product of hydrothermal alteration of the dolomitic host rocks in the district. Talc replaces dolomite and dolomitic gouge in and near faults, fractures, and bedding planes. Talc formation is more intense in thin-bedded horizons of dolomite (Shepard, 1984). It usually forms an envelope around ore bodies.

Chert nodules in altered dolomite are partially or completely altered to mixtures of talc and calcite, or talc, calcite, and chert. In partially altered dolomite with chert nodules, the chert cores are unaltered and surrounded by a mixture of talc and calcite. Such different degrees of alteration are most visible where the Aleman Formation is exposed either on surface or underground. In surface outcrops

the contrast between altered chert nodules and surrounding dolomite produces a striped appearance; local miners call this formation "Zebra Beds". Dolomites without chert nodules also are altered partially or completely to talc. Figure 19 shows the initial stage of replacement of dolomite by talc in form of what Jicha called "Liesegang-like rings". Dolomite is usually replaced from outside of the block inward. Small veins of calcite indicate post-mineralization movements and hydrothermal activities.

There is a general agreement among geologists that at relatively low temperatures the first metamorphic minerals to appear in siliceous dolomites are talc and tremolite. Reaction leading to the formation and elimination of these minerals is controlled by P CO_2 and P H_2O (Fig.20).

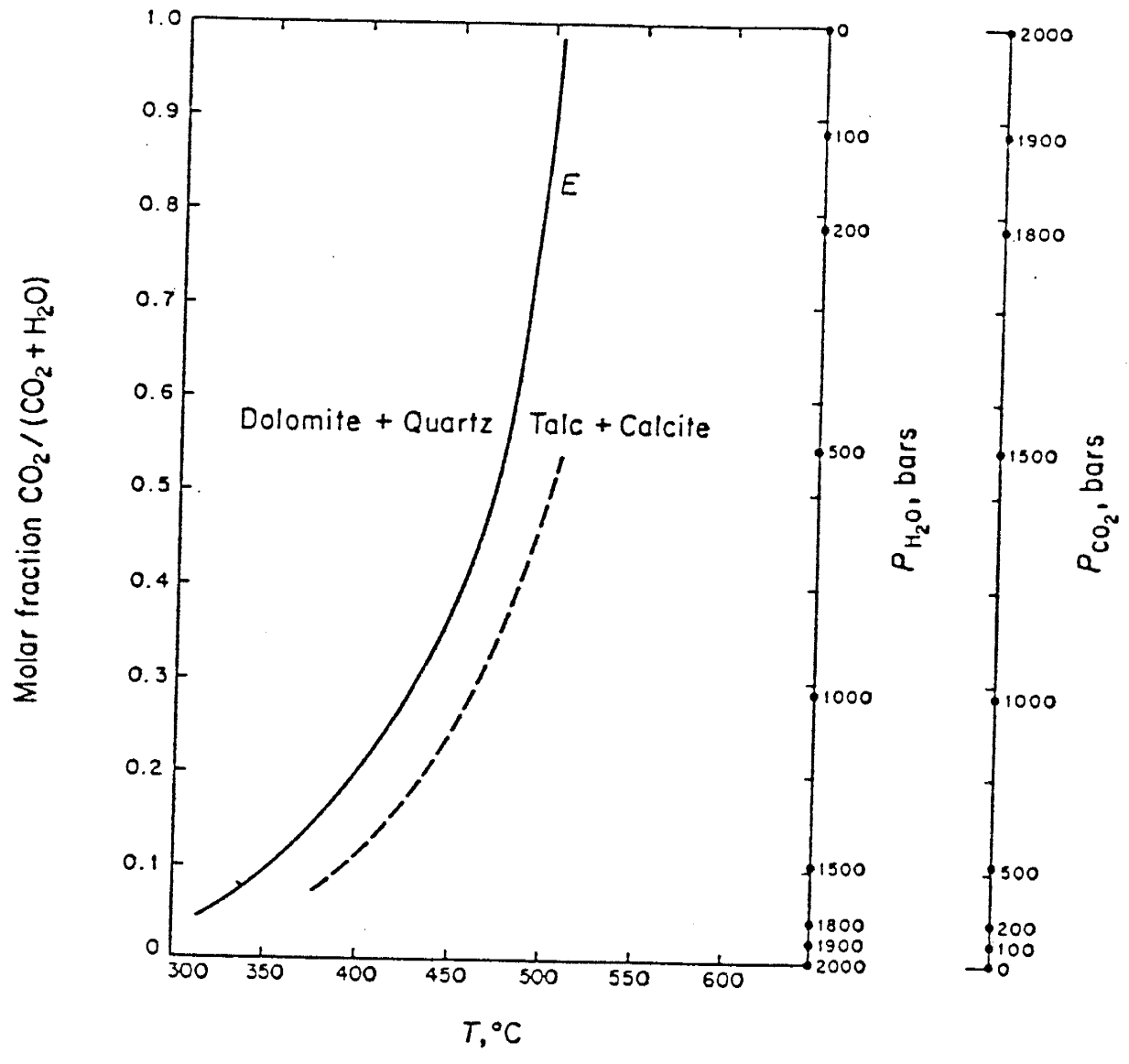
Eskola (1922), made a systematic study of metamorphic reactions occurring in carbonate rocks at some given P CO_2 in response to rising temperature. Based on field and mineralogical observations, Eskola listed the sequence of tremolite, diopside, and wollastonite as indices of increasing temperature. Bowen (1940) formulated his sequence of 13 minerals based on geological data which started with the mineral sequence of Eskola (1922). Titley (1951) included talc as the first silicate phase in a minor revision of the above sequences. In general, talc and tremolite, which are hydrous minerals, are the early products of thermal metamorphism of siliceous dolomite in the presence of water. Later, as the temperature rises, these two minerals are eliminated in favor

Figure 19.

A dolomite fragment is replaced by talc from outside inward. Calcite veins suggest post-alteration deformations and hydrothermal activity.

Figure 20.

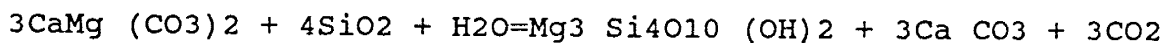
Experimentally determined curve (E) of breakdown of dolomite-quartz mixture presence of CO₂ and H₂O. The dashed curve is the same equilibrium reaction calculated from thermochemical data. (from Turner, 1968)



of anhydrous minerals such as diopside and wollastonite. Equilibria between carbonates, hydrous silicates and gases is controlled by temperature, pressure, and the respective fugacities of H₂O and CO₂ in the gas phase.

Tilley (1948) studied altered chert nodules in Cambrian age dolomites of the Strath Suarda Zone in the Broadford-Kilchrist area of Sky, Scotland. There are close similarities between altered chert nodules from Tilley's (1948) study and those of the Hermosa mining district.

Turner (1948) and Winkler (1974, 1979) have proposed the formation of talc from the reaction between dolomite and quartz in the presence of water by the following equation:



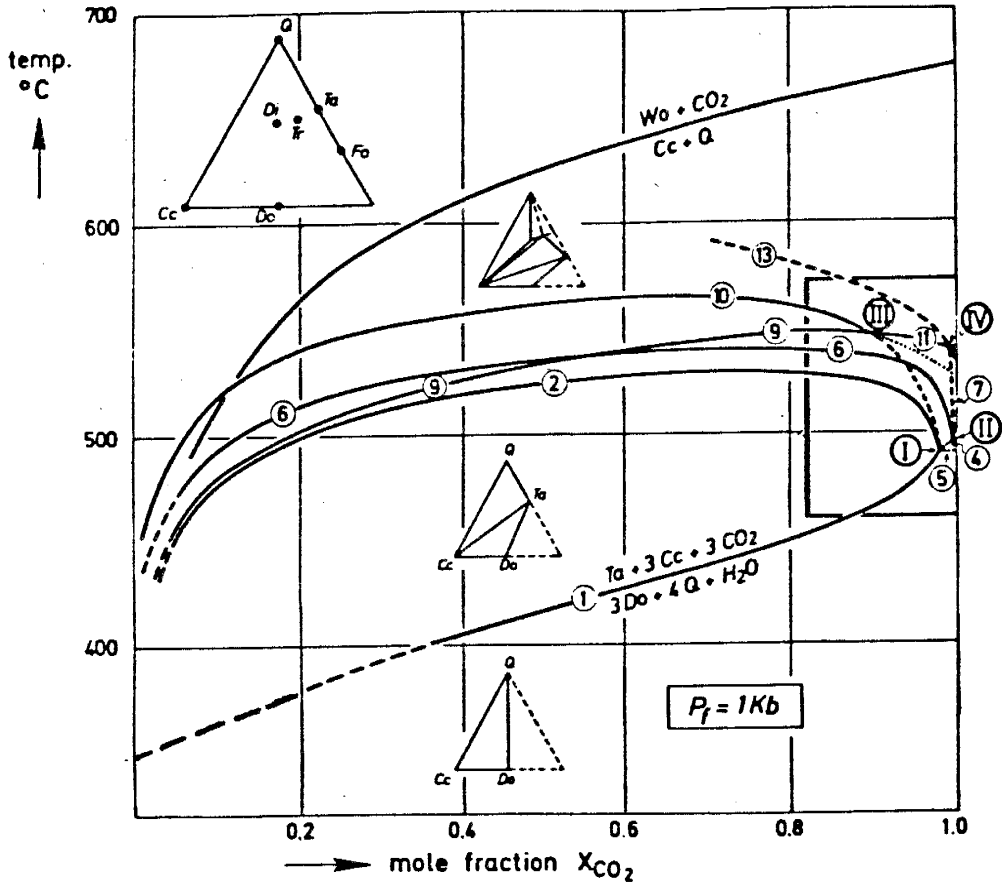
In this reaction CO₂ is released. In a hydrothermal environment pressure in the system is contributed by both CO₂ and H₂O. From the equilibrium curves of Figure 21 (from Winkler, 1974) it is clear that at 1 kb pressure reactions 1, 2, 6, 9, and 9 are relatively stable over a wide range of X CO₂. This relative stability indicates that temperature is the main equilibrium control. In the Hermosa district, no tremolite has been observed. This suggests that the hydrothermal alteration condition (temperature and X CO₂) did not reach the state of reaction 2 of Figure 21

Talc formation in the altered dolomites of the Hermosa district could be explained by reaction 1 of Figure 21. Chert

Figure 21.

Schematic isobaric T-X (CO₂) diagram for reactions during the metamorphism of carbonate rocks. Note reaction 1 for conditions of the formation of talc. (Diagram from Skippen, 1971 in Winkler, 1974)

(faint handwritten text)



nodules in dolomites become metastable at high temperatures. Release of CO₂ and hydrothermal water produce the necessary pressure for talc formation. Chert nodules in dolomites provide some of the needed silica for reaction 1, but high amounts of talc and silicification in the district suggest that the hydrothermal solutions introduced significant amounts of silica to the system (Jicha, 1954b). Fluid inclusion thermometric analysis of quartz and calcite associated with talc shows a temperature range of 240-400 C. Gas analysis of the vapor phase of fluid inclusions confirms the presence of CO₂ in the system and the pressure is higher in ores and gangue minerals associated with talc.

JASPEROID FORMATION

In many localities of the Hermosa Mining District, in particular near major faults and fractures, dolomites and limestones have been silicified or altered to jasperoid. This type of alteration occurs on a regional scale including the Chloride district to the north and the Hillsboro district to the south.

Shepard (1984) recognized most of the jasperoids of the Hermosa district. Plate 1 shows locations of jasperoid occurrences and the structural control of these occurrences. Jasperoid, commonly occurs near regional faults such as the Eastern Boundary, Hermosa, and Bull Frog faults. Some jasperoids are associated with smaller structures such as the

Pelican and Dark Canyon faults. It occurs in faults with large or small displacements, in brecciated zones, and along bedding planes of favorable horizons. Percha Shale had an important control on the silicification of underlying Fusselman and older dolomites in the district. Jasperoid occurrences in or close to the intersections of major or small faults are very noticeable in the district.

In the Antelope-Ocean Wave, Palomas Camp, and Flagstaff-American Flag mines jasperoids are directly or indirectly associated with mineralized zones. In the unexplored southern part of the district, in North Seco Canyon and Silver Queen, dolomites of the Fusselman and Montoya group are extensively silicified. Smaller jasperoid occurrences are noted between these major occurrences in the district. Large masses of jasperoid form prominent ledges and knobs. Jasperoid replacement of limestones shows different shades of light-gray to red and brownish-red. Dolomites show dark-gray to reddish-dark-gray color. In the Slater working, the jasperoid is black. Weathered outcrops of jasperoid are stained with varied amounts of iron oxides, and this colors the outcrops various shades of brown, yellow, and red.

Texturally, jasperoid occurs as massive hard and flinty bodies to well-brecciated outcrops. They are fine-grained to aphanitic in texture. Vugs are common in these rocks. Some of the chert fragments of the brecciated and silicified carbonates are preserved. In most cases, the contact between unreplaced carbonates and jasperoid is sharp. Quartz veining

in the limestones and the jasperoid of the district along the Eastern Boundary and Dark Canyon faults suggests later hydrothermal activity. In the Wolford, Antelope-Ocean Wave, Flagstaff-American Flag mines, and in the south end of the study area, scattered and disseminated sulfide mineralization is noted in jasperoid. There is no clear evidence that mineralization in the district is related to jasperoid formation. However, in many of the mining districts in the region, the ore occurrences are closely associated with jasperoid, although unmineralized jasperoid is common between mineralized zones. Paragenetic and fluid inclusion studies suggest silicification has occurred before, during, and after ore mineralization as a continuous process or as multiple mineralization and/or alteration episodes.

LIMESTONE ALTERATION

The third kind of alteration in the district involves only Lake Valley and lower Magdalena Group limestones. In this type of alteration, the limestones have been partially altered to a powdery white clay-like material that is composed of calcite and montmorillonite. This alteration forms spots in the Hermosa district but it is more extensive in the same stratigraphic horizon in Carbonate Creek, Hillsboro district, about 18 km (11 mi) south. McNeil and Evatt (1985) compared altered and unaltered limestone of the Hillsboro district by X-ray-diffraction analysis and found no mineralogical changes.

Montmorillonite has been enriched in altered rocks compared with calcite because of its resistance to leaching. Its contact with unaltered rocks is transitional.

Half way between North Seco Canyon to the south and the Flagstaff-American Flag mines in the central part of the mapped area, a small outcrop of Tertiary volcanoclastics (Sandstone of the Hermosa Area?) is highly altered. This altered rock overlies the Aleman Formation of the Montoya Group. The presence of montmorillonite, chlorite, calcite, and traces of sericite, kaolinite and biotite suggest argillic alteration of this outcrop. This alteration is limited to a small (few meters) funnel-shaped body associated with a small fracture in the underlying dolomite (Fig.22). Assay indicates that the underlying dolomite contains about 0.02 oz Au and 0.5 oz Ag per ton.

OXIDATION

Occurrences of covellite, chalcocite, native silver, malachite, azurite, limonite, anglesite, and cerussite indicate the oxidation of the primary ores in the district. Oxidation is caused by surficial exposure or penetration of meteoric waters along fractures and veins. Most of the oxidation occurred near surface. In the Wolford, Antelope-Ocean Wave, and Palomas Camp mines, oxidation is common in both dolomite and limestone hosts along faults and fractures. In the Antelope-Ocean Wave mines supergene enrichment of ores

due to oxidation is partially responsible for high gold and silver values. Secondary chalcopyrite, covellite, and tetrahedrite are common in these mines. Similar minerals are present in the Day mine except for lower gold value.

AGE OF MINERALIZATION

Field evidence in the Hermosa mining district and K-Ar dating in the Chloride mining district suggest a late Oligocene age for mineralization in the region. Mineralized structures in the region including (from north to south) Chloride, Hermosa, Hillsboro, Tierra Blanca, and Signal Peak districts are related to the Rio Grande rift opening. The rifting in south and central parts of New Mexico started about 29 m.y. ago (Chapin and Seager, 1975). Most of the unmineralized and mineralized structures with regional extent or character show trends and strikes similar to those of the Rio Grande rift. The Rio Grande rift is made up of many depressions or basins which are bounded by regional faults on their east and west sides. Winston Graben (Plate 1) is the westernmost structure of this rift in southwestern New Mexico (Harrison, 1986). Faults and fractures related to the opening stage of the Rio Grande rift cut through Paleozoic and Tertiary volcanic rocks up to the Sandstone of the Hermosa Area which is early Oligocene in age.

At the Antelope-Ocean Wave mines, the Rubio Peak Formation of late-Eocene early-Oligocene overlays the mineralized Paleozoic dolomites. Andesites and breccia flows of Rubio Peak Formation in this area are faulted and altered by hydrothermal fluids. Shepard (1984) noted some ore mineralization in this formation close to its erosional contact with Paleozoic dolomites. In the central part of the district, Sandstone of

the Hermosa Area overlays the erosional surface of mineralized Montoya Group dolomites. This mid-Oligocene volcanoclastic rock is altered by hydrothermal fluids. The alteration is limited to less than 2 m (6.5 ft) next to a small fracture in the underlying mineralized dolomite (Fig. 22).

Extensional tectonism is usually accompanied by bimodal igneous activity (Lipman et al., 1972; Christiansen and Lipman, 1972). The opening of the Rio Grande rift was accompanied by emplacement of rhyolite domes, plugs and dikes in related structures in the region. These domes, plugs, and dikes are seen in the Chlorite, Hermosa, Hillsboro, Tierra Blanca, and Signal Peak districts. Poverty Creek basaltic andesite resulted from eruptions about 28 m.y. ago as a part of extensional bimodal igneous activity.

In the Hermosa district two flow-banded rhyolite plugs and one dike were emplaced along major faults. About 6 km (4 mi) northwest of the study area, the Moccasin John rhyolite dome complex has intruded Paleozoic sediments and Tertiary volcanic rocks of early Oligocene of the Rubio Peak Formation. Rb-Sr age of the Kline Mountain intrusive of this complex has been determined by Eggleston (1987) and it is about 28 m.y. old. K-Ar age of about 28 m.y. for ore mineralization in the Chloride district is determined by Bauman (1984); it coincides with the emplacement of the Moccasin John complex and other rhyolite bodies in the region. There are strong structural control and mineralogical similarities between ore occurrences in the Hermosa district and the Stage One mineralization in

Figure 22.

Tertiary volcanoclastic sediment (the Sandstone of the Hermosa Area?) is altered by hydrothermal fluids. The underlying bed is the Aleman Formation of Montoya Group.

the Chloride district. Harrison (1986) suggests that the Moccasin John rhyolite complex has acted as the heat source for hydrothermal activity in the Chloride and Hermosa districts. Fluid inclusion analysis by this investigator (Chapter 3) indicates higher fluid temperatures around rhyolite plugs in the district. This association of higher temperature with rhyolite domes and plugs confirms Harrison's (1986) suggestion for a heat source in the region. Stacey and Hedlund (1983) studied lead-isotopic compositions of ore deposits in southwestern New Mexico, including samples from the Hermosa mining district, and concluded that ore deposits in this region were formed in mid-Tertiary time.

Based on structural control, stratigraphy, isotope age determinations of ores and rhyolite domes in the Chloride and Hermosa districts it may be concluded that ore mineralization in the Hermosa district occurred in late Oligocene time.

MINERAL ZONATION

Because of limited data for vertical variation of ore mineralization, determination of vertical mineral zoning was not possible. Lateral mineral zonation within the individual groups of mines studied is not clear or definitive but some mineralogic trends or zoning can be recognized district-wide.

Gold mineralization occurs in the vicinity and on the west side of the Bullfrog Fault. Gold occurs in the Wolford mines, Antelope-Ocean Wave mines, and in the southern part of the

district. Its value is higher in dolomite hosts. These gold-bearing locations contain 0.2-3 ppm gold except for one sample from the Slater working, which contains up to 37 ppm Au. Gold is associated with galena, sphalerite, chalcopyrite, acanthite, and pyrargyrite. In the Palomas Camp, Flagstaff-American Flag mines, and Silver-Queen prospects no gold was detected in assays. In these locations, silver values are high and little or no chalcopyrite is present. In high silver zones the amount of sphalerite decreases and argentiferous galena is abundant. Gangue minerals in the district also show zonation. Gold occurrences are associated with high silicification and less calcite and talc. Silver occurrences are associated with larger amounts of talc and calcite. In the Silver-Queen prospects barite is the dominant gangue mineral. Fluid inclusion analysis indicates a thermal zonation in the district. There is a close relationship between mineralization and thermal zonation in the district. The Bull Frog fault apparently has had a profound effect on thermal and mineral zonation in the district (Chapter 3). In general, gold, chalcopyrite, and quartz occur in the northern, southern, and western parts of the district and silver, talc, and calcite in the northeastern and central parts. The amount of gold increases northward. This northward increase of gold continues beyond the northern limit of the district. In the Chloride district, gold values are higher than in the Hermosa district.

COMPARISON OF THE HERMOSA DEPOSITS WITH OTHER Pb-Zn-Ag-Au
DEPOSITS

Field investigation, laboratory geochemical analysis, and literature review reveal that the Mississippi Valley-Type (MVT) deposits and Hermosa deposits both occur in Paleozoic carbonate rocks, but MVT deposits are larger (kms) in size. MVT deposits tend to form on the flanks or above basement highs or they occur in carbonate rocks adjacent to either sandstone or paleokarst features or faults. However, in the Hermosa district more than 80 percent of the ores occur in faults and related fractures and there are no basement highs associated with these deposits. Fluid inclusion studies (Roedder, 1972 and 1977; Norman et al, 1985) show that the mineralization temperatures in MVT deposits range from 70 to 180 C with fluid salinity higher than 25 eq. wt.% NaCl. The presence of hydrocarbons in fluid inclusions from MVT deposits and high salinity suggests that the ore-forming fluids were heated oilfield brines. In the Hermosa mining district, ore mineralization temperature ranges from 240 to 320 C and the salinity of ore-forming fluids ranges from 0 to 9 eq. wt.% NaCl. Another distinct difference between MVT and Hermosa deposits are the gangue minerals. In MVT deposits, the major gangue minerals are calcite, quartz, barite, and fluorite; but in the Hermosa deposits the main gangue mineral is talc. These geological and geochemical characteristics suggest that MVT deposits and Hermosa deposits have not formed under similar

conditions and they are not the same type of deposit.

The Irish-type base metal-silver deposits (Tynah, Silvermine, Navan, etc..) and the Hermosa deposits are both hosted by Paleozoic carbonate rocks. The Irish-type deposits typically occur in reef or back-reef facies carbonates with very diverse composition. Faulting and related fractures are the main ore controlling factors in both the Hermosa and Irish-type deposits. Morrissey et al. (1971) calculated the temperatures of ore mineralization (200-350 C) of the Irish-type deposits from stable isotope analysis. These temperatures are well within the range of those of the Hermosa deposits determined by fluid inclusion analysis. The major difference between these two groups of deposits is their genetic type. Available data indicate that Hermosa deposits are epigenetic; the Irish-type deposits are largely syngenetic to syndiagenetic. Irish-type deposits are also large (hundreds of meters) and stratiform. Texture of ore minerals, mineralogy, structure, and the depositional environment of Irish-type deposits suggest that they are sediment-hosted submarine exhalative deposits. Dolomitization of the host limestones is the only type of alteration in this type of deposit.

The Providencia Ag-Pb-Zn-Cu deposits of Zacatecas, Mexico and the Hermosa deposits have many characteristics in common. Carbonate host rocks (although Providencia deposits occur in Mesozoic rocks), tectonic setting (back-arc or inner arc), structural control (steep faults), and mineralogy (galena,

sphalerite, chalcopyrite, and acanthite) are the main similarities between these two groups of deposits. The major geological difference between them is that the Providencia deposits are in direct contact with Providencia granodiorite stock which is about 40 my old (Sawkins, 1964) while in the Hermosa district there is no direct association between ore deposits and intrusives.

Fluid inclusion studies (Sawkins, 1964) of Providencia deposits show high temperatures of mineralization (300-370 C) and high salinity (5-40 eq. wt.% NaCl) of ore-forming fluids. The high temperatures of ore deposition and related boiling condition and high salinity of the ore-forming fluids suggest a strong association of ore deposition with the large granodioritic stock in the region.

Stable isotope studies (Rye, 1966 and 1974) indicate that magmatic waters were responsible for the main stage of ore mineralization of the Providencia deposits. In the Hermosa district a relatively lower temperature of ore deposition, lower salinity of ore-forming fluids, and no contact of ore deposits with intrusives suggest that the ore-forming fluids were mainly circulating meteoric water. So, except for higher temperature, higher salinity, and magmatic source for hydrothermal fluids, there are strong similarities (structural control, mineralogy, and host rocks) between the Hermosa deposits and Providencia deposits.

The Sherman-type deposit of the Leadville district of Colorado, shows structural, lithological, mineralogical, fluid

salinity, and age of mineralization similarities with the Hermosa deposits. Three main differences are higher temperature of mineralization of the Sherman-type, close association of this type with igneous bodies, and larger (in size) deposits. Thompson, et al. (1983) and Johansing (1982) determined mineralization temperature of 310-410 C for Leadville-type and 260-347 C for Sherman-type deposits.

Gold-silver-base metal deposits in north-central Nevada occur in a wide variety of geologic environments related to stratigraphic and structural features in the region. In the case of the Carlin gold deposits, Eureka Ag-Au-Pb-Zn deposits, and Copper Canyon Cu-Au-Zn-Pb-Ag deposits, the ores are associated with Paleozoic carbonaceous carbonate rocks, and they occur as disseminates, replacements and veins. Carlin-type deposits are characterized by: young age and shallow-seated occurrence in carbonaceous carbonate rocks; ore bodies that usually are conformable with or parallel to bedding or extending out from deep steep faults; association with dikes and flows; and hydrothermal alteration.

Fluid inclusion studies (Nash, 1972, and Radtke et al., 1980) of the Carlin-type deposits indicate that mineralization temperatures of these deposits range from 175 to 275 C with widespread boiling at higher temperatures. The salinity of ore-forming fluids ranges from 1 to 4 eq. wt.% NaCl, but at boiling temperature it reaches to approximately 17 eq. wt.% NaCl. Data from fluid inclusion analysis of the Hermosa deposits show relatively higher temperatures and low to

moderate boiling condition in quartz crystals at about 290 to 345 C. Stable isotope studies (Rye, 1974; Radtke et al, 1980) suggest that meteoric waters were the main source of water for ore-forming fluids in Carlin-type deposits. From the geological and geochemical comparisons of the Carlin-type and the Hermosa deposits, it could be concluded that, except for the lack of Precambrian basement, higher gold contents of the Carlin-type, and the unique gangue mineral (talc) of the Hermosa deposits, other characteristics of these two deposits suggest they have formed under relatively similar conditions (structural control, host rocks, ore-fluid composition and temperature of mineralization).

The Chloride mining district is located about 13 km (8 mi) north of the Hermosa mining district. The Minnehaha-Great Republic, Silver Monument, U. S. Treasury, St. Cloud and Hoosier-Wall St. mines comprise this mining district. Epithermal base and precious-metal deposits in this district were formed during a mid-Tertiary thermal event related to bimodal volcanism that occurred concurrently with initial development of the Rio Grande rift in southwestern New Mexico (Harrison, 1986, 1988). The dominant structural style found in the district is high-angle normal faulting along north, northwest, north-northeast to northeast and lesser east trends (Harrison, 1988). The structure in the Chloride district is a continuation of structures in the Hermosa district (Fig.6). Major structures in both districts have the same trends and age. Early normal faulting in both districts

resulted in a series of north-northeast elongated horsts and grabens that were truncated by the north-northeast trending Winston graben. Winston Graben is the westernmost structure related to extensional movements of the Rio Grande rift of about 29 m.y. ago in this region. Epithermal deposits in this district occur as open-space, fissure-filling veins with or without disseminated replacement mineralization. Except for higher gold and copper contents, the mineralogy in the Chloride district is very similar to that of the Hermosa district. Harrison (1986, 1988) divided the Chloride mining district into northern and southern subdistricts based on differing metal content, mineralogy, Ag/Au ratios, and, to a lesser extent gangue mineralogy and alteration. Mineralogy of the northern district is dominantly fine-grained acanthite, tetrahedrite, and pyrite with lesser bornite, chalcocite, and native gold occurrences in bands, pods, and streaks.

Two stages of mineralization are present in the southern subdistrict. Mineralogy in the first stage consists of galena, sphalerite, and chalcocite with lesser amounts of polybasite, pyrargyrite, and pyrite. Mineralogy in the second stage consists of bornite, chalcocite, argentite, digenite, covellite, and bethekenite (Harrison, 1986). K-Ar age of mineralization for both stages ranges from 26.3 ± 1.1 m.y. to 28.9 ± 1.1 m.y. (Bauman, 1984).

The first stage of mineralization in the southern subdistrict is much poorer in precious metal content than the second stage. Mineralogy, mineralization style, and metal

content suggest that there are strong similarities between Stage One mineralization in the Chloride district and sulfide mineralization in the Hermosa district. Geologic data and fluid inclusion analysis from the region suggest that it is quite possible that the Stage One mineralization of the Chloride district and the mineralization in the Hermosa district represent the same hydrothermal activity associated with the emplacement of the Moccasin John flow-banded rhyolite dome located midway between the two districts (Fig.2). A main difference between the two districts is that mineralization in the Chloride district occurs in Tertiary volcanic rocks of the Rubio Peak Formation, but in the Hermosa district it occurs in Paleozoic carbonates. The main gangue minerals in the Chloride district are quartz, calcite, adularia, and sericite but, in the Hermosa district, talc is the dominant gangue mineral with lesser amounts of calcite and quartz. The differences in gangue mineralogy in the two districts reflect different interactions between hydrothermal fluids and different types of host rocks.

The ore mineralization of Carbonate Creek in the Kingston mining district, which is located about 16 km (10 mi) south of the Hermosa district, occurs as vein and replacement deposits, typically as manto type replacing host carbonates. At the intersections of faults and fractures in the district, pipe-like ore bodies are common. As in the Hermosa district, Fusselman Formation and Montoya Group are the main host rocks for ore mineralization in the Kingston district. Sanders and

Giordano (1986) attributed the main faults and fractures in the district to the development of the Emory Cauldron. The Kingston mining district is situated inside the cauldron near its eastern margin. It is quite possible that ore deposits in this district are related to the formation of the Emory Cauldron as has been stated by Elston et al., (1976). In the larger picture, considering structural controls of ore deposition in the Chloride and Hermosa districts to the north, and deposits with similar characteristics in Lake Valley, Tierra Blanca, and Signal Peak to the south of the Kingston district, it seems that the main structural controls have been structures related to the initial stage of the Rio Grande rift opening. Chapin and Seager (1975) have shown that the initial stage of the Rio Grande rift opening occurred about 29 m.y. ago. The dominant northwest to northeast trending mineralized faults and fractures; occurrences of bimodal volcanism related to extensional tectonism which includes rhyolite domes, plugs, and dikes and basaltic andesites in the region; and the age of mineralization (about 26-28 m.y.) in southwest New Mexico suggest that structural controls and thermal events, younger than those of Emory Cauldron, were responsible for ore deposition in the region.

Ore minerals present in the Kingston mining district consist of acanthite, pyrargyrite, and polybasite with some native silver, native gold, chalcocite, and small amounts of azurite and malachite. These occur in pipes and pockets with some replacement in the wallrocks. Alteration in the district

is restricted to the alteration of limestones to a powdery, soft, calcite-clay mixture (Canby and Evatt, 1985) and the silicification of carbonates. Canby and Evatt (1985) analyzed a few fluid inclusions in quartz samples from this area. Temperature of ore mineralization in this area ranges from 214 to 231 C which is about 30 to 60 C lower than that of the Hermosa district. Salinity of the ore-forming fluids is slightly lower than that of the Hermosa district. Lower temperature of mineralization and the type of alteration in the Kingston district explain the absence of talc which is the dominant gangue mineral in the Hermosa district with higher temperatures of mineralization and alteration.

Structural and stratigraphic control, host lithology, ore mineralogy, precious metal value, fluid chemistry, and tectonic setting similarities between the Hermosa deposits and the Kingston deposits suggest that these deposits were formed under the same physicochemical conditions. Minor differences in gangue minerals and gold values are due to local variations of the mineralizing conditions in the two districts.

GEOCHEMISTRY OF THE HERMOSA MINING DISTRICT

PART I

MICROTHERMOMETRIC ANALYSIS

INTRODUCTION

Aqueous fluid inclusions in minerals and rocks have been noted for centuries, but the classical paper by Sorby (1858) generated interest among geochemists in these usually small (< 40 microns) inclusions. In the last three decades, fluid inclusion studies have been applied in geologic thermometry to determine the temperature at which minerals form in igneous rocks, metamorphic rocks and ore deposits. Such studies are also done to determine the temperatures at which diagenesis, recrystallization, and alteration of sedimentary rocks occur. A review of a vast numbers of fluid inclusion studies with different purposes suggests that the ultimate purpose of fluid inclusion studies in minerals is the determination of temperature and pressure of mineralization and the composition of fluids which formed these minerals.

Fluid inclusions are small droplets of aqueous solution, carbon dioxide, oil, or other fluids trapped in minerals. These inclusions are samples of fluids that were present when the enclosing mineral grew or recrystallized, usually from these same fluids (Roedder, 1972). By analyzing these preserved fluids with various techniques, the physicochemical conditions under which the host minerals were formed can be determined.

Concerns have been expressed that inclusions may have leaked or their physicochemical conditions may have changed

irreversibly and consequently, the analytical data from fluid inclusion investigations do not necessarily represent actual physicochemical conditions of the mineralization. However, studies by Roedder and Skinner (1968) Roedder (1972, 1981, and 1984) indicate that leakage is rare and that any other physical or chemical changes, after the entrapment and cooling of the fluid inclusions, are negligible.

Fluid inclusion studies in combination with other geochemical techniques, in particular with stable isotope analyses, are used to study ore deposits. More recently, these analyses are being used seriously in mineral exploration. Studies by Roedder (1960b, 1967d, 1968c, 1971b, 1976a, and 1977b), Sawkins (1964, 1966), Kelly and Turneaure (1970), and many others, have shown that the conditions of ore mineralization can be determined, and that such data can be used to develop conceptual "models" for ore deposition.

In any meaningful fluid inclusion study, a correct distinction of the origin or type of the analyzed inclusion is crucial. Roedder (1967a, 1972, and 1981) has discussed most of the criteria for recognition of the origin of fluid inclusions. These criteria are used in this study in order to classify and analyze the fluid inclusions from the study area. According to these criteria, fluid inclusions have been classified as primary, secondary, and pseudosecondary.

Primary fluid inclusions are formed contemporaneously with the host mineral and usually are found along growth zones or within crystal irregularities. The fluids trapped in these

inclusions represent the physicochemical conditions during the formation of the host mineral. Secondary inclusions are those that formed after crystallization of the host mineral has been completed. If a crystal is fractured and a different fluid enters this fracture when the fracture heals some inclusions are trapped, these inclusions are called secondary fluid inclusions. This process is very common in all geological environments particularly in tectonically active regions such as the study area. Secondary fluid inclusions represent physicochemical conditions present some time after the deposition of the host mineral. If a crystal was fractured during growth, the fluid from which it was growing will enter this fracture and will be trapped in the crystal. Such inclusions are called pseudosecondary fluid inclusions. Pseudosecondary inclusions may represent the conditions present during the time of the host crystal growth.

Daughter minerals in fluid inclusions are solid phases which have crystallized out of the fluid after trapping and cooling.

Daughter minerals indicate saturation (or supersaturation) of the fluid with respect to the phases at their formational conditions (Roedder, 1972). The daughter minerals are mainly halite and sylvite, but chalcopyrite, pyrite, hematite, sulfates, and other daughter minerals also have been observed. Identification of these daughter minerals reveals valid information about the composition of fluids which formed the fluid inclusions and host minerals.

METHOD OF STUDY

SAMPLE COLLECTION

About 2000 samples of ore and non-ore rocks were collected from underground workings, old mine dumps, and the surface exposures of veins and silicified carbonates (jasperoids) in the Hermosa mining district. The sampled area is about 47 square km (18 square mi). Four hundred and fifty of these samples were chosen for fluid inclusion analysis. One hundred and eighty are ore minerals or directly associated with ores in the district. The remaining 270 samples are from veins with little or no ore and fractured, brecciated, and mineralized localities.

The selected samples contained quartz, calcite, sphalerite, and barite. These doubly polished samples were reduced to a thickness of 0.1 to 0.3 mm.

METHODS

Two techniques have been used to analyze fluid inclusions from the Hermosa mining district. In the first technique, which is a non-destructive method, a heating-freezing stage was used to determine the composition of the liquid phase, density of the fluid, and the formation temperature and in some cases pressure of the host minerals. The second technique, quadrupole mass spectrometry, is a destructive

method (Norman, 1977) and is discussed in detail in the gas analysis section of this chapter.

A Linkham TH-600 stage (Fig.23) made in Surrey, England, designed and described by Shepherd (1981) was used to analyze fluid inclusions. When this stage is used in conjunction with an optical microscope, it is possible to observe phase changes in fluid inclusions as small as three microns in diameter. In the non-destructive method of analysis, the phase changes during heating and freezing experiments are reversible which means the analysis can be repeated as a check on the precision of the obtained data.

The TH-600 system is a heating freezing stage for the microthermometric analysis of inclusions over the range of -180 to +600 C, with a maximum resolution of 0.1 C (Shepherd, 1981). A fully automatic programmable temperature controller with digital temperature display is used to control heating and freezing rates during the analysis. The sample rests on a thermal block, and heating is achieved by thermal conduction. For freezing, dry nitrogen gas (N₂) flows through copper tubing submerged in liquid N₂ and the cooled N₂ gas goes through a thermal block monitored by a temperature controller. Figure 24 shows the layout of the TH-600 Stage and cooling mechanism. A choice of 27 different linear rates of temperature (0.1 C/min to 90 C/min) is available. Shepherd (1981), Shepherd, et al. (1985), Roedder (1984), and Hollister, et al. (1981) have described the Linkham TH-600 and other stages in detail.

Figure 23.

Schematic cross section through the Linkham TH 600 stage.
(From Shepherd, 1981)

HOLLISTER & OTHERS - PRACTICAL ASPECTS

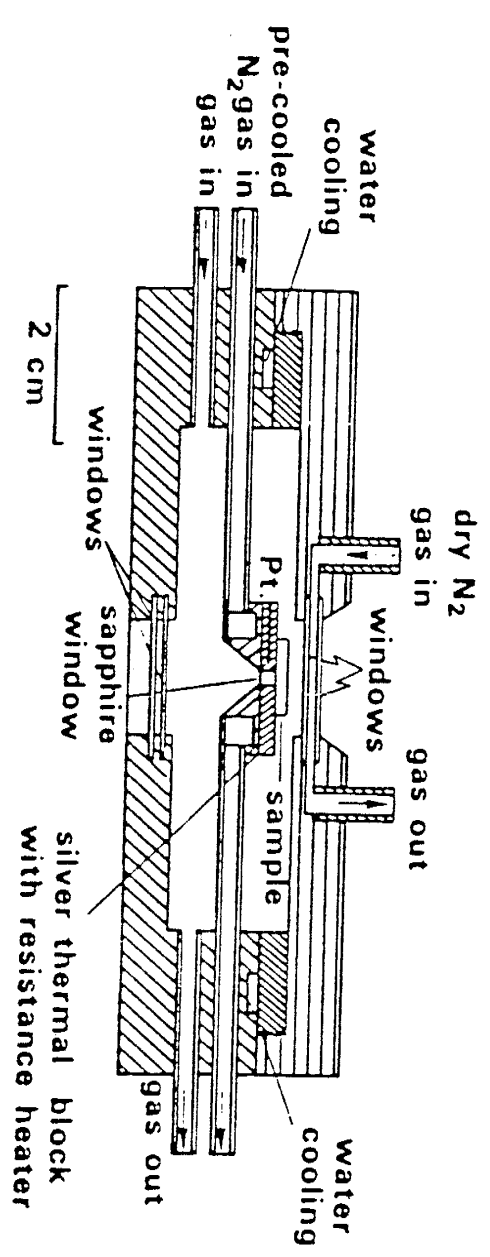
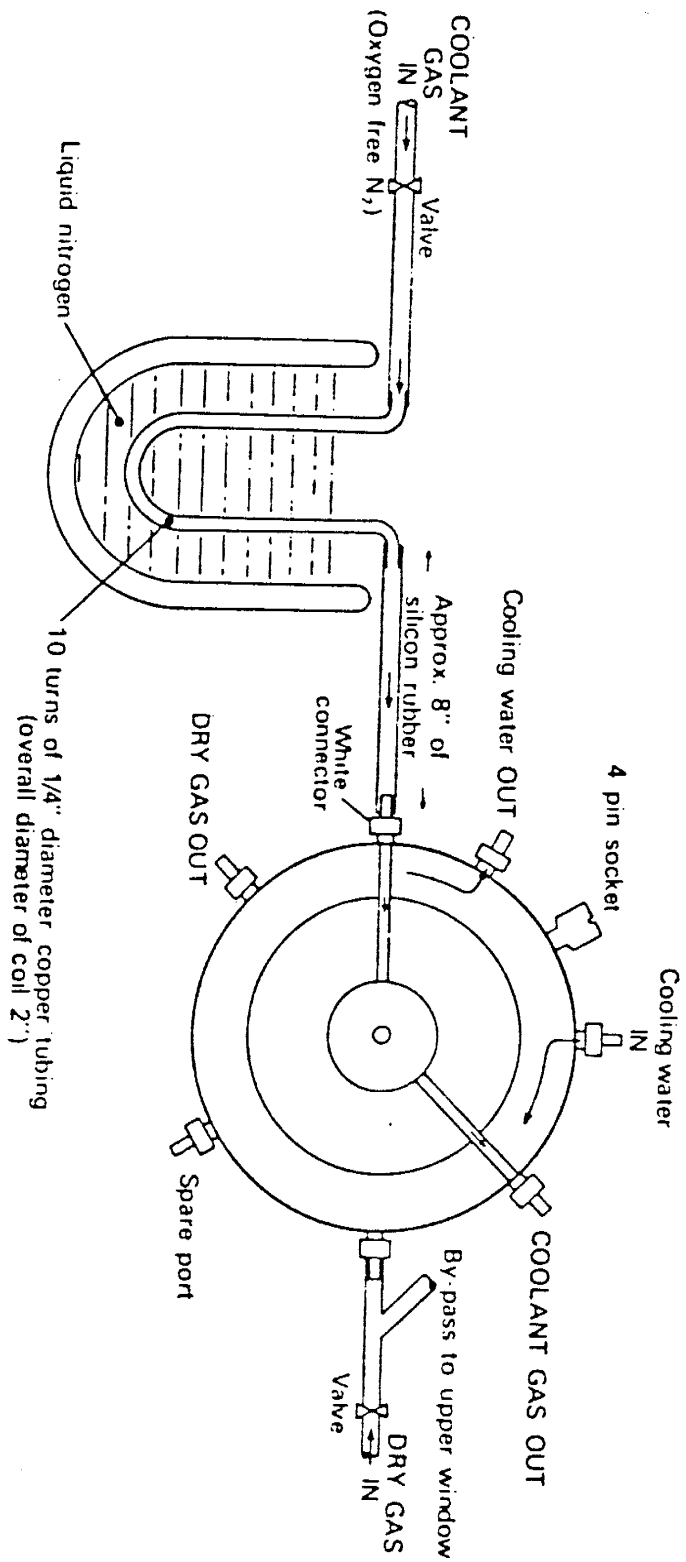


Figure 24.

Layout of the Linkham TH 600 stage for heating and freezing.
(From MacDonald and Spooner, 1981)



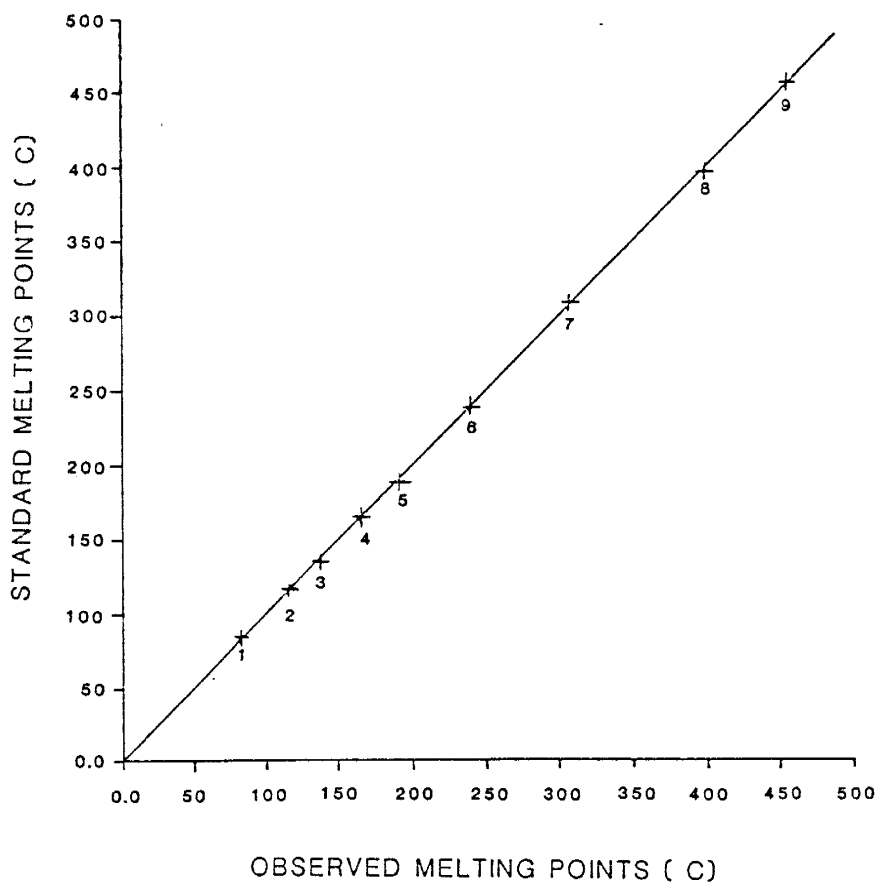
CALIBRATION

Temperature data from fluid inclusion analysis during heating and freezing experiments could be reproduced with a precision of better than $+ 0.1$ C. However, these data may not represent the actual temperature of phase changes or temperatures of mineral formation. This difference increases in higher working temperatures. Because of this discrepancy between the actual temperatures of mineral formation or of phase transformations and the temperatures given by the instrument, the latter has to be calibrated. A calibration curve is constructed by measuring the melting temperatures (points) of standards. By using the constructed curve, the true temperature of the sample is determined. Figure 25 shows the calibration curve constructed on the Linkham TH-600 stage for this study. The standards and their actual melting points are also shown in this figure.

For lower or freezing temperatures, deionized distilled water was used and the final melting temperature of ice was observed. When the final temperature of complete melting of ice was higher or lower than 0.0 C, the system was adjusted to show zero for the final melting point of ice. Once a week the freezing point of water was checked for possible temperature drift of the stage. When a temperature drift was observed, the necessary adjustment of the stage or of the data was carried out. During calibration experiments, it was concluded that the best heating rate for the temperature

Figure 25.

Calibration curve constructed for this study. The standards and their melting points are listed. The observed melting points in a few runs were slightly (1-2 C) different from the reported melting temperatures of the standards.



standard	melting temperature (°C)
1. vanilla	81-82
2. acetanilid	114-116
3. acetophenetidin	134-136
4. sulfanilamide	164.5-166.5
5. sulfapyridine	190-193
6. caffeine	235-237.5
7. sodium nitrate	307
8. potassium dichromate	398
9. silver chloride	455

measurements was 0.5 C/min. MacDonald and Spooner (1981) concluded that the best heating rate of temperature measurement is 0.4 C/min.

BOILING OF A FLUID SYSTEM AND RELATED FLUID INCLUSIONS

Boiling in a hydrothermal system is recognized by the following characteristics: (1) random proportions of liquid and vapor are trapped in fluid inclusions; (2) two distinct populations of inclusions are present, one with a low liquid to vapor ratio and the other with a high liquid to vapor ratio (Kamilli and Ohmoto, 1977). When there is a wide range of liquid to vapor ratios, an anomalously high homogenization temperature (T_h) is observed. In such cases, the true temperature of entrapment is the minimum T_h . In a boiling system, the T_h of inclusions with different liquid to vapor proportions are identical or very close to each other and these are the true trapping temperatures. Under these conditions, because the hydrothermal fluids are trapped on the boiling curve, no pressure correction for temperature is necessary.

In a boiling hydrothermal system, the gas phase or bubbles can be water vapor or minor amounts of different gas species such as CO_2 , CH_4 , N_2 , H_2S ,...etc. This composition represents the immiscibility condition of the hydrothermal system at lower temperatures. Each volatile species has its own partition coefficient between the vapor and liquid phase under the prevailing condition but most of these partition coefficients have not been measured (Roedder, 1984). Evidence for boiling is seen in some of the samples from the Hermosa mining district but it is not very common.

DENSITY OF FLUIDS IN FLUID INCLUSIONS

Assuming fluid pressure approximately equals total pressure, the density of the fluid in a fluid inclusion constrains the host mineral to P-T conditions on the isochore for that fluid. Knowing the salinity and degree of fill (F) of primary inclusions, it is possible to calculate or graphically estimate the densities of mineralizing fluids at different stages of mineralization.

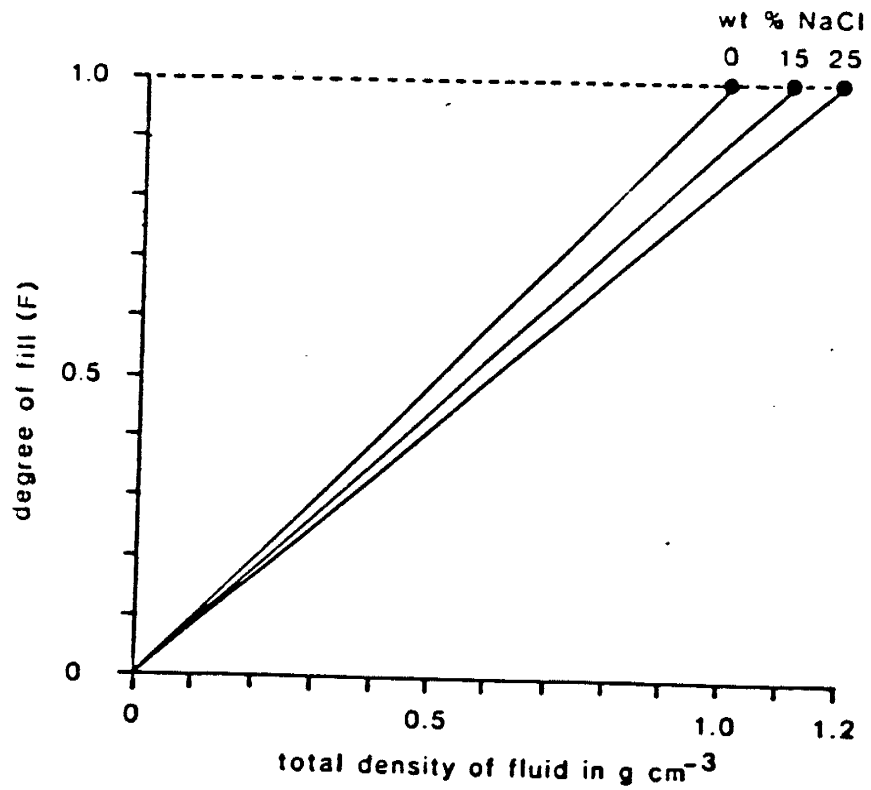
Shepherd et al. (1985) developed a useful diagram relating degree of fill to the overall fluid density as a function of salt concentration (Fig.26). Using this figure, the densities of the fluids which formed Type I and II inclusions in quartz and calcite were estimated, and these range from 0.8 to 0.4 g./cm³. For the same types of inclusions in sphalerite, the densities of the fluids range from 0.82 to 0.88 g./cm³. The fluid density of about 0.8 g./cm³ is common for inclusions in quartz and calcite, and 0.85 g./cm³ is common in sphalerite.

PRESSURE CORRECTION

Pressure corrections for measured T_h is necessary to determine the true trapping temperature (T_t). During the entrapment of fluid inclusions in the growing host minerals the pressure of the hydrothermal system may exceed its vapor pressure, thus requiring a temperature correction. If the pressure on the fluid system is equal to or less than the

Figure 26.

The relationship between the degree of fill (F) at 25 C and the total density of the contents for different NaCl solutions. (From Shepherd et al., 1985)



vapor pressure, no correction is needed. When the fluid system boils, the pressures of liquid and vapor are equal and no pressure correction is required. Roedder and Bodnar (1980) have reviewed methods of estimating the pressure and depth of crystallization from fluid inclusion data. Shepherd et al. (1985) also have reviewed other methods of pressure determination by using (1) vapor pressure of the fluid at T_h , (2) fluid isochore + independent geothermometer, (3) intersecting isochores for immiscible fluids, and (4) dissolution of halite daughter minerals.

The maximum pressure exerted on a fluid is usually from the overlying rocks, which is known as lithostatic pressure. However, if the fluid system is open to the surface (by faults or fractures) then the pressure is lower and it is known as hydrostatic pressure ($P = 2.5 P_h$). To estimate lithostatic pressure on the fluid system in the Hermosa mining district, geologic reconstructing of the stratigraphy of the area is used.

COMPOSITIONAL TYPES OF FLUID INCLUSIONS

Three main types of fluid inclusions were distinguished in samples from the Hermosa mining district based on their degree of fill. The degree of fill (F) is defined by Shepherd, et al., (1985) as the volumetric proportion of liquid relative to the total volume of the inclusion. Each type may represent a distinct type of original fluid or special condition of

formation. None of these types are restricted to a particular mineral. All types occur as primary and/or secondary inclusions, although type I occurs more as primary in quartz and sphalerite. The intent of this study is to exclude secondary or necked-down inclusions in the compositional classification. The three main types of inclusions are described in the following paragraphs.

Type I (liquid-rich inclusions). This is the most common type and accounts for about 70% of the analyzed inclusions. Type I inclusions occur in all minerals studied. This type is characterized by high degree of fill. In Type I, vapor content ranges from a few percent to about 30% (Fig.27), with a vapor content of 10 to 20% being most frequent. Type I inclusions represent the entrapment of an originally undersaturated and homogeneous aqueous brine at elevated temperature. All inclusions of Type I homogenize to liquid. Only very few decrepitated before homogenization.

Type II (vapor-rich inclusions). These inclusions are characterized by a vapor phase that occupies 60 to 90% of the volume of the fluid inclusions (Fig.28). With few exceptions, inclusions of Type II homogenize to a gas phase. They represent high-temperature and low-density (undersaturated) water vapors which condensed when the temperatures cooled down. It is possible that some of these inclusions are the results of the necking-down phenomenon, in which most of the liquid portion of the original inclusion has migrated or leaked out. If this is the case, it is not possible to

Figure 27.

Type I fluid inclusions in quartz (A, B, C) and sphalerite (D) at 25 C. Numbers refer to the sizes of the inclusions.

A = 7 microns
B = 18 microns
C = 20 microns
D = 30 microns

Figure 28.

Type II fluid inclusions in quartz at 25 C.

28-A: Interstitial gas-rich fluid inclusion (25 microns).

28-B: Regular gas-rich fluid inclusion (20 microns).

Figure 29.

Type II (gas-rich) fluid inclusions in sphalerite at 25 C.

Figure 30.

Type II (gas-rich) irregular fluid inclusions in sphalerite at 25 C (2-40 microns).

distinguish these inclusions from the true primary gsa-rich inclusions. Necked-down vapor-rich and fluid-rich inclusions are abundant in the samples from the study area. Type II inclusions account for 10 to 20% of analyzed inclusions. They mainly occur in quartz and sphalerite. In quartz crystals, Type II inclusions show regular shapes and behavior, they occur in early to late quartz of the mineralized zones. In sphalerite crystals, gas-rich inclusions exhibit both regular and irregular shapes (Fig.29). The irregular shape inclusions occur in forms of blebs or interconnected tubes or pipes (Fig.30). Type II and Type I inclusions occur together in some samples, they suggest different conditions of entrapment in a continuous process of crystallization.

Type III (transitional type). Type III inclusions occur in all analyzed minerals from the study area. Type III is characterized by an intermediate degree of liquid filling (Fig.31). Vapor content in this type ranges from 35 to 60% of the volume of the inclusions. Type III inclusions account for about 10 to 15% of the 7000 analyzed inclusions. The condition of formations represent a transition between those responsible for the formation of Type I and Type II. At elevated temperatures, some inclusions of this type homogenize to liquid and some to gas.

Daughter minerals were observed in only a few inclusions from the district. Inclusions with daughter minerals are therefore not classified as a separate type. Most of the daughter minerals occur in Type I inclusions and, based on

Figure 31.

Type III fluid inclusion in quartz at 25 C (15 microns).

the optical characteristics and chemical behavior (not dissolving at high temperatures), they were tentatively identified as hematite and sulfates.

Another type of inclusions was observed which were completely filled with liquid. They occur in all examined minerals but are not abundant. Several freezing experiments on these all-liquid inclusions produced no new phase or change. They may represent late dilute liquids at lower temperatures. Their shapes, in most cases, indicate they are primary inclusions and not results of necking down of Types I or II.

From the classification of fluid inclusions in the district, it is concluded that two conditions were dominant during the entrapment of the fluid inclusions. In one condition the mineralizing fluids were partially boiling, and during this period Type II, I and some of the Type III inclusions were trapped. In the other condition the mineralizing fluids were not boiling and inclusions of Type I and some of the Type III were trapped.

COOLING AND HEATING OBSERVATIONS

After mapping the distribution of fluid inclusions in the polished sections and after the origin (primary or secondary) were determined, small chips of the samples were used for microthermometric analysis. The phase changes observed during these analyses are used to identify fluid composition, to determine the fluid density, and to infer the relative abundance of fluid components.

The most common ions detected in fluid inclusions are: Na⁺, K⁺, Ca⁺⁺, Mg⁺, Cl⁻, SO₄ , CO₃ and HCO₃ (Roedder, 1972). There are published phase diagrams for different systems or fluids which contain different concentrations of these ions. The determination of compositions in fluid inclusions depends on closely matching observed phase changes with experimentally determined phase transition in published known systems, and where possible, identification of the solid phases formed both at low and high temperature (Crawford, 1981). During microthermometric analyses of fluid inclusions, several observations and steps are recommended by Crawford (1981): "(1) cooling the inclusion until the contents solidify; freezing of liquids, liquefaction of gases, or vapor bubble nucleation in liquids on cooling, generally require several tens of degrees of undercooling; therefore all temperature measurements of phase changes are recorded; (2) determination of the eutectic melting temperature; (3) observation of melting (congruent or incongruent) of a salt-hydrate phase;

(4) measurement of the melting of ice; (5) determination of the temperature of solution of mineral solids which persist after the melting of hydrate and ice; clathrate compounds will also be present if CO₂ or hydrocarbons are present in the inclusions along with H₂O; (6) measurement of the homogenization temperature of liquid and vapor phases (Th)." In each of these observations, enough time was taken to assure that equilibrium, after phase changes, was achieved in the inclusion. In order to check the precision of the results, repeated measurements of the same experiment on the same inclusions were carried out, and reproducibility of the measurements was verified. The complexity of the fluid system in the inclusions affects the analysis results. The fewer the components of the fluid system, the fewer phase changes, and, as a result, more accurate interpretation of the analyses could be made.

FREEZING BEHAVIOR

In theory, two-phase inclusions containing pure water or nonaqueous fluid, such as CO₂, should freeze to solid + vapor at a well-defined temperature. For example, water should freeze at 0 C and CO₂ should freeze at -56.6 C. However, because of the metastability condition in most fluid inclusions due to their small sizes, and because fluids in these inclusions rarely consist of a single chemical component, the fluid inclusions do not freeze at predictable

temperatures. Because of this, fluid inclusions must be supercooled before they freeze. The freezing temperatures for inclusions from the study area range from -28 C for less saline fluids in quartz and calcite to -48 C in quartz, sphalerite, and calcite. The freezing is sudden, the bubble shrinks, as the frozen liquid expands. The supercooling temperature for freezing does not provide a good estimate of composition, but the temperature of the phase changes during the reheating or melting process provides compositional and density information. When inclusions are frozen, a variety of new solid phases may be formed and the identification of these phases gives compositional information (Roedder, 1962 and 1963). The most common new phase was ice and it could be identified by its index of refraction, very low birefringence, volume increase on freezing, and temperature range of stability. Except for one inclusion in a sample from the Slater working (Slt-14-c), all the analyzed inclusions formed ice upon cooling. The range of melting temperature is a direct function of composition and therefore it was used to estimate fluid composition from experimental P-T-X data.

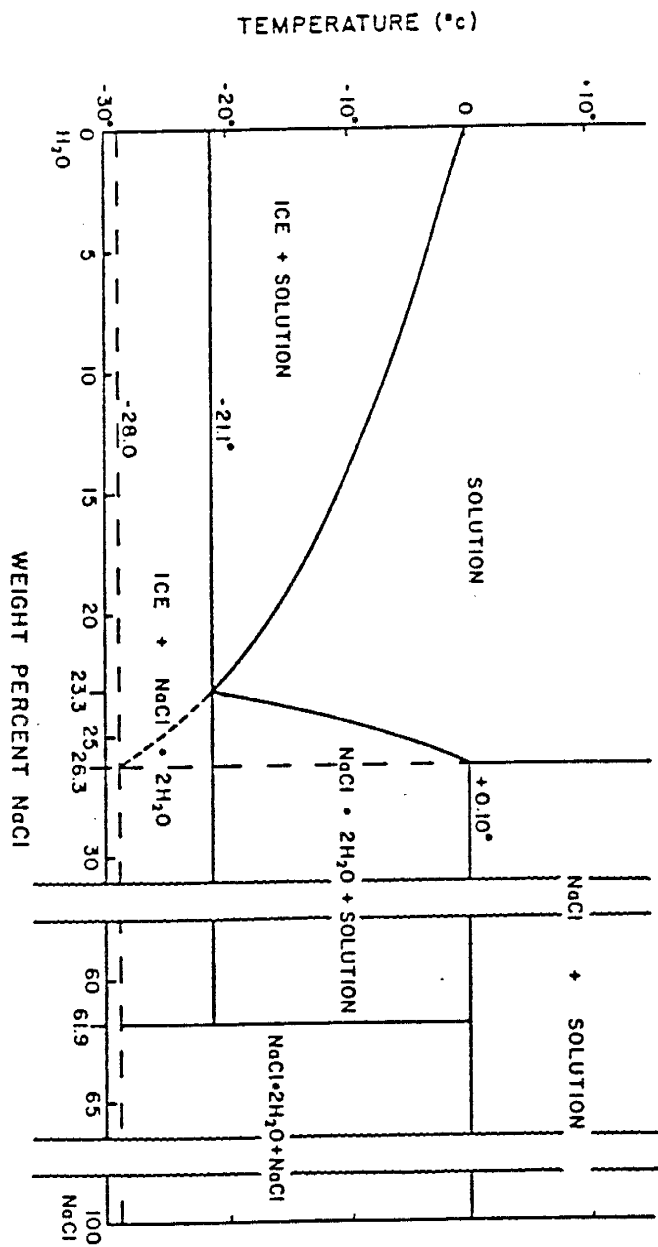
Accurate determination of the first-melting temperature (eutectic temperature) is important for the determination of the composition of the fluid system. A first melting temperature (T_e) of -20.8 C is diagnostic of the NaCl-H₂O system (Potter et al., 1978). According to Crawford (1981) the addition of KCl to a NaCl-H₂O system would lower the eutectic point by about 2.1 C from -20.8 to -22.9 C. The addition of

other chlorides such as CaCl_2 or MgCl_2 would depress the eutectic point to -52.0 and -35.0 C respectively. Because the fluids from the Hermosa mining district are dilute brines, it is very difficult to measure the first melting temperatures (T_e) of all frozen inclusions. However, from the relatively few observations of T_e in inclusions in quartz, sphalerite, and calcite, a range of eutectic points from -22 to -30 C is determined. This range of eutectic points suggests that in addition to NaCl some KCl or MgCl_2 is in the fluid system.

During freezing experiments ice forms in fluid inclusions. As ice melts gradually, it is recognized as rounded grains of high negative relief and low birefringence in the inclusion liquid. From the final melting temperature (T_m) of the inclusions the salinity of the fluids is determined by using the data of Potter et al. (1978) or the T-X plot (Fig.32) for the low temperature part of the $\text{NaCl-H}_2\text{O}$ system of Roedder (1962a). The salinity of inclusions is presented as "equivalent weight percent NaCl " (eq. wt. % NaCl) because it is assumed that the amount of NaCl that produced the measured freezing point depression is roughly equal to the total salts (NaCl , KCl , MgCl_2 , CaCl_2 ,...) present in the solution.

Figure 32.

T-X plot for the low-temperature part of the NaCl-H₂O system in equilibrium with vapor at 1 bar total pressure. (From Roedder, 1962a)



FREEZING DATA

Freezing experiments were carried out on more than 80% of the analyzed inclusions in quartz, sphalerite, calcite, and barite from the study area. The majority of these runs were performed on primary inclusions. About 5% were done on secondary inclusions from different mines or areas of the district. Necked-down fluid inclusions were also analyzed in order to see if there are any compositional changes of the fluid phase after the physical changes.

All freezing experiments were performed before heating runs in order to avoid any possible effects of stretching or leakage due to heating.

Type I inclusions in all minerals showed the characteristics of unsaturated NaCl solutions. The freezing temperature for this type ranged from -29 to -45 C. The first melting temperature ranged from -22 to -29 C indicating the presence of some KCl and MgCl₂ in the solution. Salinities were calculated from the melting point depression and it ranged from 0 to 9 eq. wt.% NaCl. The dominant range of salinity in quartz and calcite is 0 to 2 eq. wt.% NaCl. Some inclusions in sphalerite (both early and late stages) showed a range of 0.7 to 2 eq. wt.% NaCl. Sphalerites with low salinity fluids have lighter honey-yellowish color and these observed in the mineralized zones throughout the mining district. Low salinity inclusions in quartz and calcite are very common in the district and occur with or without ore

mineralization. Calcite crystals associated with ore mineralization contain higher numbers of low salinity inclusions than those in quartz in the same location. Quartz crystals associated with little or no ore mineralization contain higher numbers of low salinity inclusions than those in calcite from the same location. In general, about 80% of the analyzed inclusions showed a low salinity.

The second range of salinity in Type I inclusions was 2 to 5 eq. wt.% NaCl. The majority of inclusions within this range occur in quartz, sphalerite, and calcite in mineralized zones. This range occurs in primary and secondary inclusions. Calcite crystals associated with ore mineralization contain a higher numbers of this second range of salinity than quartz in the same condition. In the areas with little or no ore mineralization a reverse association is true. The association between ore occurrences and the second range of salinity suggest definite correlation.

Less than 5% of the analyzed Type I inclusions showed salinities higher than 5 eq. wt.% NaCl (5 to 9). The high salinity inclusions are largely restricted to sphalerite and calcite. Very few inclusions in quartz from the southern part of the district showed high salinity. The quartz crystals with high salinity associated with sulfide mineralization are in areas of good ore potential.

Type II (vapor-rich) inclusions are difficult to freeze even at -150 C), because of their high gas to liquid ratios and also it is hard to see ice melt. A few of the inclusions

which were frozen showed 0.7 to 3 eq. wt.% NaCl. The majority of this type occur in quartz and sphalerite. In most cases, these inclusions are associated with ore occurrences and boiling condition.

Type III inclusions show the same ranges of salinities as Type I. The same associations of salinity range, mineralization, and mineral type (quartz, calcite, or sphalerite) for Type I are true for Type III.

During freezing analysis, one secondary fluid inclusion in a calcite sample (Slt-14-c from Slater working), behaved differently from other inclusions from the same sample and location. This inclusion was about 50 microns in diameter with a bubble of 20 microns and fluid density of about 0.73 g./cm³ (Fig.33-A). The inclusion froze at -41 C, and at the same time a new liquid phase developed inside the bubble. This new phase was of darker and more greenish color. This phase developed in three separate blebs and grew larger as cooling continued. At -58 C the new phase stopped growing (Fig.33-B). Cooling was continued until -135 C, but no change occurred in any of the blebs. Upon heating, at about -31 C the size of the new phase blebs started to decrease (Fig.33 C and D), at -13.5 C the new phase in the bubble disappeared and at -3.1 C the ice completely melted. A primary inclusion in the same field of view (Fig.33 A, B, and C) was monitored for comparison with the described inclusion. Almost the same final melting point (-3.2 C) was observed for this primary inclusion, and no new phase developed even at -135 C. The behavior of the secondary

Figure 33.

Secondary inclusion in calcite (50 microns).

A: At 25 C.

B: At -65 to -135 C. The inclusion is frozen. A new phase is developed. Note the primary inclusion is also frozen.

C: At -22 C. The new phase decreasing in size.

D: At -14.5 C. Just before the new phase homogenizes. Note the changes in the primary inclusion.

inclusion in response to freezing suggests that the new phase was liquid CO₂ with some CH₄ or N₂. Why three separate blebs of the new phase were developed instead of a large one is not understood. This particular inclusion was analyzed two more times, and the same results were produced each time.

Many of the freezing runs were repeated one or two more times. The reproducibility of the same results in the same inclusions after two or more times was almost 100%. In all freezing runs, the heating rate was reduced to +0.5 C as the final melting temperature was approached.

HEATING BEHAVIOR

The homogenization temperature (Th) is the temperature at which different phases in an inclusion homogenize to a single phase upon heating. Sorby (1858) recognized the significance of phase changes which occur after trapping in an inclusion. Heating analysis simply reverses these changes and theoretically reproduces the original fluids and related restraining conditions again.

HOMOGENIZATION DATA

Homogenization temperatures (Th) of about 7,000 fluid inclusions in quartz, calcite, sphalerite, and barite from mineralized and non-mineralized zones were determined by about 2,700 separate runs. The same chips and inclusions which were

used for freezing experiments are used for these heating runs. The results of these analyses are listed in Appendix II. Many runs are not listed because the analyzed inclusions either leaked or exploded. About 700 of the runs were repeated in order to check the reproducibility of the results. The reproduced data are within 1 to 2 C of the first runs. The homogenization temperature of each inclusion was recorded when the fluid phase homogenized either by the expansion of the liquid or the expansion of the gas phase.

Two main types of homogenization were observed in these analyses. More than 95% of the inclusions of Type I and about 70% of the inclusions of Type III homogenized into a liquid. About 80% of the inclusions of Type II and 20 to 30% of Type III homogenized into a gas phase. Not all heating runs for Type II and Type III were successful because of leakage or decrepitation before homogenization. In the first type of homogenization, the bubble gradually decreases in size and at a certain size or temperature (different for each individual inclusion) the bubble starts vibrating and moving in different directions. During this movement, the bubble continues to decrease in size and finally disappears (Th).

In the second type of homogenization, two types of behaviors are observed. In the first one, the bubble volume does not change for much of the heating period but then gradually expands and homogenizes into a vapor phase. In the second behavior, the bubble decreases in size for a short period during heating until it reaches a certain minimum

volume; it remains constant for much of the heating period and finally starts to expand and homogenize into a gas or vapor phase. These different modes of homogenization reflect the fluid density and pressure formation of the inclusions.

In this study few inclusions were seen with daughter minerals. Heating experiments for inclusions with daughter minerals were carried out. The liquid and vapor phase behaved normally, and the inclusions homogenized into a liquid phase. However, the daughter minerals did not homogenize or dissolve even at temperatures above T_h . For two inclusions in quartz samples from the Slater working and Day mine, heating runs of long duration were performed in order to dissolve these solid phases. The temperature of the heating stage was held constant at T_h . After 8 hours the solid phase was still present, but slightly rounded at the edges. After 21 hours no additional changes were observed. The temperature of the stage was raised 30 C above T_h for another 5 hours and still no change was observed. At this point the experiments were ended. From these observations it could be concluded that these daughter minerals either did not precipitate from the fluids in the inclusions or a very strong chemical disequilibrium was present during the formation of the fluid inclusion.

PRESSURE CORRECTION FOR T_h DATA FROM THE HERMOSA DISTRICT

In the previous chapter it was concluded that the mineralization occurred in late-Oligocene time (29-26 m.y.

ago). Geologic reconstruction of the area suggests that in the Antelope-Ocean Wave mines, during ore mineralization, the overlying rocks (mainly the Rubio Peak Formation) were about 210 m (689 ft) thick thus exerting a pressure of about 60 bars. Using the salinity data (about 1 eq. wt.% NaCl) and Potter's (1977) pressure correction curves, the pressure correction for the obtained Th would be less than 5 C. Geologic reconstructions for the Wolford, Protector, Flagstaff-American Flag mines, and the southern part of the study area show even thinner overlying rocks. The same method of pressure correction was used for these areas, and the corrections were found to be negligible.

Lithostatic pressure on the fluid system in the uplifted and highly mineralized Palomas Camp area is generally much higher than in other mineralized zones in the district. Ore mineralization occurs in the Fusselman dolomite and Onate formation which underlie Mississippian, Pennsylvanian, and Permian rocks. Although, no Rubio Peak Formation is present in this area currently, evidence (Shepard, 1984) suggests that the it was present during mineralization period. A total thickness of overlying rocks of at least 800 m (2625 ft) thick is estimated. This column of rocks exerted a pressure of about 230 bars on the fluid system, and a pressure correction of 15-20 C is needed to obtain the Tt of inclusions from this camp.

In order to use this method of pressure correction the salinity of the fluid must be known, because the amount of the dissolved salts in the fluid system affects the density of the

fluid and in turn the density will affect the vapor pressure.

RESULTS OF FREEZING-HEATING EXPERIMENTS IN MINERALIZED ZONES

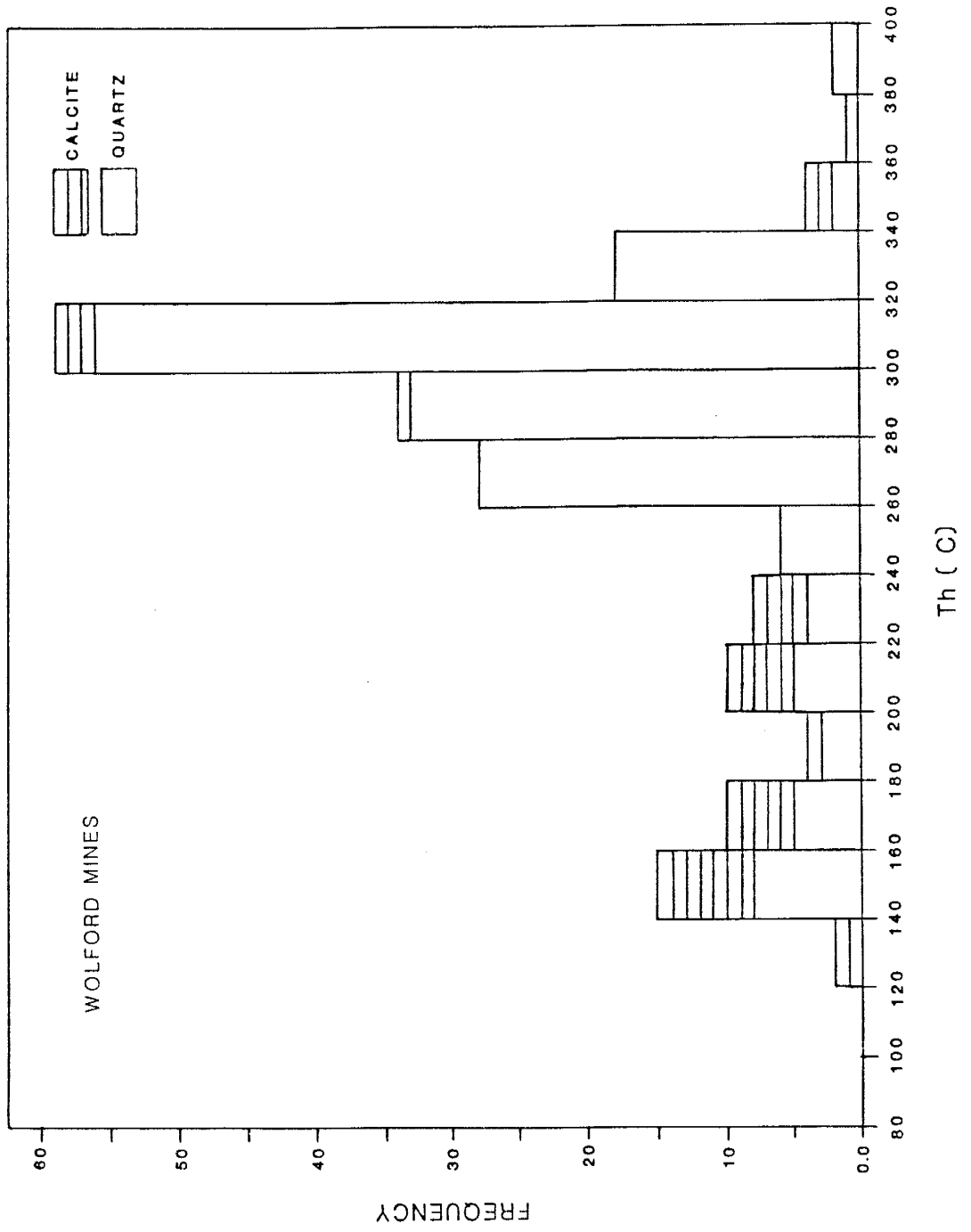
WOLFORD MINES

In the Wolford mines, about 175 inclusions in 13 samples were analyzed. About 80% of these inclusions are in quartz and the rest are in calcite. As described earlier, mineralization in the Hermosa mining district was a continuous process, and there are no clear cut stages in these deposits. However, for purposes of this study, the mineralization is divided into several stages. Early quartz is the predominant mineral in the Wolford mines. Th of inclusions in this early quartz ranges from 300 to 380 C regardless of their compositional type. The majority of the inclusions homogenize between 300 and 340 C (Fig.34). Quartz sygenetic with ore mineralization is the next predominant mineral, and inclusions in this quartz homogenize between 260 to 300 C. Quartz associated with late-stage ore mineralization shows a 220 to 260 C Th range. Inclusions in late-stage quartz and calcite homogenized between 160 to 220 C. Calcite occurrences are not common in this location, but, when present, they appear before, during and after ore mineralization stages (Fig.34). Chalcopyrite, tetrahedrite, and acanthite are associated with quartz which deposited between 260 and 300 C.

A large quartz crystal with five distinct zones was analyzed to determine if any temperature or fluid composition zoning exists. Except for zone 2, no temperature change was

Figure 34.

Histogram of the homogenization temperature (T_h) of fluid inclusions in quartz and calcite from the Woldford mines. Note the dominant temperature range of 260-340 C for early-stage quartz and ore mineralization.



observed, and the change in this zone was in the order of 10 to 15 C. Th for zones 1 (early), 3, 4, and 5 (late) ranged from 310 to 320 C. The salinity in zones 1, 2, 3, and 4 was about 1 eq. wt.% NaCl. Zone 5 showed a salinity of 3.5 eq. wt.% NaCl in every analyzed inclusion. The increase of salinity in zone 5 suggests that a different fluid was responsible for crystallization of this zone. Two different ranges of salinities of 0.5 to 1.5 eq. wt.% NaCl and 2 to 5 eq. wt.% NaCl have been measured in all types of inclusions in this location.

ANTELOPE-OCEAN WAVE MINES

About 350 inclusions in 25 samples of quartz, calcite and sphalerite from the Antelope-Ocean Wave mines were analyzed. These samples are directly or indirectly associated with the ore mineralization. Calcite crystallization occurs from the early to late stage of mineralization. Th of inclusions in calcite range from 340 to 100 C (Fig.35-A). Calcite is more abundant below 300 C. The majority (more than 70%) of the inclusions analyzed in calcite are primary. Quartz is the dominant mineral in the 280-320 C range and it rarely occurs below 200 C.

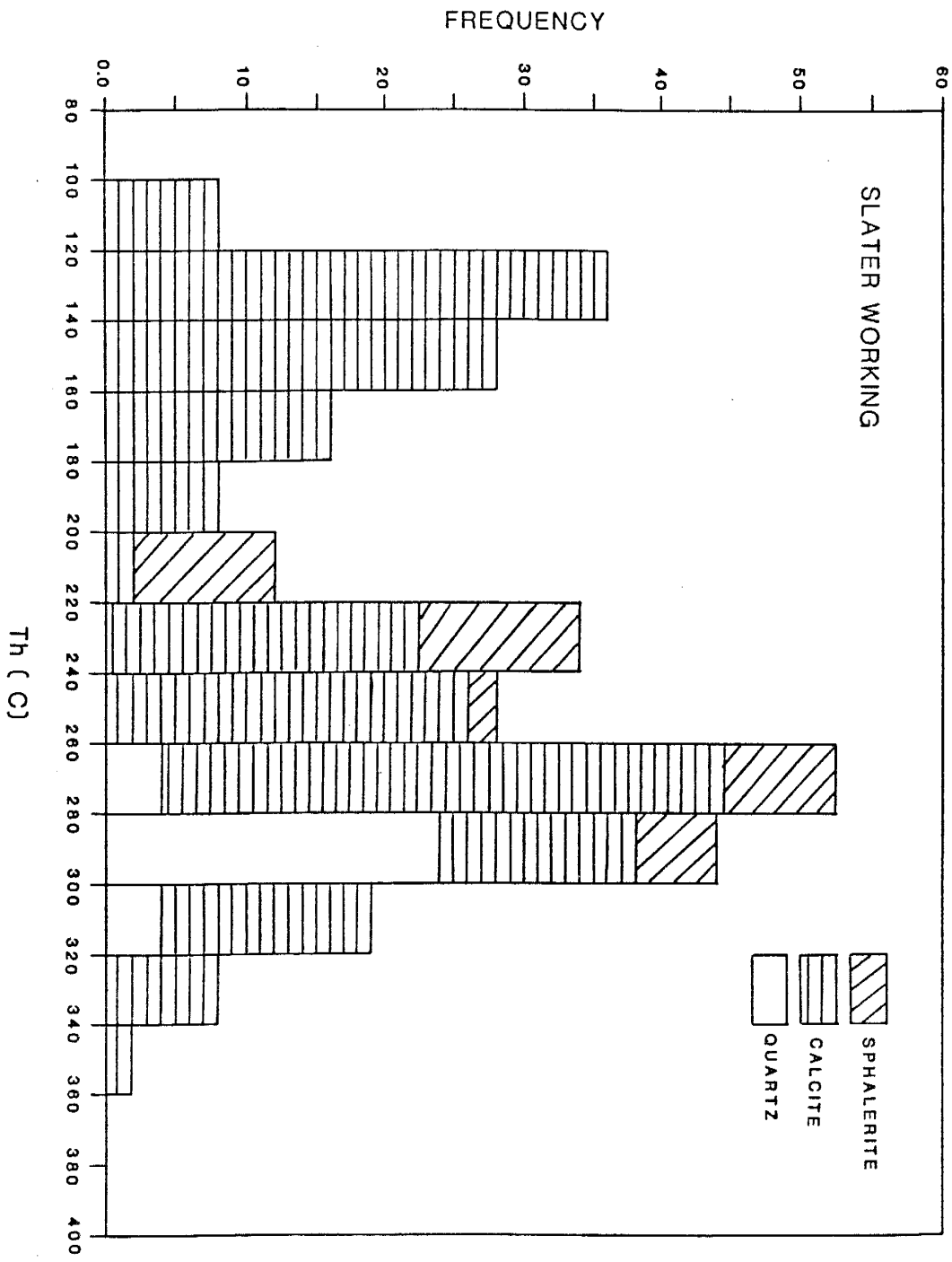
Figure 35-B shows Th of inclusions in quartz, calcite, and sphalerite in the Slater working. Two distinct populations of Th are observed in this location. One group shows a 200 to 360 C Th range and the other group shows a 100 to 200 C Th range.

Figure 35-A.

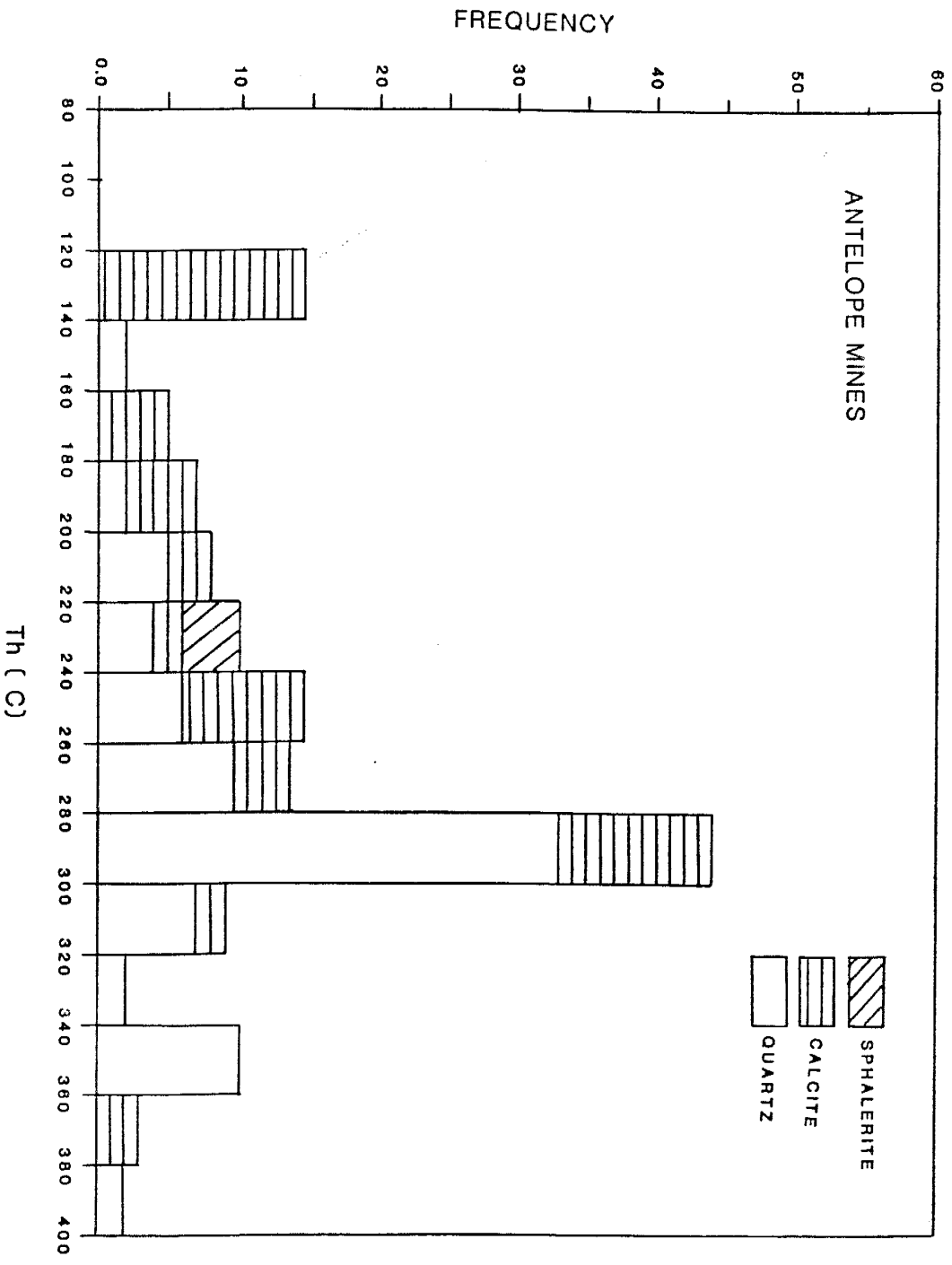
Histogram of the homogenization temperature (Th) from fluid inclusions in quartz, calcite, and sphalerite from the Antelope-Ocean Wave mines. Note the limited temperature range of sphalerite in this area.

Figure 35-B.

Histogram of the homogenization temperature (Th) from fluid inclusions in quartz, calcite, and sphalerite from the Slater working (Antelope-Ocean Wave mines). Note the high temperature of sphalerite (200-300 C).



B



A

The first group represents the early quartz and calcite mineralization with the Th range of 300-360 C. Ore mineralization in this group starts at 300 C and ends at 200 C. Chalcopyrite, tetrahedrite, and sphalerite are associated with quartz and calcite which formed between 280 and 300 C. Sphalerite, galena, acanthite, pyrargyrite, and native silver are associated with quartz and calcite that formed at 200 to 280 C range. Gold has been detected in samples from the early stage of ore mineralization (about 290 C). The second population in Figure 35-B represents a late stage of hydrothermal activity and calcite is the only mineral that has formed in this stage.

In general, it can be seen that fluid temperatures in the Antelope-Ocean Wave mines are cooler than those of the Wolford mines. Evidence of boiling is indicated by large numbers of gas-rich inclusions. Higher quartz and lower calcite occurrences in the Wolford mines suggest the association of high temperature with higher silicification. There is no clear-cut correlation between high, medium, and low Th and different salinities in these inclusions. However, most of the sphalerites with high Th show high salinities. Inclusions in quartz and sphalerite have regular prismatic to round shapes, but in calcite they have irregular shapes. The sphalerite in sample Slt-13 which contains the highest gold value in the district has a 242-289 C range of Th with a mean temperature of 276 C. The mean Th for inclusions in calcite in this sample is about 230 C. Mineralizing fluids in these mines have a

salinity range of 0.3 to 7 eq. wt.% NaCl.

In summary, Th of inclusions in quartz, calcite and sphalerite from the Antelope-Ocean Wave mines for early ore mineralization stages ranges from 240 to 300 C, and for late stages of ore mineralization, it ranges from 200 to 240 C. A 100-200 C event represents the final stage of mineralization.

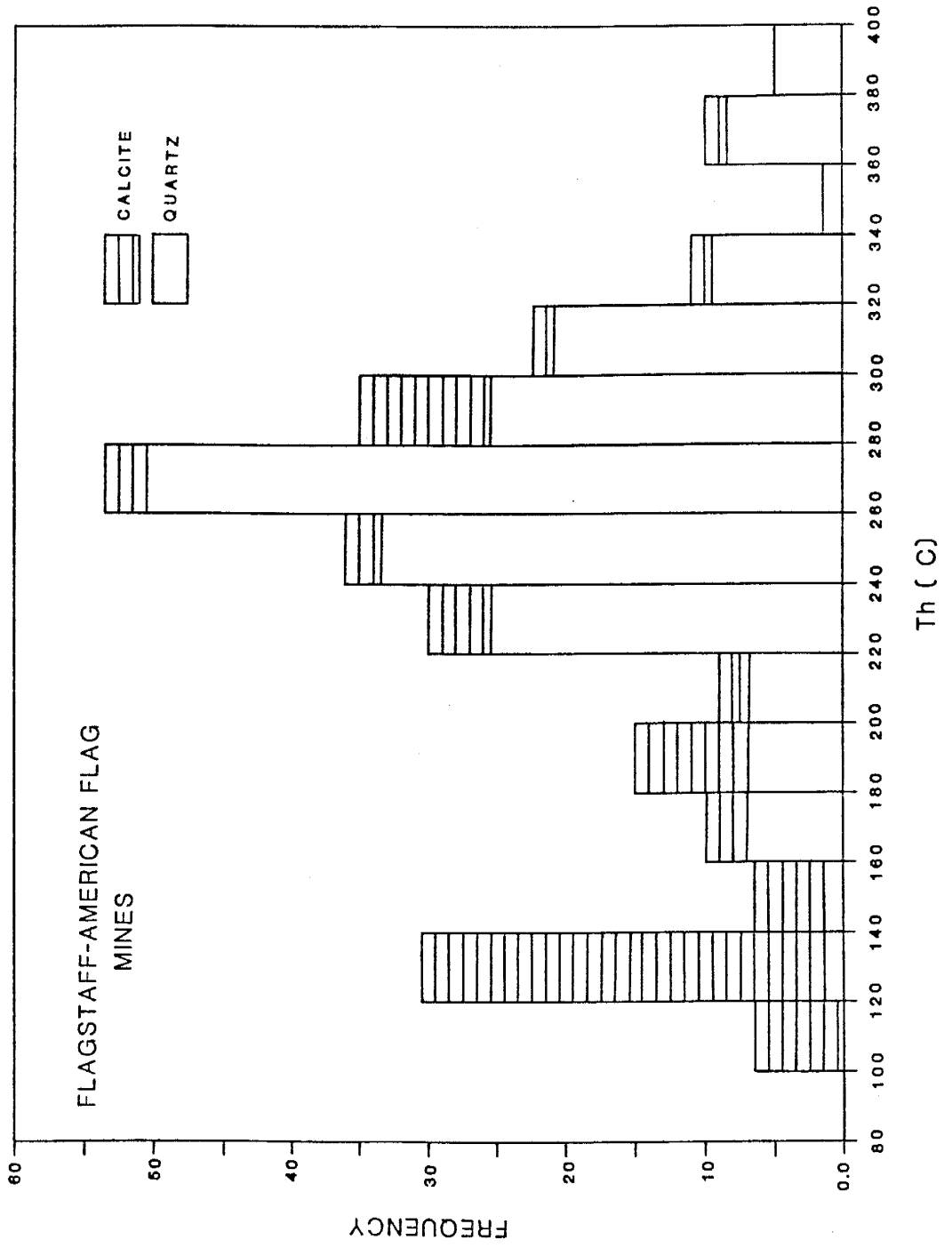
FLAGSTAFF-AMERICAN FLAG MINES

Farther south, in the Flagstaff-American Flag mines, about 270 inclusions in 15 samples of quartz and calcite were analyzed. Two distinct populations can be recognized which are characterized by their Th ranges (Fig.36). Th of the main group ranges from 220 to 320 C covering early quartz and calcite crystallization and early to late ore mineralization. Acanthite and galena are syngenetic with quartz crystallized between 240 and 300 C. In this population Type III inclusions are dominant with type I and II less so respectively. The second population is dominated by calcite with a Th range of 100 to 200 C. No ore mineralization is associated with this temperature range. Type I inclusions are characteristic for this population.

Fluid salinity in the Flagstaff-American mines Flag ranges from 0.5 to 2 eq. wt.% NaCl. A large number of Type II and III fluid inclusions, high Th, increasing salinity and large calcite crystals suggest a partial boiling condition during the early and ore stages of hydrothermal activity.

Figure 36.

Histogram of the homogenization temperature (T_h) from fluid inclusions in quartz and calcite from the Flagstaff-American Flag mines. Note the presence of calcite from high to low T_h .



SOUTHERN AREA

About 524 fluid inclusions in 24 samples of quartz, calcite, sphalerite, and barite from the southern part of the district were analyzed. The dominant range of Th is 240-300 C. This area has not been explored adequately, but its lithology and structure suggest a very favorable condition for ore occurrence. Assay values (Appendix III) show relatively high values of silver (50-300 ppm) and gold (1-3 ppm). Figure 37-A is a histogram of Th values from this area. Type II and III inclusions are relatively abundant and they homogenized in the 240-320 C range. Quartz and calcite occur in a wide range of temperature (100-400 C), but quartz tends toward higher temperatures than calcite. The main ore mineralization started at 300 C and ended at 240 C. Figure 37-B shows Th of inclusions in a smaller but intensely mineralized locality in this area. This figure shows two populations of Th. The first population at higher temperature represents the ore mineralization temperature (240-300 C) and quartz is the dominant gangue mineral. The second population represents the late-stage of mineralization and calcite is most abundant.

Salinity of the fluids in the southern area ranges from 0 to 7 eq. wt.% NaCl. The salinity data also show two populations, one with 2.5 to 3.5 and the other with 0.5 to 1.5 eq. wt.% NaCl. Ore mineralization in this area is associated with the higher salinity range. In comparison with other mineralized areas in the mining district, sphalerite has

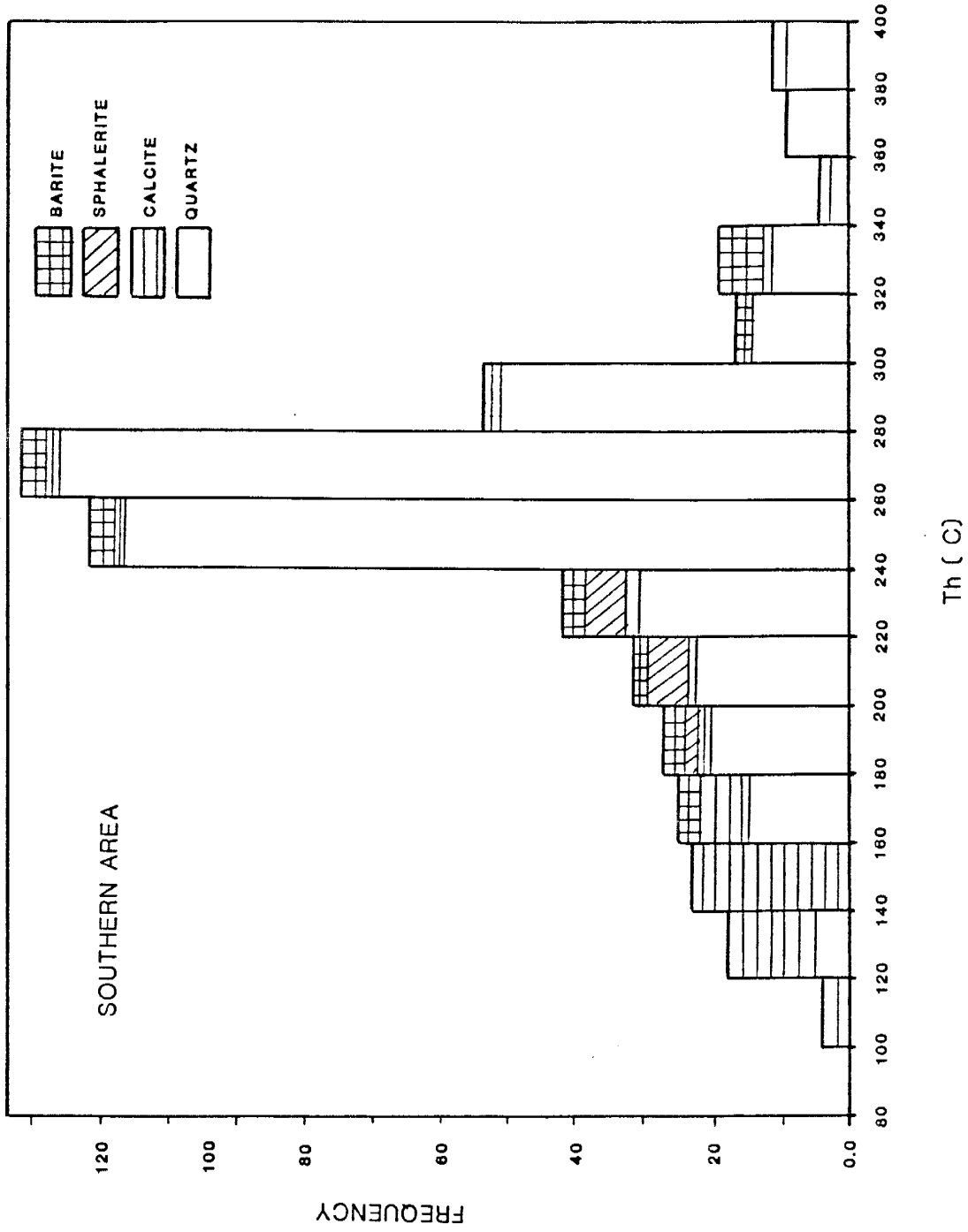
Figure 37-A.

Histogram of the homogenization temperature (Th) from fluid inclusions in quartz, calcite, sphalerite and barite from the southern area.

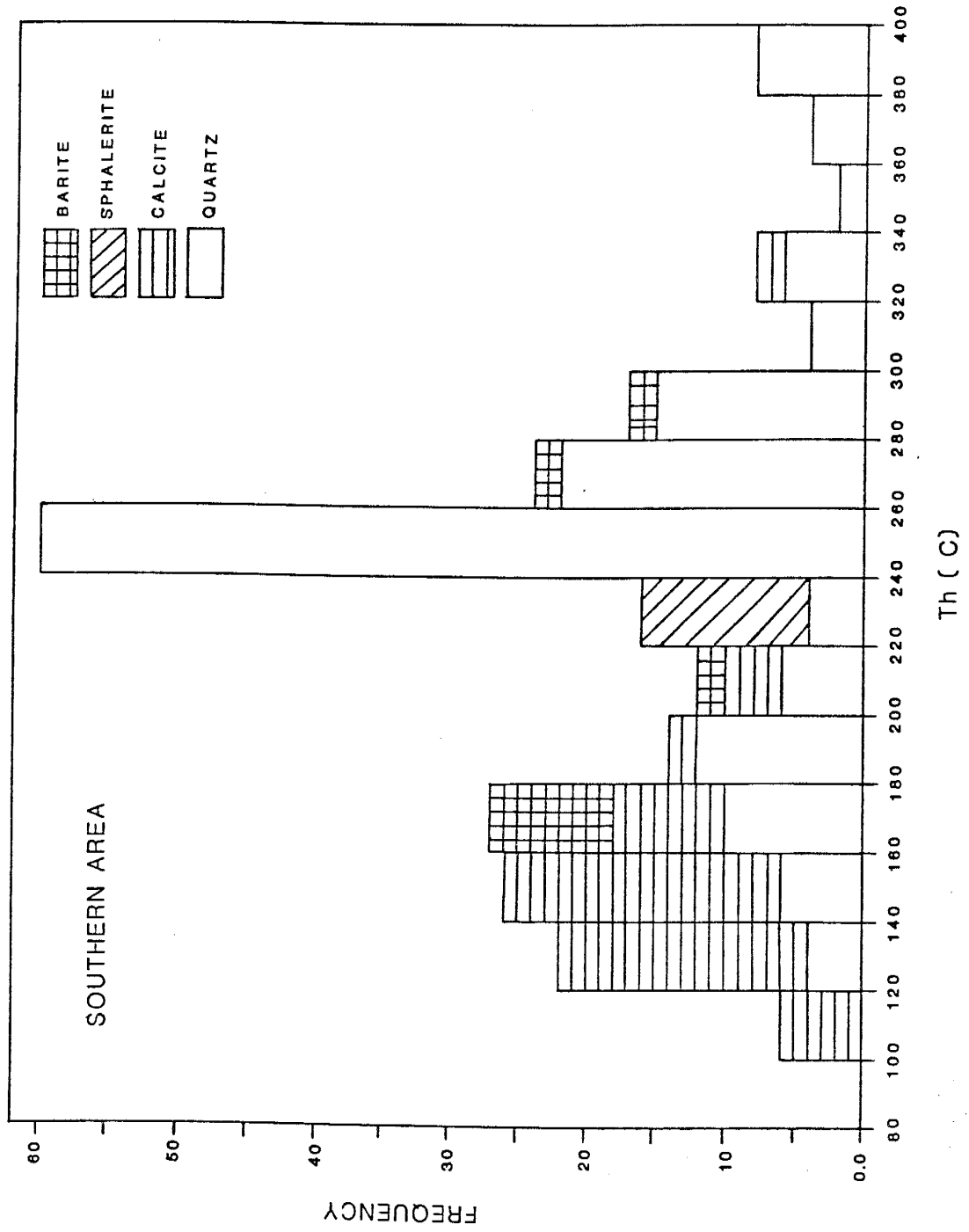
Figure 37-B.

Histogram of the homogenization temperature (Th) from fluid inclusions in quartz, calcite, sphalerite and barite from a smaller but intensely mineralized locality in the southern area. Note the wide temperature range of barite occurrences.

37-A



37-B



formed from cooler (220-240 C) and less saline (0.5-1 eq.wt.% NaCl) fluids. Fluid inclusions in calcite show both ranges of the salinity, but barite inclusions have lower (0.5-1.5 eq. wt.% NaCl) range.

Most of the samples analyzed in this area are from jasperoid exposed on the surface. Generally, fluid inclusions in jasperoid from other studies have lower temperatures of formation than the majority of jasperoid samples analyzed in this study area. The higher Th of inclusions from this area result from the exposure of deeper levels in the silicified hosts. The absence of Fusselman dolomite and younger formations confirms such a conclusion.

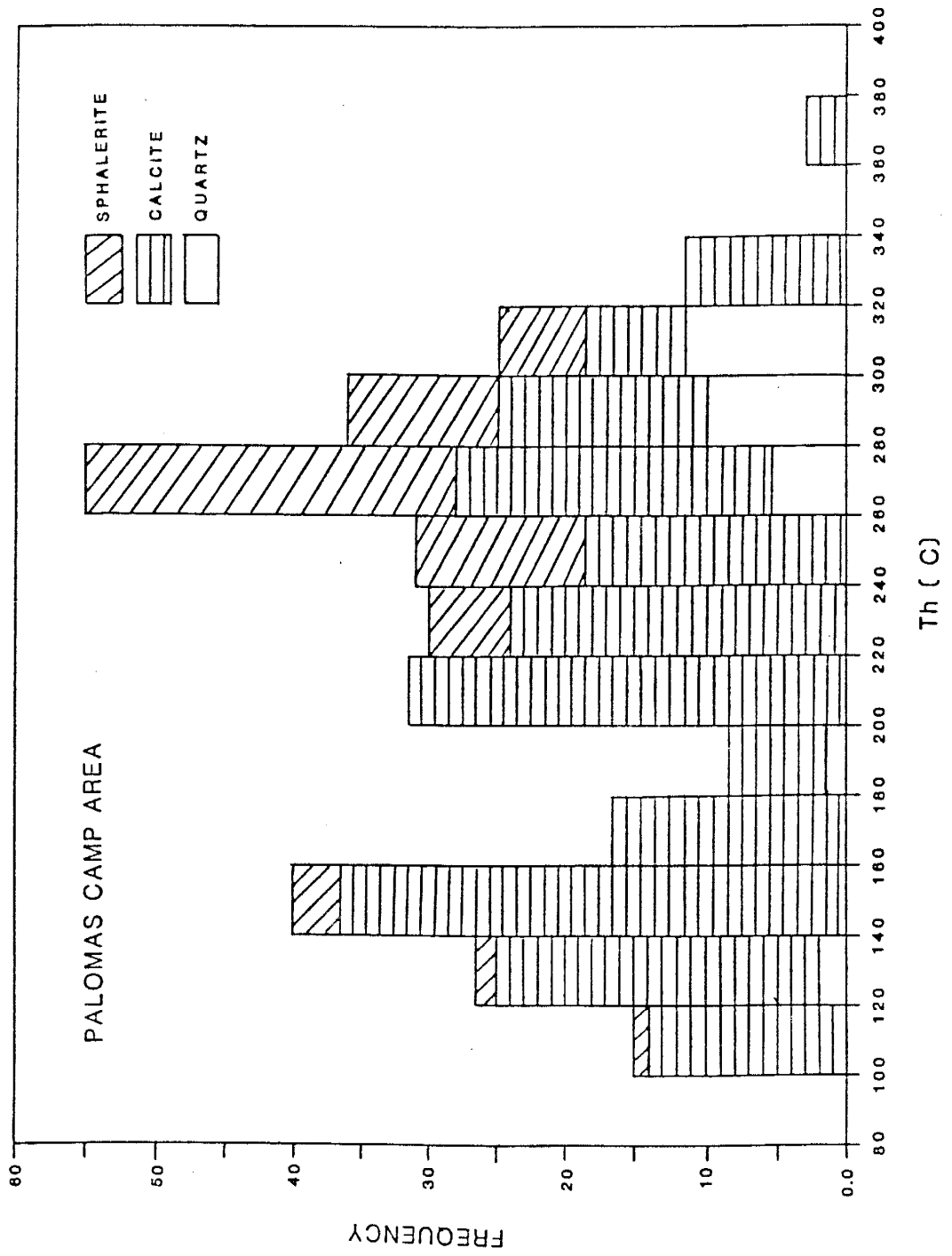
Although the samples from this area are jasperoid, the inclusions were large (5-25 microns), which is unusual for jasperoids. Types I, II, and III inclusions were observed and analyzed. Evidence of boiling in the form of gas-rich inclusions is fairly common.

PALOMAS CAMP

The Palomas Camp, which has been mined extensively, is located in the east-east central portion of the mining district. More than 2000 inclusions were analyzed from different workings. The results of 350 analyses from three important mines (Day, Wood, and Palomas Chief) are representative of inclusions from the Palomas Camp, and are shown in Figure 38. Inclusions in quartz show a wide Th range,

Figure 38.

Histogram of the homogenization temperature (Th) from fluid inclusions in quartz, calcite, and sphalerite from the Day, Wood and Palomas Chief (Palomas Camp) mines. Note the wide temperature range of calcite and sphalerite occurrences.



from 120 to 340 C with a dominant range of 260 to 320 C. Quartz is not abundant. Most of the analyzed samples are calcite. Th of inclusions in calcite ranges from 100 to 340 C. Two populations of Th can be observed in this figure. The first is associated with ore mineralization and the temperature range of 240-320 C. Inclusions of Type I and III in quartz, calcite, and sphalerite are dominant. Sphalerite, galena, and acanthite are associated with quartz and calcite which formed between 260 and 320 C, and sphalerite, acanthite, pyrargyrite, and polybasite are associated with calcite that crystallized in 220-260 C range. The second population is dominated by calcite and represents the late-stage of mineralization with a Th range of 100 to 180 C. The salinity of the first population ranges from 1 to 9 eq. wt.% NaCl and the second population from 0.5 to 4.5 eq. wt.% NaCl.

The results of temperature analysis from the Antelope-Ocean Wave mines and the Palomas Camp provide an east-west temperature profile of the mining district. This profile indicates that the temperature of mineralization in Palomas Camp is lower than that of the Antelope-Ocean Wave mines.

Approximately 3500 fluid inclusions, in samples from other workings, prospects, veins, and outcrops between the described areas, were analyzed. These analyses were done in order to determine possible trends of temperature or fluid composition change or fluid flow, from one location to another in the district. These analyses are the basis for the temperature distribution maps, fluid composition maps, and related maps

which show possible correlations among fluid composition,
fluid temperature, and ore mineralization.

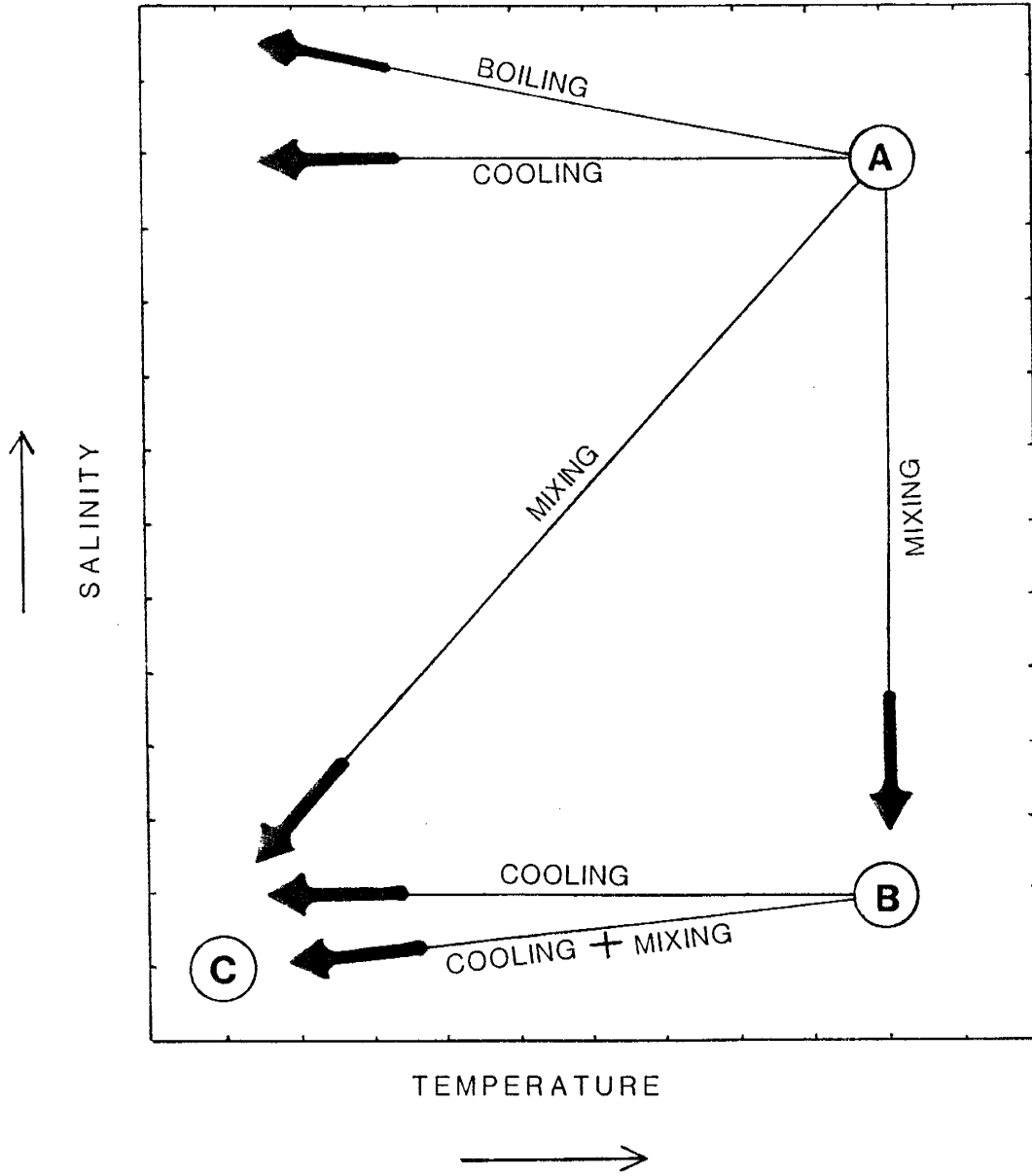
INTERPRETATION OF THE FREEZING AND HEATING DATA

Based on the temperature and salinity data obtained from various locations, it is clear that several fluid systems, with different temperatures and compositions, have been involved in the hydrothermal history of the district. Before discussing the results from each location, it is necessary to explain fluid behaviors in hydrothermal systems with different characteristics. Figure 39 shows the possibilities of boiling, mixing, and cooling behaviors of fluids A, B, and C in an hydrothermal system. ^{Fig 39} The possible behaviors are as follows:

- 1) The high temperature and salinity fluid A mixes with the high temperature and low salinity fluid B.
- 2) Fluid A mixes with the low temperature low salinity fluid C.
- 3) Fluid B mixes with fluid C.
- 4) Fluid A or B cools down with no salinity changes.
- 5) Fluid A or B cools down with some salinity changes (mixing).
- 6) Fluids A or B boil and cool down with some salinity increase because of the loss of water and other volatiles. During boiling a loss of 10 to 20 percent of fluid may occur and this will result in decreasing temperature and increasing salinity of the fluid system. Knowing this, it is possible to make a distinction between cooling due to boiling and cooling

Figure 39.

This diagram depicts the theoretical existence of different types of fluids in a hydrothermal system and the interactions between these fluids. Trends for boiling, mixing or cooling of one or more fluids are shown.



because of normal loss of heat to the ambient environment.

WOLFORD MINES

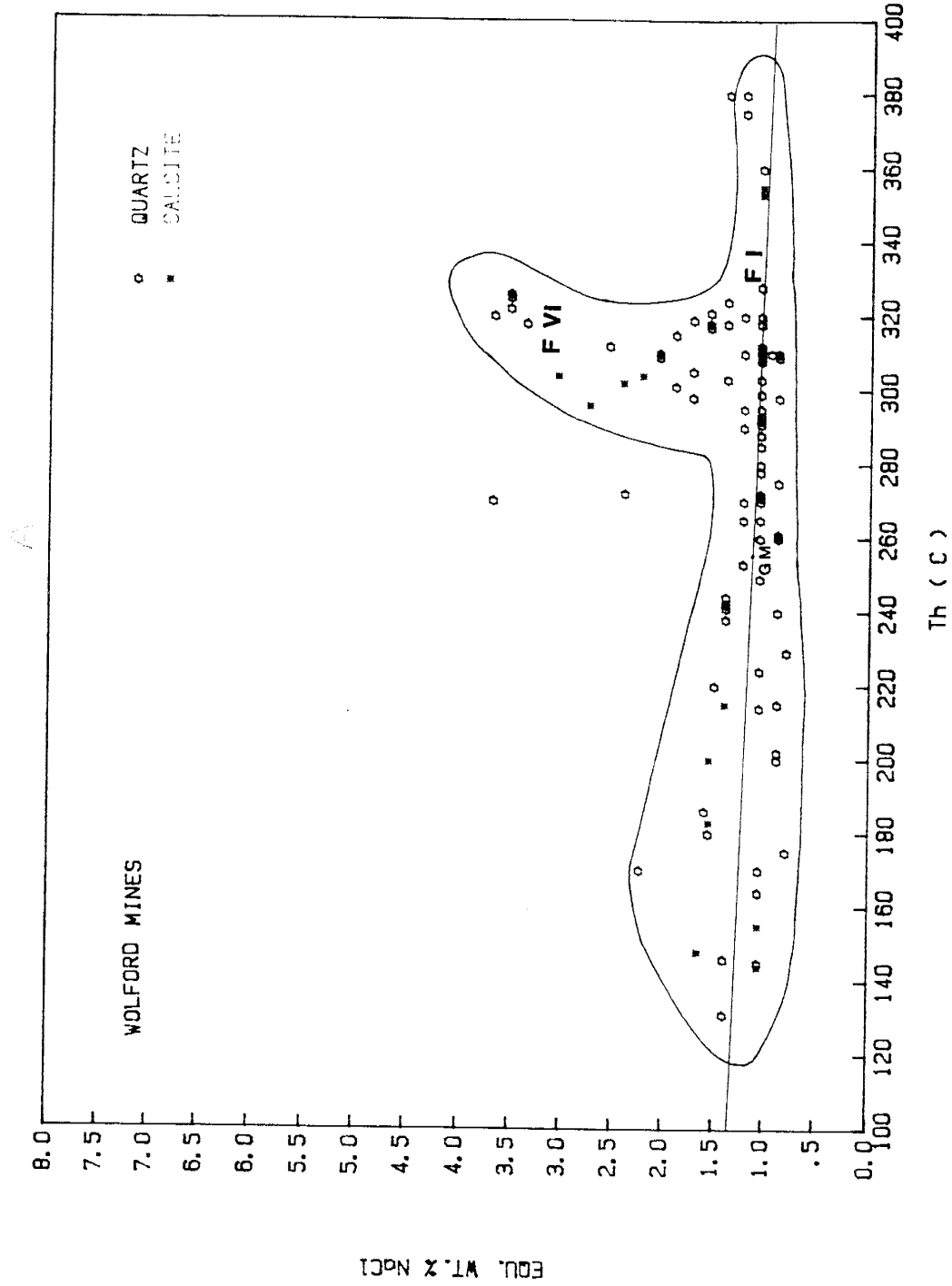
The results of freezing and heating analyses of inclusions at different stages of mineralization in the Wolford mines are shown in Figures 40-A and 40-B. Figure 40-A shows the presence of two types of fluids with different salinities during the early stage of mineralization. Fluid VI (F VI) with a high salinity of 3.5-4 eq. wt.% NaCl and a high temperature of 300-340 C mixes with fluid I (F I) with low salinity of 0.5-1.5 eq. wt.% NaCl and slightly lower temperature of 280-320 C. F VI fluid is mainly observed in Type I and III inclusions, and F I is observed in Type II and III inclusions at higher Th and Type I inclusions at lower Th.

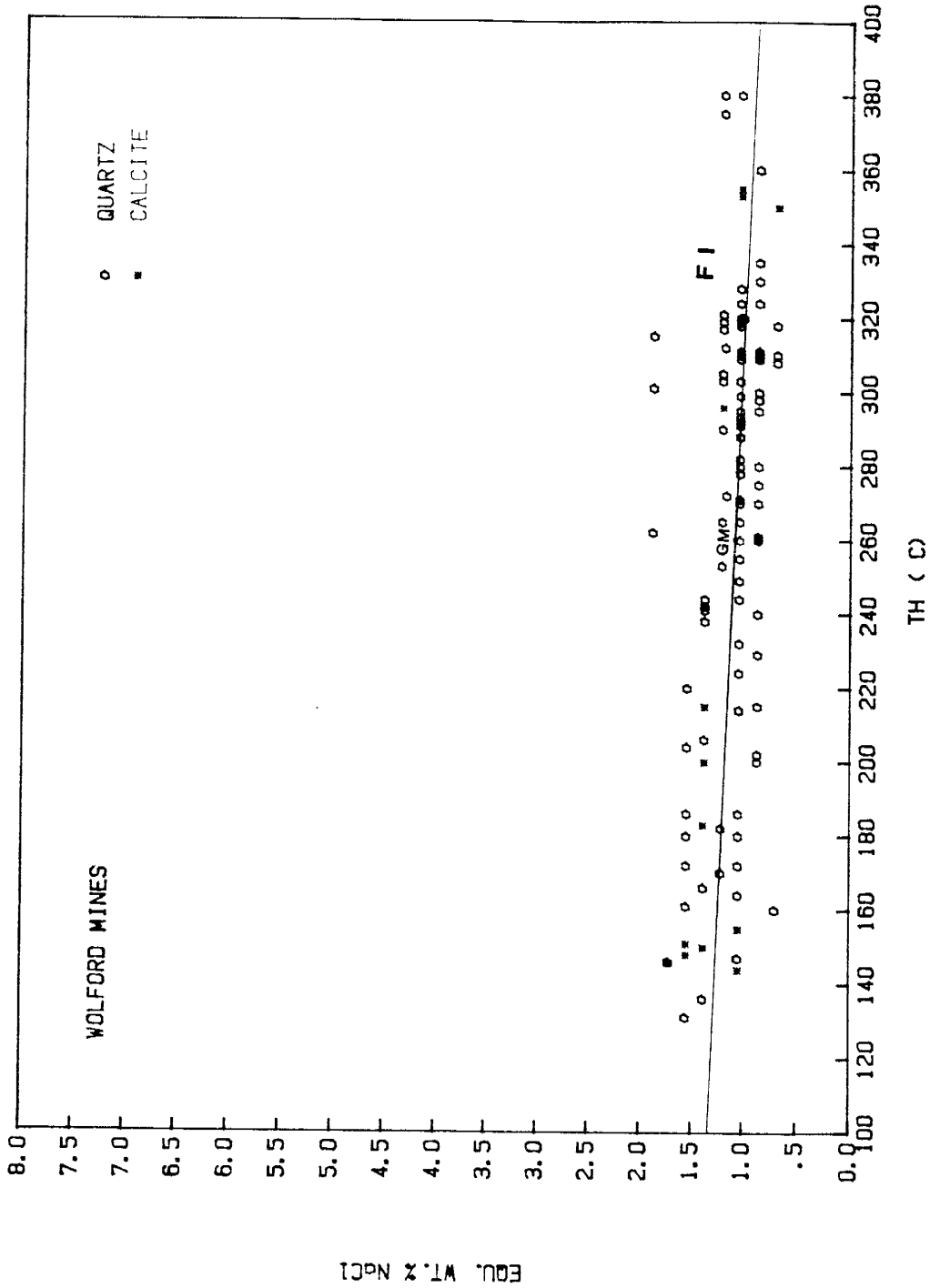
Figure 40-B shows Th and salinity data for ore and late stages of mineralization in the Wolford mines. Paragenetically, it was possible to separate the inclusions in the early quartz and calcite from the rest of the inclusions. If this separation is correct, then Figure 40-B indicates that boiling prevailed during the ore mineralization after the early-stage. This assumption is supported by a higher number of Type II and III inclusions and the increase of salinity as the fluid cools due to boiling. Another possibility is to conclude that the increase of salinity in the cooler fluid was the result of mixing of F I and F VI fluids. Furthermore, based on the limited number of inclusions

Figure 40.

Plot of temperature (T_h) versus salinity for the Wolford mines.

- A: F I fluid with salinity of 0.5-1.5 eq. wt.% NaCl mixes with F VI fluid with salinity of 3.5-4 eq. wt.% NaCl. F VI fluid is largely seen in Type I and III inclusions.
- B: F I fluid boils and the salinity of the fluid increases as it cools down due to boiling. The increase of salinity is about 20%. The Grand Mean (GM) and the slope of the line has been calculated using a formula from Renault (1970). All types (but fewer Type III) inclusions are present in this group. Gold and silver mineralization is associated with F I fluid.





with high salinity (F VI fluid), it is concluded that the volume of this fluid was small, so that in mixing with the F I fluid, salinity was increased by 10 percent or less. In Figure 40-B the grand mean (GM) of all the heating and freezing data and the slope of the line are calculated from the formula given by Renault (1970). The calculated line shows about 18% increase of salinity at the closing stage of mineralization. Mixing of F I and F VI fluids may have initiated mineralization, but boiling was the main mechanism of ore deposition in the Wolford mines.

ANTELOPE-OCEAN WAVE MINES

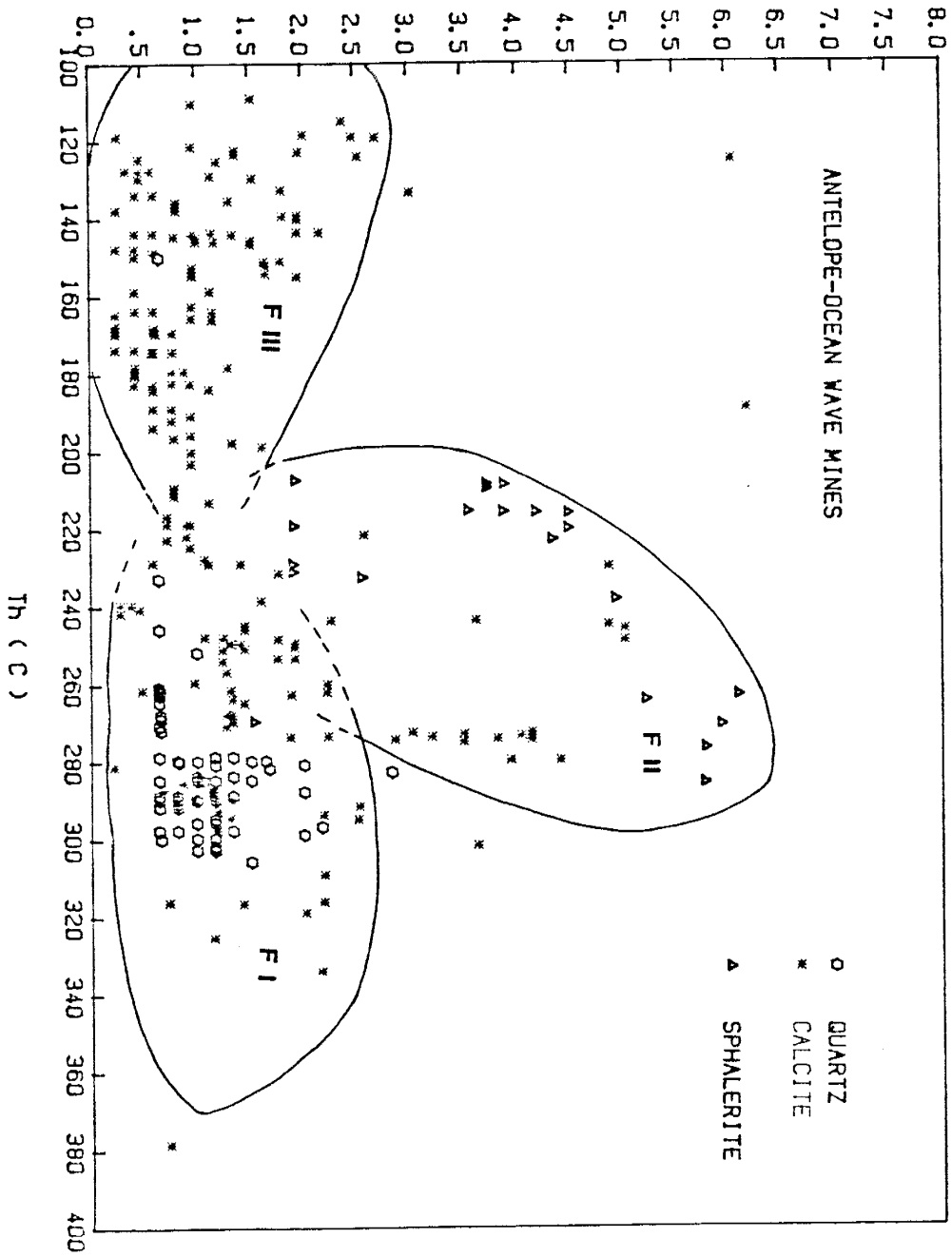
Figure 41 shows the Th and salinity data of all primary inclusions (Type I, II, and III) analyzed in samples from the Antelope-Ocean Wave mines. Three types of fluids with different salinities and temperatures are recognized in these mines. The first fluid (F I) represents the main ore forming fluid with a temperature range of 240-300 C and a salinity of 0.3 to 2.5 eq. wt.% NaCl. Th and salinity of this fluid is similar to that of F I in the Wolford mines in the north of the mining district. This fluid is responsible for most of quartz mineralization in these mines. The second fluid (F III), with the temperature range of 120 to 180 C and salinity of 0.3 to 2.5 eq. wt.% NaCl, represents the late stages of mineralization. No ore deposition is associated with this fluid. The majority of inclusions from this fluid are Type I

Figure 41.

Plot of temperature (Th) versus salinity from the Antelope-Ocean Wave mine. Three types of fluids are recognized:

F I fluid with salinity of 0.5-1.7 eq. wt.% NaCl
F II6 to 9
F III.....0.3-2

EQU. WT. % NaCl



inclusions. Calcite is the dominant mineral that was deposited by this fluid. A limited mixing between fluids F I and F III is inferred from the data. Little or no ore mineralization was associated with this mixing. The third fluid (F II), with the temperature range of 260 to 280 C and the salinity of about 6 eq. wt.% NaCl, represents a different ore forming fluid. Sphalerite is the main ore that was deposited by this fluid. The F II fluid cools down and its salinity decreases at the same time. This behavior suggests that the F II fluid is mixing with cooler and less saline fluid or fluids. The F III fluid could be the fluid that mixed with F II fluid. If this is true, the salinity increase of F III fluid at about 120 to 140 C could be explained. In addition to the fact that mixing of F II and F III fluids would increase the F III salinity, a careful study of Figure 41 reveals that this increase could also be the result of a short period of boiling at lower temperature due to a sudden decrease of pressure. If this latter interpretation is correct, the presence of gas-rich inclusions (Types II and III) in calcite of low temperatures, could be explained.

Figure 41 shows that all three types of fluids are mixing at one point (200-220 C range). The mixing of the F I and F II fluids caused the main stage of ore deposition and the late stage sphalerite mineralization. Galena, sphalerite, chalcopyrite, tetrahedrite, and gold were deposited first in the temperature range of 260-290 C, and acanthite, polybasite, native silver, and sphalerite were deposited later between 240

and 270 C.

From the analysis of the microthermometric data and paragenetic analysis of ore and gangue minerals, it is concluded that mixing and a short period of boiling (evidenced by a limited number of Type II inclusions) were the main mechanisms of ore mineralization in these mines. The fluid which contained most of the metals had the temperature range of 260-300 C and salinity of 0.5 to 2.5 eq. wt.% NaCl.

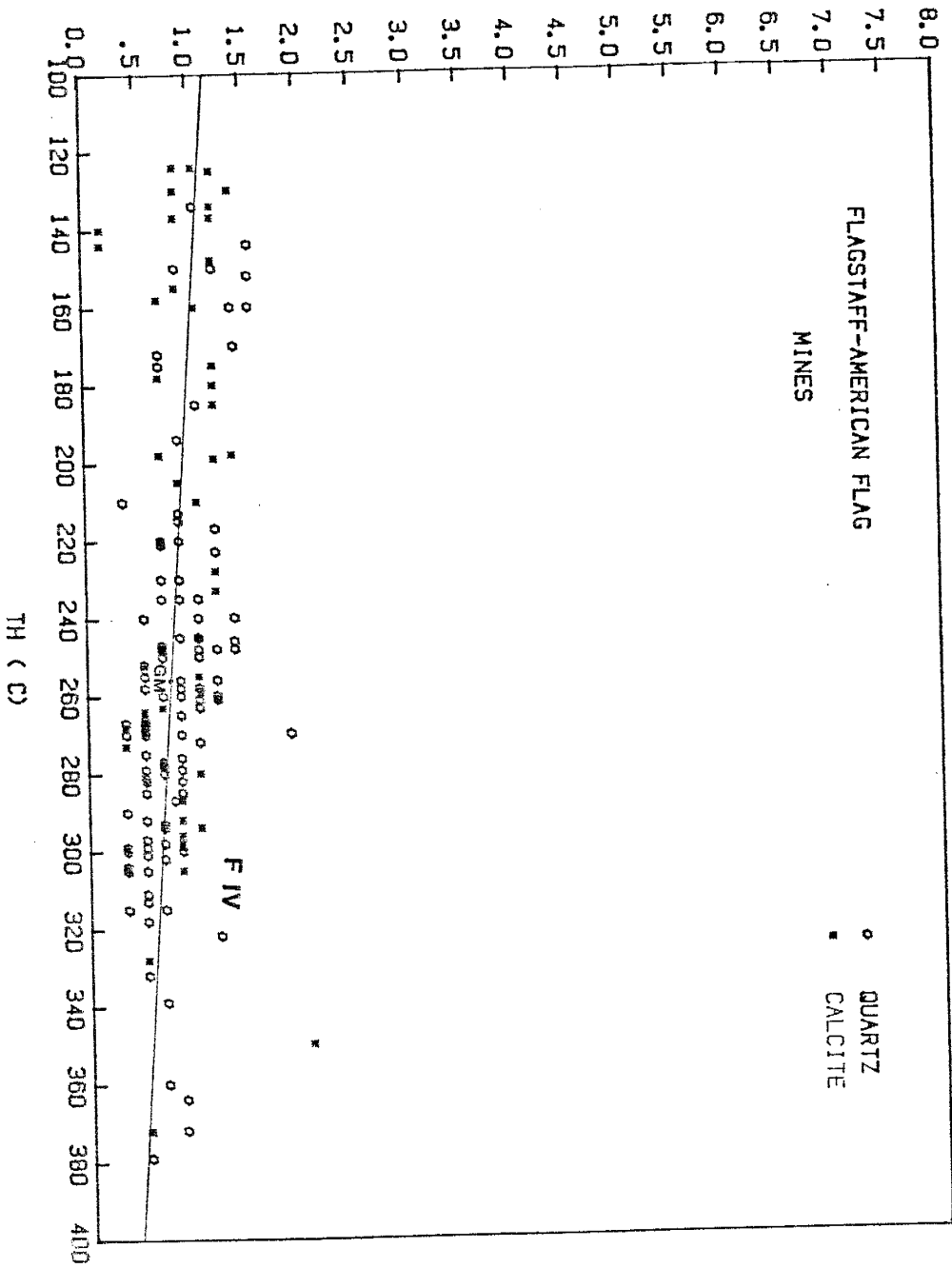
FLAGSTAFF-AMERICAN FLAG MINES

Salinity and Th data from Flagstaff-American Flag mines (about one mile south to southeast of the Antelope-Ocean Wave mines) are presented in Figure 42. Silver minerals and galena are associated with quartz and calcite deposited in the temperature range of 250 to 300 C. Inclusions of Type III and II are abundant in quartz and calcite as gangue minerals. The salinity of the hydrothermal fluid in all types of inclusions increased constantly with decreasing temperature. The salinity of the fluid system increased from 0.3-1 eq. wt.% NaCl in the 300-320 C temperature range to 1-1.6 eq. wt.% NaCl between 160 and 240 C. This reverse change of salinity and temperature indicates the presence of a boiling condition during the early stage of quartz and calcite mineralization and during the ore deposition stage in these mines. In Figure 42, the calculated line indicates that the salinity of the boiling fluid increased about 15-25% while it was cooling down

Figure 42.

Plot of temperature (T_h) versus salinity from Flagstaff-American Flag mine. Note the increase of salinity as the fluid cools down due to boiling.

EQU. WT. % NaCl



108

as a result of boiling. In comparison to the other fluids in the district, the fluid system in these mines is similar to F I in the Wolford and the Antelope-Ocean Wave mines.

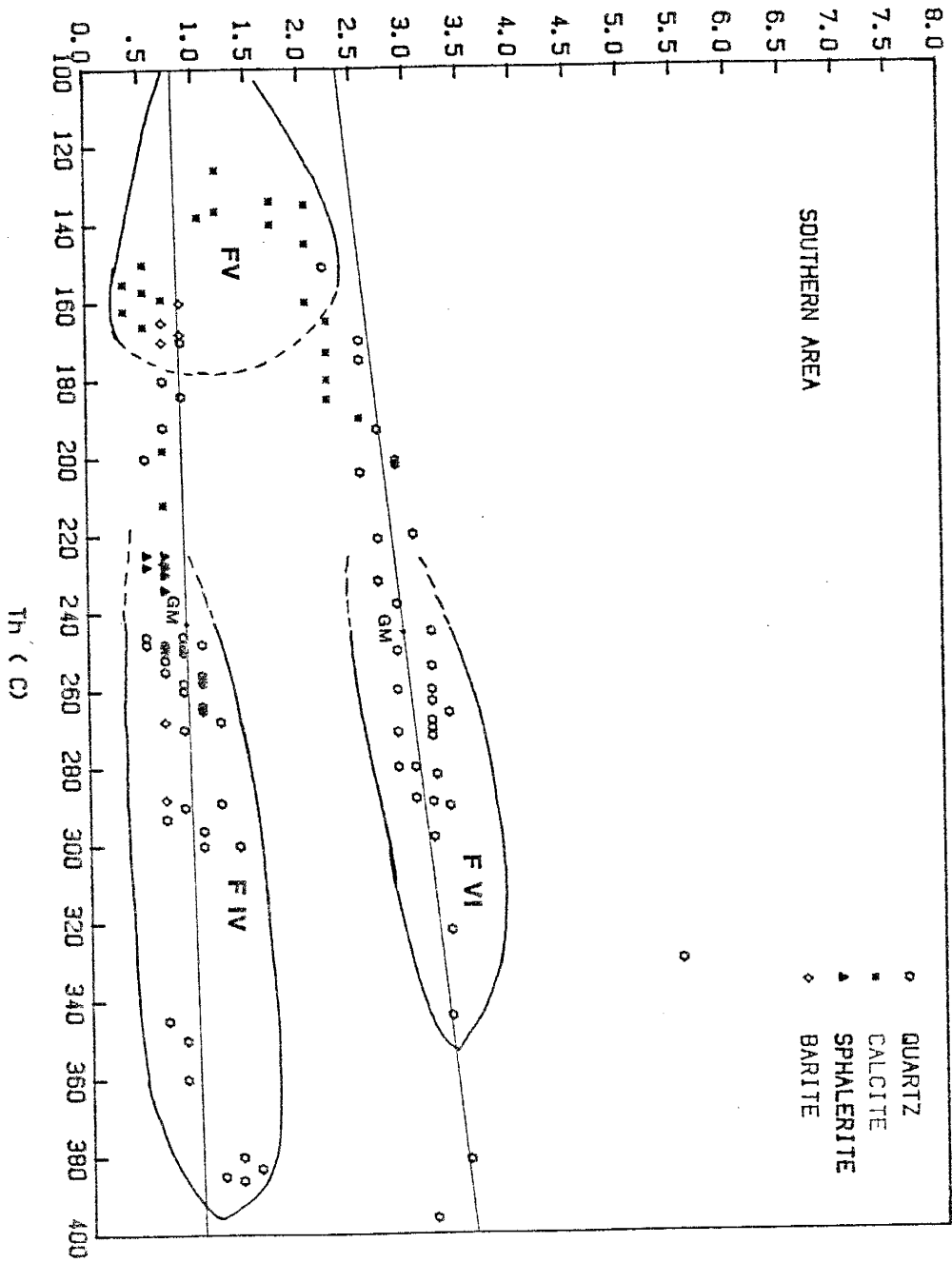
SOUTHERN AREA

Results of Th and salinity analyses from the southern part of the district (about 2.5 miles south of the Flagstaff-America Flag mines) are shown in Figure 43. Three types of fluids with different salinities and temperatures are recognized. F IV fluid with the Th range of 250-300 C and salinity of 0.7 to 1.5 eq. wt.% NaCl is the fluid responsible for the low grade ore mineralization. F VI fluid with the Th range of 250-300 C and salinity of 2.5-3.5 eq. wt.% NaCl caused the main ore mineralization stage in this area. The third fluid (F V) has a low temperature (120-140 C) with salinity of 0.3-.7 eq. wt.% NaCl. It appears that this fluid was cool (20-40 C) ground water, and that it warmed up because of mixing with F V and F VI fluids. Because the F VI fluid was more saline than F IV fluid, the calculated mixing line with F V (Fig.43) has a steeper slope. Several gas-rich (Type II and III) inclusions with high Th (320-390 C) suggest the presence of an early boiling condition in this area. However, the main mechanism of ore mineralization was the mixing of F VI and F IV fluids with cool ground water (F V). As is true in other areas in the district, quartz and ore mineralization occurred at higher temperatures and calcite, with little or

Figure 43.

Plot of temperature (T_h) versus salinity from the southern area. F IV fluid with 0.7- 1.5% salinity and F VI fluid mix with F V fluid and cool down. Note that F IV and F VI do not mix with each other due to their density difference.

EQU. WT. % NaCl



no ore mineralization occurred in cooler environments. However, this is not true everywhere.

Sphalerite from the southern area shows lower salinity and Th than sphalerite from other parts of the district. Sphalerite in the southern area is deposited in the late stage of ore mineralization. The relatively high (1-3 ppm) gold values in this area were deposited by F VI fluid.

PALOMAS CAMP

Temperature-salinity data from the Day and Nana-Humming Bird mines in Palomas Camp, the most productive area in the Hermosa mining district, are plotted in Figure 44. Palomas Camp has three types of fluids with different salinities and temperatures. F I has a temperature range of 260-320 C and salinity of 0.7 to 2.3 eq. wt.% NaCl, which is very similar to the F I fluid in other areas in the district. Sphalerite, galena, chalcopyrite, acanthite, and polybasite have been deposited by this fluid. The second fluid is F II with a temperature range of 270- 310 C and salinity of 6.5-9 eq. wt.% NaCl. Sphalerite, and argentiferous galena were deposited by this fluid. The third fluid is F V, a cool (40 C) fluid with salinity of about 0.5 eq. wt.% NaCl. This temperature and salinity are those of ground water in the district at the time of the hydrothermal activity.

F I and F II fluids do not mix with each other, but they mix with the F V fluid separately. Figure 44 shows that mixing

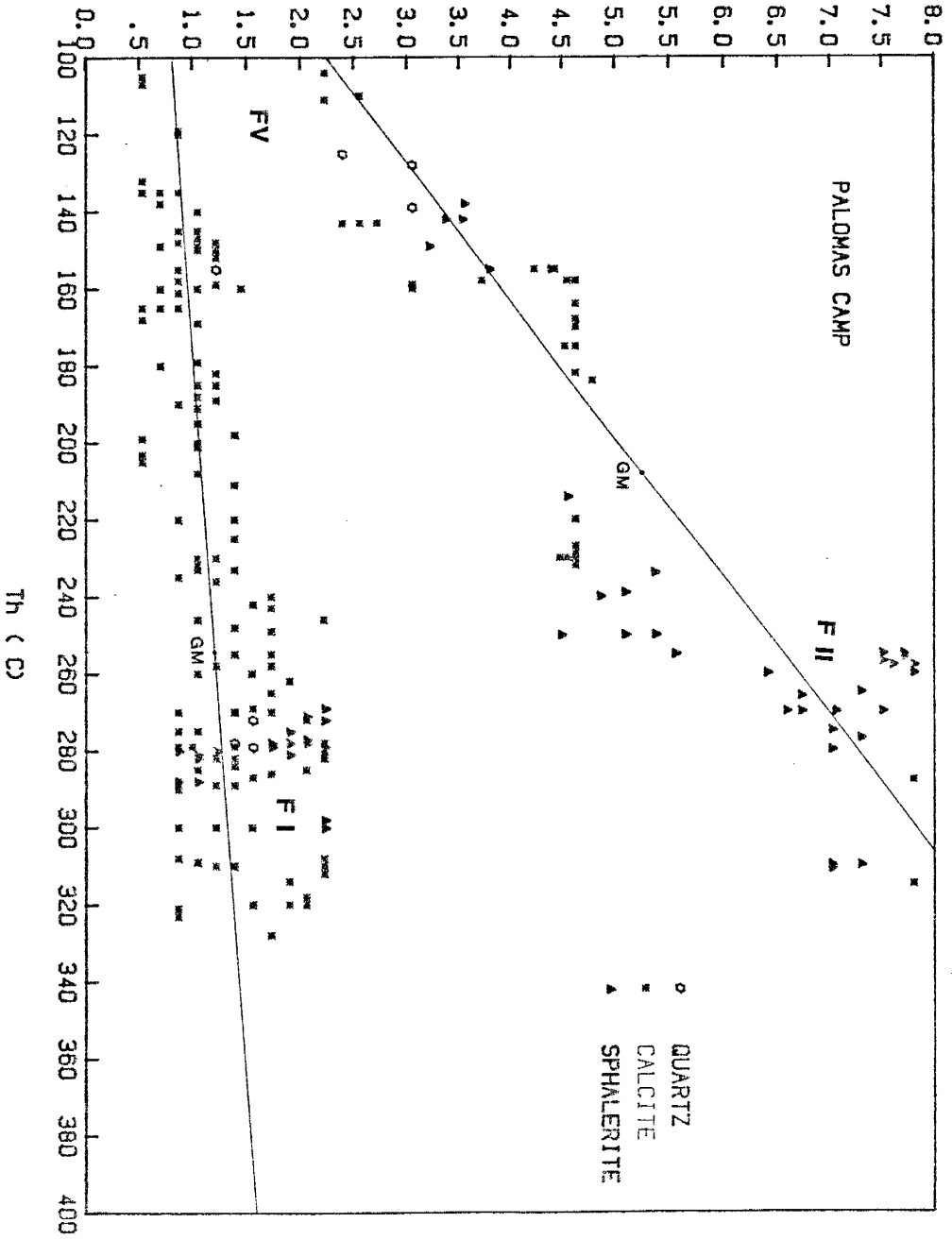
Figure 44.

Plot of temperature (Th) versus salinity from the Paloma Camp area.
Three types of fluids are recognized:

F I fluid with salinity of 0.7-2.3 eq. wt.% NaCl.
F II6.5-9
F V0.5.....

The mixing trends of F I and F II fluids with F V fluid are
calculated.

EQU. WT. % NaCl



was the main mechanism of ore deposition in the Palomas Camp area. The mixing lines of F I and F II fluids with F V fluid intersect at about 40 C at a salinity of about 0.5 eq. wt.% NaCl which is very similar to ground water.

PART II

GAS ANALYSIS

GAS ANALYSIS OF THE FLUID INCLUSIONS

INTRODUCTION

The study of the composition of volatiles in hydrothermal systems has provided useful information about physicochemical conditions of mineral solubility and deposition in such systems (Ewers and Keays, 1977; Henley and Ellis, 1983; Henley et al., 1984; Henley, 1986; Henley, 1989). The preserved liquid and gas phases of paleohydrothermal systems in fluid inclusions from ore deposits have been used to determine the physicochemical conditions of ore deposition in different environments (Henley, et al. 1984; Henley 1989; Norman, 1977; Norman and Sawkins, 1987; Piperov and Penchev, 1973).

Different techniques and related problems of the analysis of gases in individual inclusions or bulk analysis of inclusions in several grams of samples are discussed in detail by Norman (1977), Norman and Sawkins (1987) and Piperov and Penchev, (1973). Bulk analyses were made of volatiles of both primary and secondary inclusions from quartz and calcite.

SAMPLE PREPARATION

Of 75 quartz and calcite samples, district-wide, selected for gas analyses all but five were associated with ore mineralization stages. The samples were first ground by mortar and pestle to -10 to +40 mesh. Impurities, which were mostly

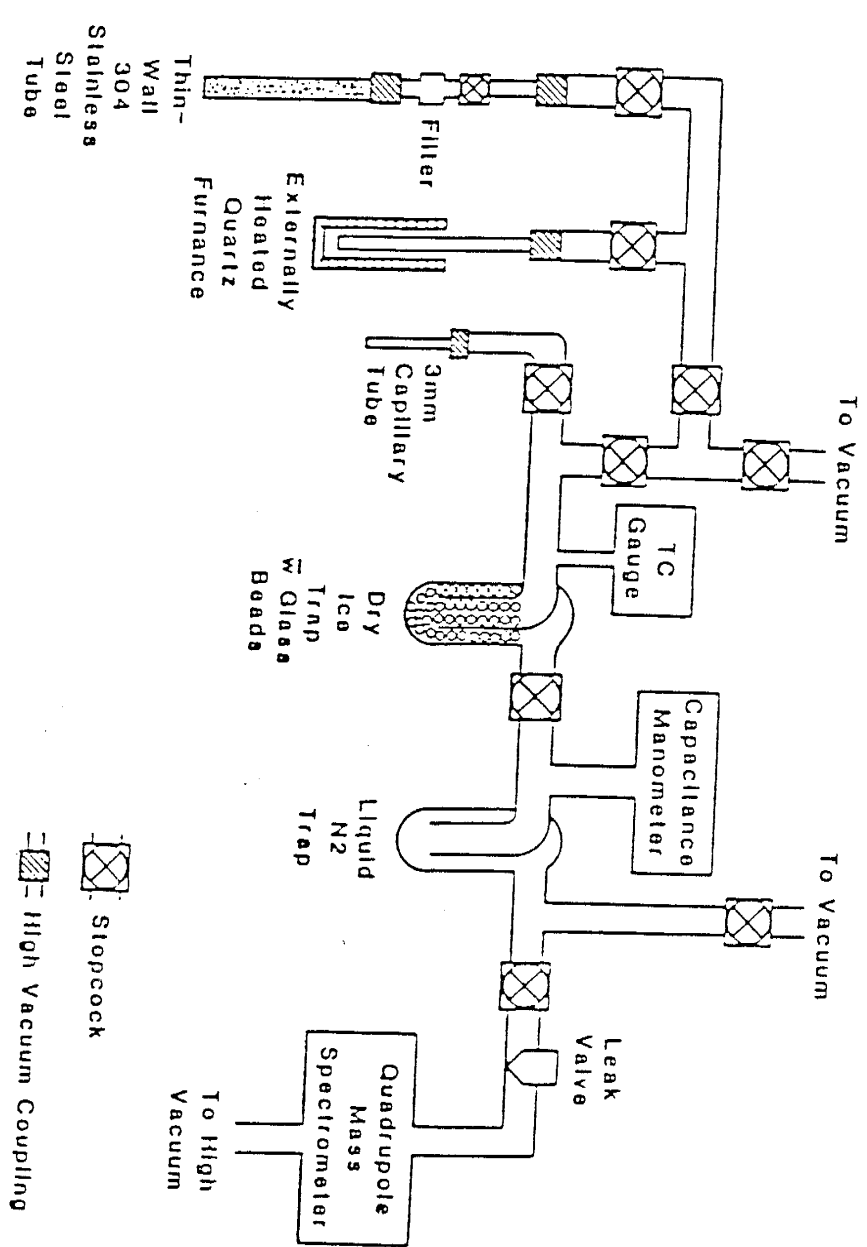
sulfide minerals, were sorted out by hand . Each sample was placed in a beaker containing a solution of 50% distilled-deionized water and 50% HCl. The beaker was placed on a hot plate at 90-100 C temperature for 24 hours. The sample was rinsed in distilled-deionized water several times, and water was added to the sample and was placed on the hot plate for another 24 hours. The sample was rinsed several times and a solution of 10% of sodium hydroxide was added and placed on the hot plate for 10 hours. The sodium hydroxide solution dissolves and removes any organic material on the surface of the grains. The sample was rinsed in distilled-deionized water, put in water and placed on the hot plate for about 24 hours. After rinsing, the sample was placed in an oven at the temperature of 70-80 C.

INSTRUMENTATION

The apparatus used in these analyses consists of a vacuum extraction line and a quadrupole mass spectrometer (Fig.45). The extraction line consists of two external heaters which thermally decrepitate and release volatiles from fluid inclusions, a high vacuum Pyrex tubing with vacuum Teflon valves in different sections of the line for separating different species of gases, a capacitance monometer for measuring the pressure of the released volatiles in the line, a leak valve for releasing the gas sample into the mass spectrometer, and a turbo molecular vacuum pump with attached

Figure 45.

Schematic diagram of the gas analysis apparatus.



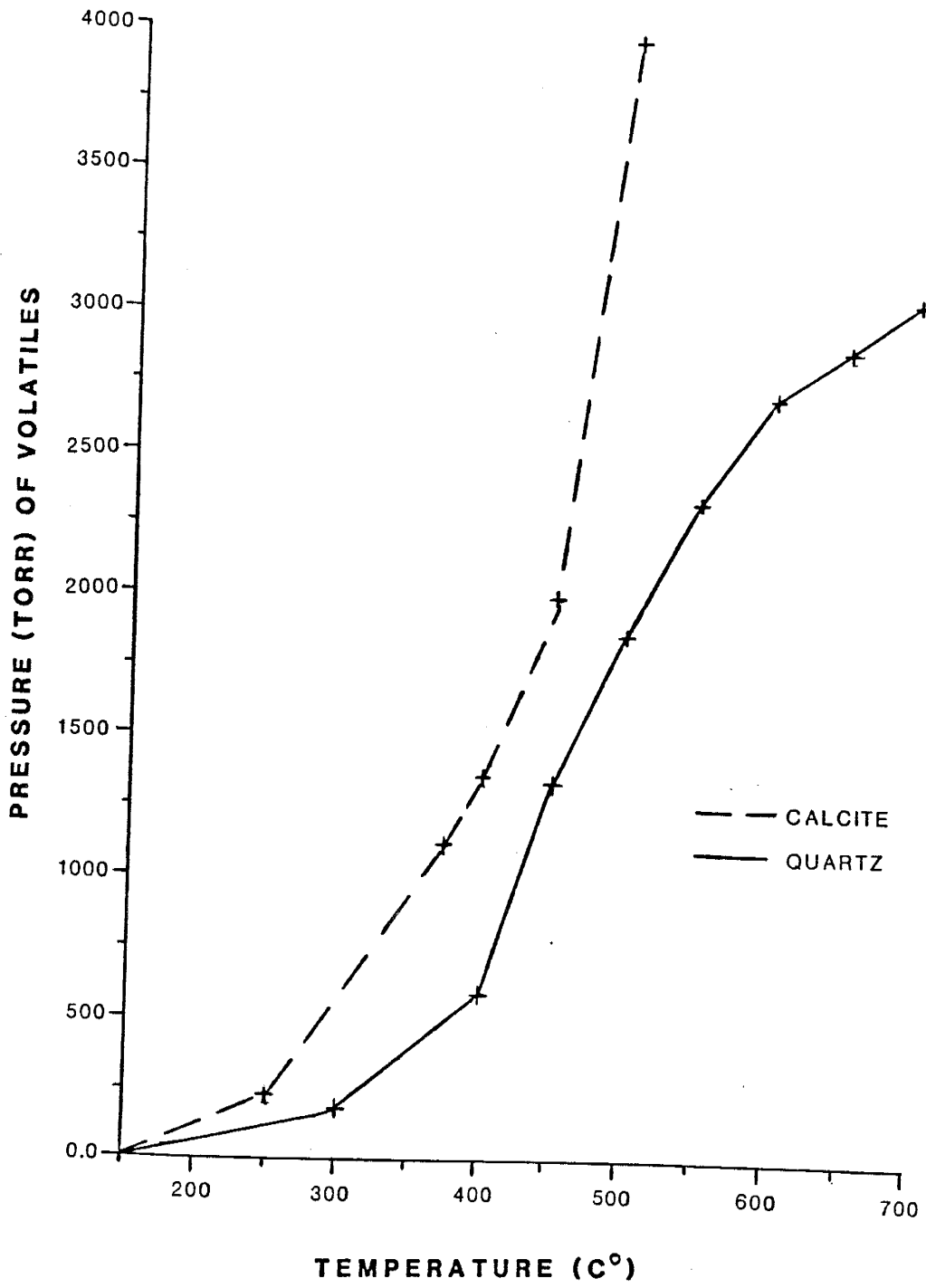
rotary vane pump. The quadrupole mass spectrometer is an INFICON IQ200. It can measure and identify gases of mass number 1 to 200. The mass spectrometer is connected to a second turbo molecular vacuum pump. The instrument is interfaced with a Hewlett Packard 85 computer for recording and reducing the gas data.

For each analysis, approximately 5 grams of cleaned sample was placed in the fused-quartz furnace connected with the vacuum-extraction line (Fig. 45). The quartz tube with the sample was evacuated by rotary vane pump to a pressure of 1×10^{-2} torr and followed by the high vacuum. The sample was heated for at least 6 hours at a temperature of 150 C. The high vacuum and heating remove the absorbed air, water, and other contaminants from the sample. After heating and pumping, a pressure of 3×10^{-3} torr or lower was attained in the line. The pressure in the mass spectrometer was kept at 1×10^{-2} torr at room temperature (25 C). The electron multiplier of the mass spectrometer was set at 2200 volts.

At high temperature, some minerals such as calcite may decompose and produce gases which do not belong to the gas phase of fluid inclusions under study. To avoid this problem, samples of quartz and calcite were step-heated in the extraction line and the pressure for each step was recorded (Fig.46). At approximately 400 C, calcite samples showed a sudden increase of gas pressure. The analysis of the volatile phase showed large amounts of CO₂, which confirmed the decomposition of the calcite sample. A minor increase of

Figure 46.

Decrepitation and decomposition curves for calcite and quartz samples from the Hermosa mining district due to step heating. Note the sudden volatile pressure increase of the calcite sample around 400 C which indicates the decomposition of calcite.



volatile pressure was observed for quartz samples above 500 C. Based on these observations, it is concluded that the safe and proper decrepitation temperature for quartz samples from this district is 500 C and, for calcite samples, 400 C.

In order to analyze volatiles in the samples, the following procedure was followed for each sample. The extraction line was isolated from the quadrupole mass spectrometer and vacuum pumps. Quartz samples were heated to 500 C and calcite samples to 400 C for about 15 minutes to decrepitate the fluid inclusions in the samples. The volatile components were separated into three portions, according to their boiling points. Water was trapped with a mixture of dry ice and alcohol (-78 C) in a cold trap. The condensable gases such as CO₂, H₂S, SO₂, and C_nH_n hydrocarbons were trapped with a liquid nitrogen cold trap (-196 C). Noncondensable gases such as H₂, He, Ar, N₂, CO, and CH₄, remained in the vacuum line. Before each analysis, a background run was performed. After the background run, the noncondensable phase was scanned from mass 1 to 40. After evacuating the remaining noncondensable phase by high vacuum pump, the condensable phase was evaporated by removing the liquid nitrogen cold trap. The condensable phase was scanned from mass 2 to 100. After removing the rest of the condensable phase, the water was evaporated and trapped in a capillary tube with liquid nitrogen bath, sealed, removed, and weighed.

The relative amounts of each gaseous species were calculated from the mass spectra using a least-squares matrix

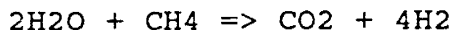
computation and sensitivities determined from standards. Using the amount of gas, volume of the extraction line, and the pressure of the gas, total moles of gases were calculated. The volume of the extraction line was calculated with liquid nitrogen and dry ice-alcohol traps on. The amounts of water and gas were measured with an accuracy of + 3% (Norman and Sawkins, 1987). The measured internal precision of the mass spectrometer is + 1.7. Shepherd (1985) and Norman and Sawkins (1987) noted that the changes of the original gaseous phase in fluid inclusion due to gas reactions by derepitation are quantitatively insignificant.

RESULTS OF GAS ANALYSIS

The volatile species measured by bulk analyses of fluid inclusions from different localities are listed in Appendix IV. The results are recorded as mole % including water as a gaseous species. The principal gases observed were CO₂, CH₄, H₂S, N₂, H₂, C_nH_n, CO, He and Ar. Total gas measured varied between 0.1 to 5 mole % with an average of 0.5 to 1 mole %.

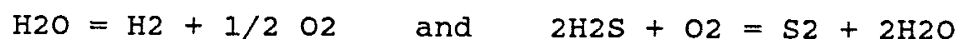
The amount of volatiles in inclusions varies in different localities and elevations. The concentration of gas species such as CO₂, H₂S and CH₄ is higher in samples which show boiling condition illustrated by high numbers of gas-rich inclusions. Different species of volatiles have higher concentrations in different localities. Higher H₂S concentrations are present in the Wolford mines, the Antelope-

Ocean Wave mines, the Flagstaff-American Flag mines, and the southern area. The southern area shows the highest concentration of H₂S. All these localities are closely associated with the Bull Frog fault in the center of the district. The highest concentrations of CO₂ are observed in the Palomas Camp area. The amount of CO₂ decreases in samples closer to the Bull Frog fault. The CO₂:H₂S ratio in these deposits is in the range of values (1-100) from active and fossil geothermal systems reported by Henley (1986). The higher concentration of CO₂ in Palomas Camp may reflect analytical problems due to the thermal decrepitation of calcite samples in this area. In addition to a high concentration of CO₂ and H₂S, Appendix IV also shows a high concentration of hydrogen in the analyzed samples. Considering that the volatiles were released by thermal decrepitation, it is possible that, at high temperature of decrepitation (400-500 C), the gases have reequilibrated. This reequilibration would increase the amount of CO₂ and H₂ according to the reaction:



Norman (unpublished) has developed a computer program (GASFIX) to calculate gas concentrations more representative of the phases present at the trapping temperature of the fluid. This program also calculates oxygen and sulfur fugacities from the measured gas concentrations based on the

reactions:



Appendix V lists the recalculated gas concentration. Oxygen and sulfur fugacities, Th, and salinity of inclusions are also listed in the appendix.

STABLE ISOTOPE ANALYSES

Decrepitated quartz and trapped water of six samples from different localities in the Hermosa mining district were subjected to oxygen and hydrogen isotope analyses at Yale University by Dr. A. Campbell.

The δD values were determined from the extracted waters of the fluid inclusions. These values ranged from -33 to -170 per mil. For present day groundwater the δD is -88.6 to -90.5 per mil and for Tertiary meteoric waters this value is -42 to -43.8 per mil (Taylor, 1974). The $\delta^{18}\text{O}$ values for quartz ranged from 5.68 to 11.16 per mil. The $\delta^{18}\text{O}$ value of the water of the fluid inclusions was calculated from the $\delta^{18}\text{O}$ compositions measured in quartz and average Th using the following equation by Clayton (1972):

$$\delta^{18}\text{O water} = \delta^{18}\text{O qtz} - 3.57 (10^{+6} / \text{Th})^2$$

The calculated $\delta^{18}\text{O}$ values from water ranged from 0.94 to -

5.41 per mil. The results of the isotopic analyses and calculations are listed in Table 4.

Figure 47 is a plot of δD vs. $\delta^{18}O$ of analyzed samples (calculated water) from the district. Values for present-day and Tertiary meteoric waters (Taylor, 1974) and magmatic water values are shown. The $\delta^{18}O$ values of all analyzed sample (except for CP Int-25) vary within a narrow range. These values suggest isotopic exchanges between Tertiary meteoric waters with magmatic water or with Tertiary igneous rocks in the district during hydrothermal events. The analyzed samples are associated with an ore mineralization stage. Epithermal systems that are composed of only meteoric waters have a fairly constant δD value. The δD values of the analyzed samples do not show any particular trend or characteristic. The wide range of δD could be attributed to the thermal decrepitation of the fluid inclusions for gas analyses. The high decrepitation temperature (500 C) may have effected the isotopic composition of the released water and gases. The volatiles may have reequilibrated at the decrepitation temperature which is above the T_h of the fluid inclusion. These possible reequilibrations and isotopic exchanges between different components of the fluid system may be responsible for the wide range of the δD values in the district. Another possible source for the wide range of the δD is contamination of the extraction line by air leaking into the system.

Table 4. Oxygen and Hydrogen stable isotope data (per mil).

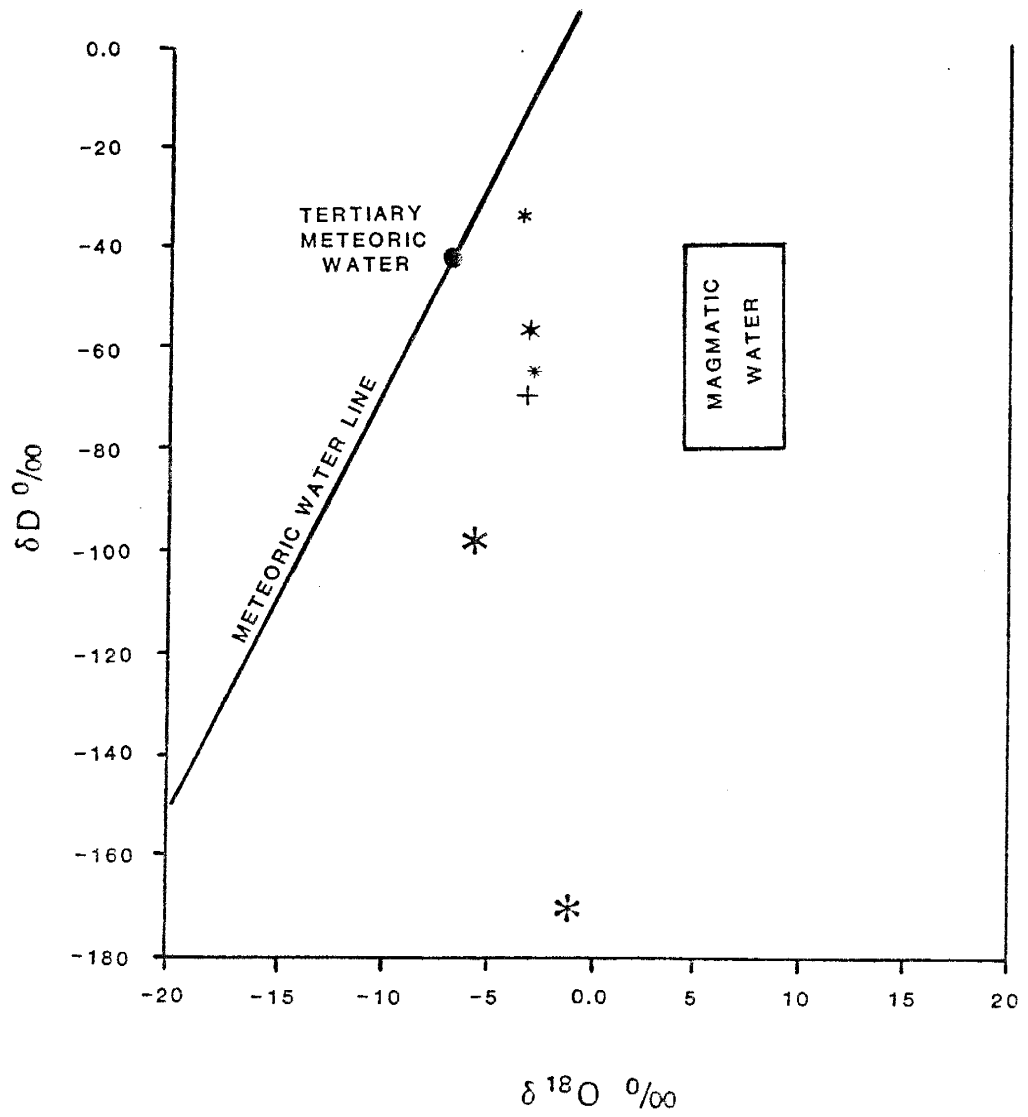
Sample	δ O Quartz	δ O Water	δ D Water
Prt-86-Ore	6.04	-3.38	-33
Prt-86-Up	6.26	-3.11	-69
Flagsataff	5.99	-2.95	-57
Wlf-83-3	5.68	-2.85	-64
MK-4	7.67	0.94	-170
CP Int-25	11.16	-5.41	-97

Figure 47.

Plot of $d D$ versus $d O$ for samples (calculated waters) from the Hermosa mining district.

- * Prt-86-ore (ore)
- * Flagstaff (ore)
- * Wlf-83-3 (ore)
- + Prt-86-up (non-ore)
- * CP-Int-25 (non-ore)
- * MK-4 (ore)

The accuracy of the $d D$ values is unknown because the effect of the decrepitation procedure has not been evaluated.



HELIUM ISOTOPE ANALYSES

The different ranges of helium isotopic compositions in different geologic environments have been used as tracers to determine the origin of fluids and gases in these environments. Helium isotope data are denoted as ratio (R) of ^3He to ^4He compositions and is expressed in a ratio with the R-value of air ($R_a : 1.4 \times 10^{-6}$). Helium isotope ratios $R/R_a > 2$ occur only in magma-based geothermal systems (Welhan et al. 1988). A direct correlation exists between geothermal reservoir temperature and helium isotope ratio of fluids, suggesting that both heat and helium in a geothermal reservoir are derived from a shallow magmatic source. The helium isotopic compositions from various environments and the analyzed sample from the Hermosa mining district are shown in Table 5.

The R/R_a value measured for the Hermosa sample suggests a mantle helium component in the inclusion fluid. This value suggests that the heat source, and possibly, some of the volatiles of the fluid system responsible for mineralization in the district were magmatic. The $\delta^{18}\text{O}$ data and the presence of igneous intrusives in the vicinity of this sample support this conclusion. A possible source of error in the helium isotope data from the Hermosa sample is the presence of the Abo Formation in the district, which contains uranium-bearing minerals. Uranium and thorium continue to decay and produce ^3He after the hydrothermal system has ceased to operate. The

Table 5. Helium Isotope Data

	R/Ra
Hermosa (Wlf-83-3)	1.46
Mantle	8-9
Atmosphere	1.00
Crust	0.01
U-Th-minerals	0.0007

generation of ^3He due to this decay would change the R/Ra value of the Hermosa sample (mantle derived ?) resulting in an incorrect interpretation of the data.

PART III

DISCUSSION

DISCUSSION

The precious-base metal epithermal deposits are the results of large scale hydrothermal convective systems driven by magmatic heat in the upper 5-10 km of the crust (Henley, 1989). Henley and McNabb (1978) in their study of porphyry copper emplacement in Tertiary and older orogenic-volcanic belts around the world, concluded that a continuum does exist in ore-forming hydrothermal systems in volcanic terrain from magmatic fluid to almost entirely meteoric-ground water environments. Studies by Henley and Ellis (1983), Henley (1985), Hedenquist and Henley (1985a), and White (1981) indicate that present-day active geothermal systems show the same physicochemical characteristics as those of the epithermal deposits (fossil geothermals) around the world. Therefore, studying the present-day active geothermal systems and determining their physicochemical behavior (temperature, pressure, fluid composition and related changes, metal solubility and deposition, size, age, and structural control) will help to understand characteristic of precious-base metal epithermal deposits and to develop exploration models for this type of deposit. The model of fluid flow in the Broadlands and Wairakei systems in New Zealand suggests that these systems are upwelling plumes with gold mineralization close to the center and the hottest zone at shallow depths. Silver-base metal mineralization occurs away from the plume in a cooler and deeper environment.

Seward, 1973; 1976; 1984; Henley, 1973; 1985; Henley and brown, 1985; Drummond and Ohmoto, 1985 discuss metal complexing, metal deposition and depositional mechanisms in the present-day geothermals and forssil geothermals (epithermal precious-base metal deposits).

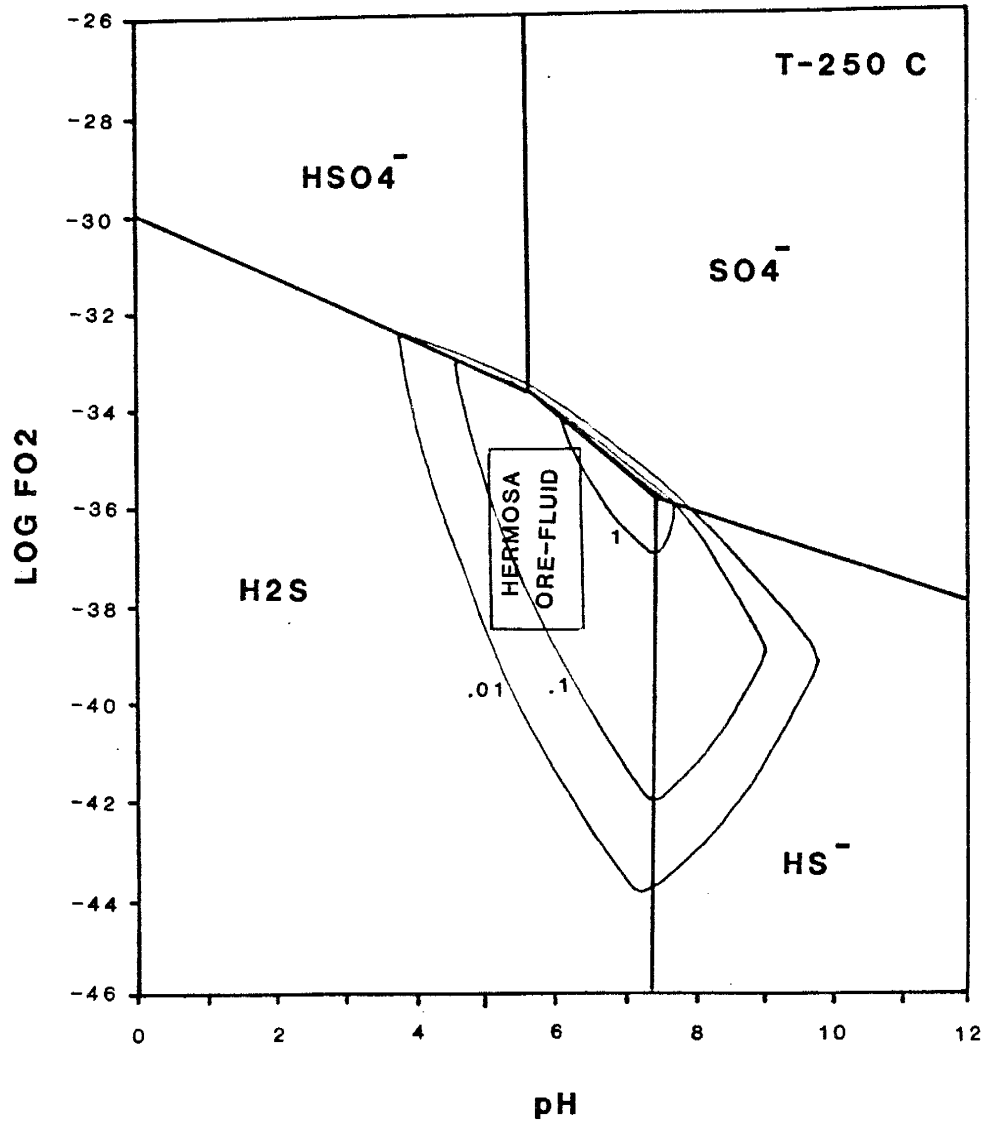
Microthermometric, gas, isotope, and chemical analyses of ore and non-ore samples from the Hermosa mining district have helped to define the conditions required for ore mineralization in the district. Lithological and structural studies define the favorite horizons and locations with relation to certain rock types or structures in the district.

Oxygen and sulfur fugacities and pH of the ore-forming fluids during mineralization were calculated based on the results of microthermometric and gas analyses of the fluid inclusions from the district. The fluids which were responsible for mineralization were neutral, slightly reduced, dilute sodium and calcium-chloride solutions. The volatile components ranged from 0.1 to 0.5 mole% of the total fluid. In some samples this value was as high as 10 mole%.

Figure 48 shows the f_{O_2} and the corresponding pH of the ore-forming fluids. This diagram was constructed at 250 C, using total sulfur of 0.02 molal accordant with the average for the different mineralized localities in the district. The oxygen fugacity and pH ranges of the ore-forming fluids are shown in the boxed area. The latter is below the sulfate-sulfide boundary, which indicates that the gold and silver were transported as bisulfide complexes. These complexes are

Figure 48.

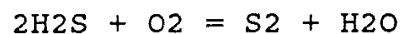
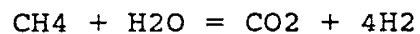
Log fO_2 -pH diagram calculated at 250 C using a total sulfur concentration of 0.02 molal accordant with the average for different mineralized localities in the Hermosa mining district. The boxed in area shows the ore-forming fluid characteristics in the district.



stable in the sulfide field (pyrite and pyrrhotite), but dissociate when the fluid is oxidized. Solubility of gold in ppm as Au(HS) is contoured on the diagram.

The calculated pH is approximately neutral at 250 C. This may be because the ore-forming fluids have interacted with the carbonate hosts which could have acted as buffers.

Figure 49 is the log FO₂-FS₂ diagram that shows the stability fields of sulfide mineral assemblages at 250 C. The fields are on the boundary between pyrite, magnetite, and pyrrhotite fields. Different ranges of oxygen and sulfur fugacities for fluids of high ore grade, low ore grade, and non-ore are indicated. Oxygen and sulfur fugacities were calculated using the redox reactions:



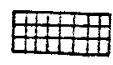
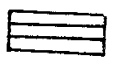

The calculated FO₂ and FS₂ values fall well within the range of other epithermal systems (both active and fossil).

Th data were used to develop the temperature distribution map of the district. The data were plotted by different computer programs.

For presentation of the Th and other types of data districtwide, contouring of the values was the best method. Figure 50 shows the mean temperature distribution and Figure 51 the Th data corresponding to the first stage of ore mineralization in the district. Gold deposition occurred mostly

Figure 49.

Log FS2-F02 diagram at 250 C showing sulfide mineral assemblages for the Hermosa mining district.

-  Fluids of high ore grade
-  Fluids of low ore grade
-  Fluids of non-ore grade

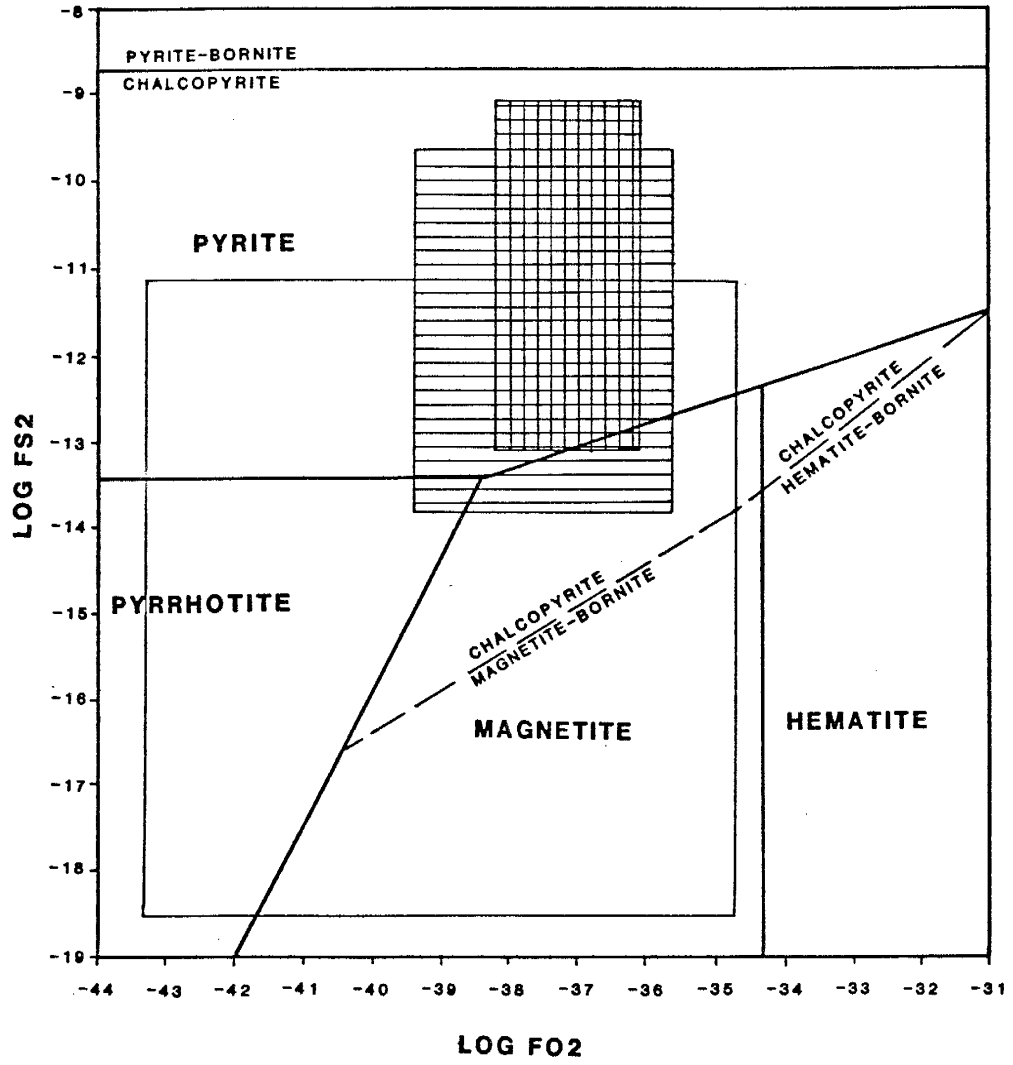


Figure 50.

Mean temperature (C) distribution of the Hermosa mining district.

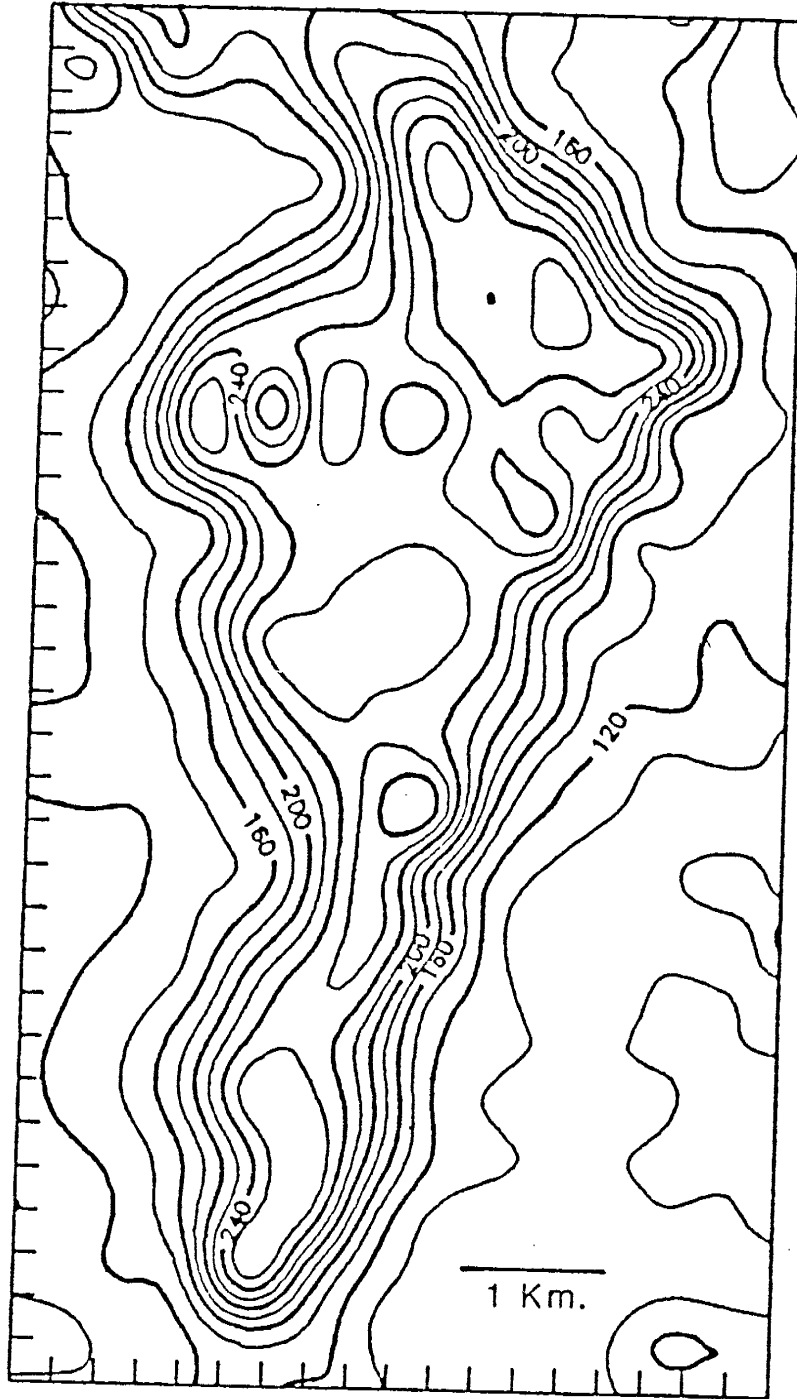
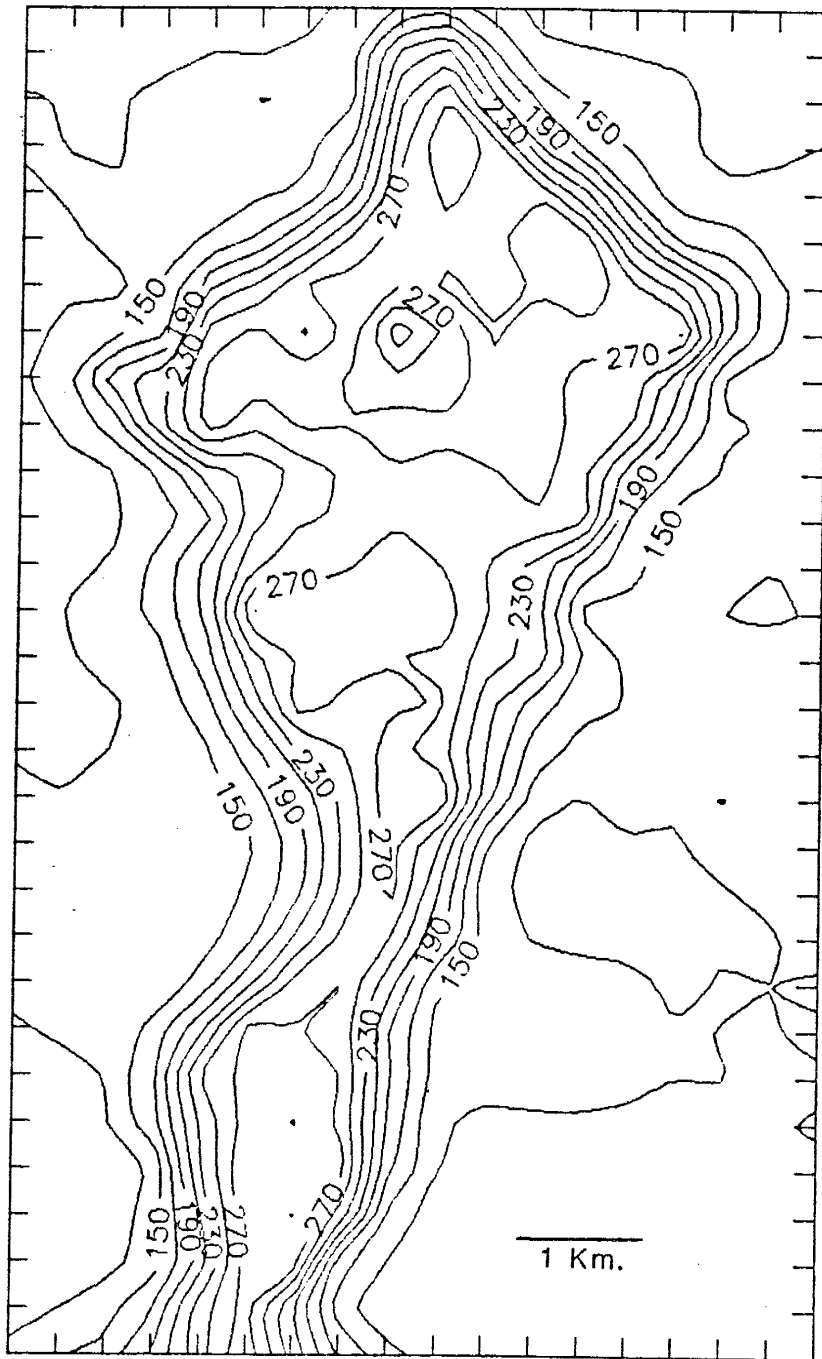


Figure 51.

The (C) distribution of the first-stage of quartz and calcite and ore mineralization in the Hermosa mining district. Note the high-temperature centers that indicate upwelling zones in the district.

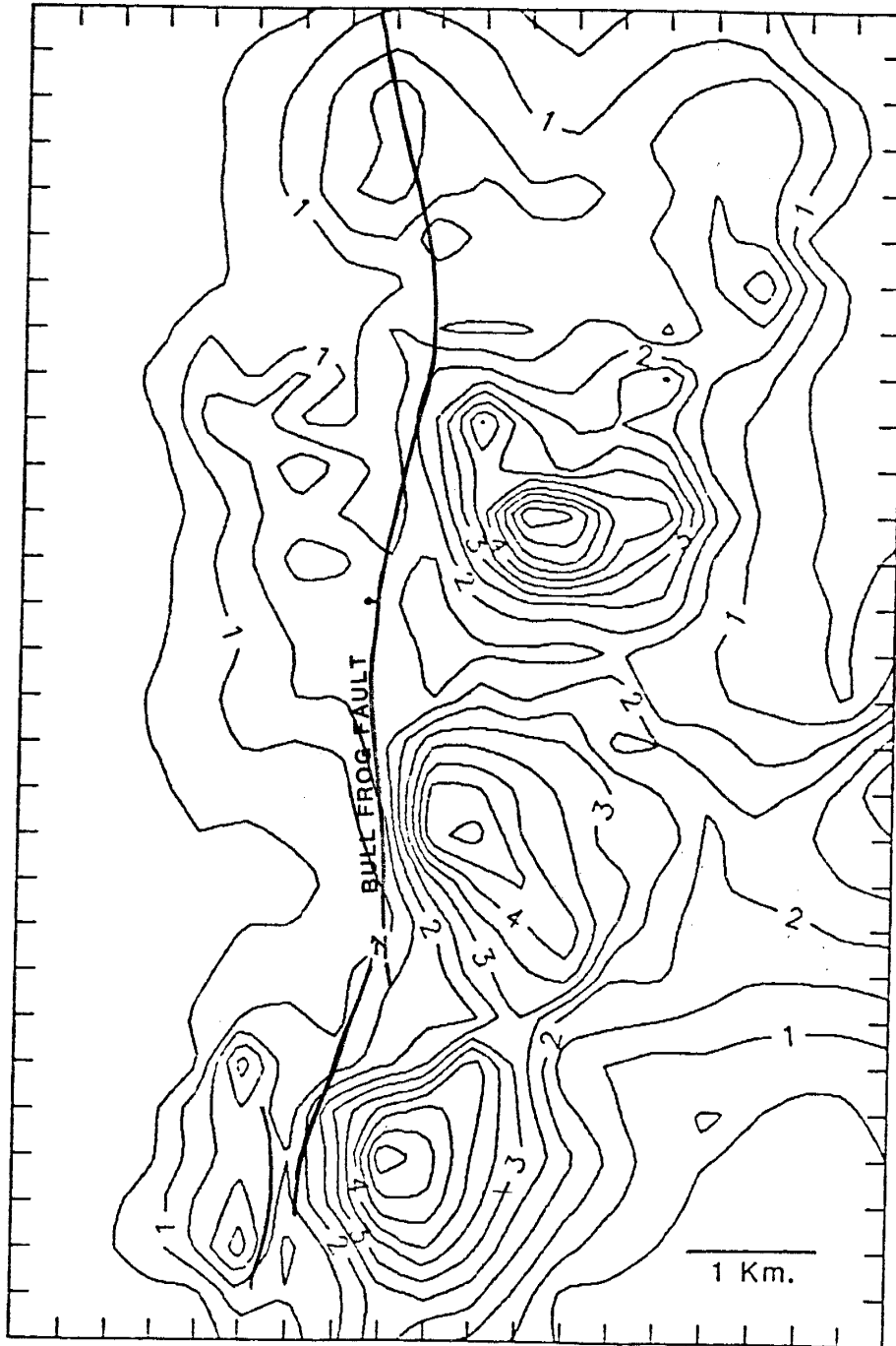


during the first stage of mineralization. Both figures show distinct high temperature centers. The temperature decreases away from these centers. The correlation of high temperature centers in Figures 50 and 51 indicates that although different fluids were active in the system, the mineralization in the district was a continuous process. Microthermometric analyses of the first and last stages of quartz and calcite show the same correlation. In the northern part of the district, the high temperature zone coincides with the occurrence of a rhyolite plug. This association indicates that the rhyolite plug was the heat source in that part of the district. Numerous rhyolite domes, plugs, and dikes are present in the region. In the study area, the occurrences of these intrusives are controlled by the Bull Frog fault. Thus it could be concluded that hydrothermal fluids, driven by heat from rhyolite domes, plugs, and dikes, ascended through the Bull Frog fault and related fractures and mineralized the district. The same association between mineralization and rhyolite complexes is observed in the Chloride mining district just north of the study area.

The salinity data were plotted the same way as the Th data. Figure 52 shows the salinity of the fluids in the district. The most obvious feature is the concentration of high-salinity fluids (2-6 eq. wt.% NaCl) on the eastern side of the Bull Frog fault. One explanation for this bimodal salinity is that the ascending hot, but low salinity, hydrothermal fluid mixed with local high salinity fluids on the eastern side of the

Figure 52.

Salinity distribution in the Hermosa mining district. Note the concentration of high salinity values on the eastern side of the Bull Frog fault.

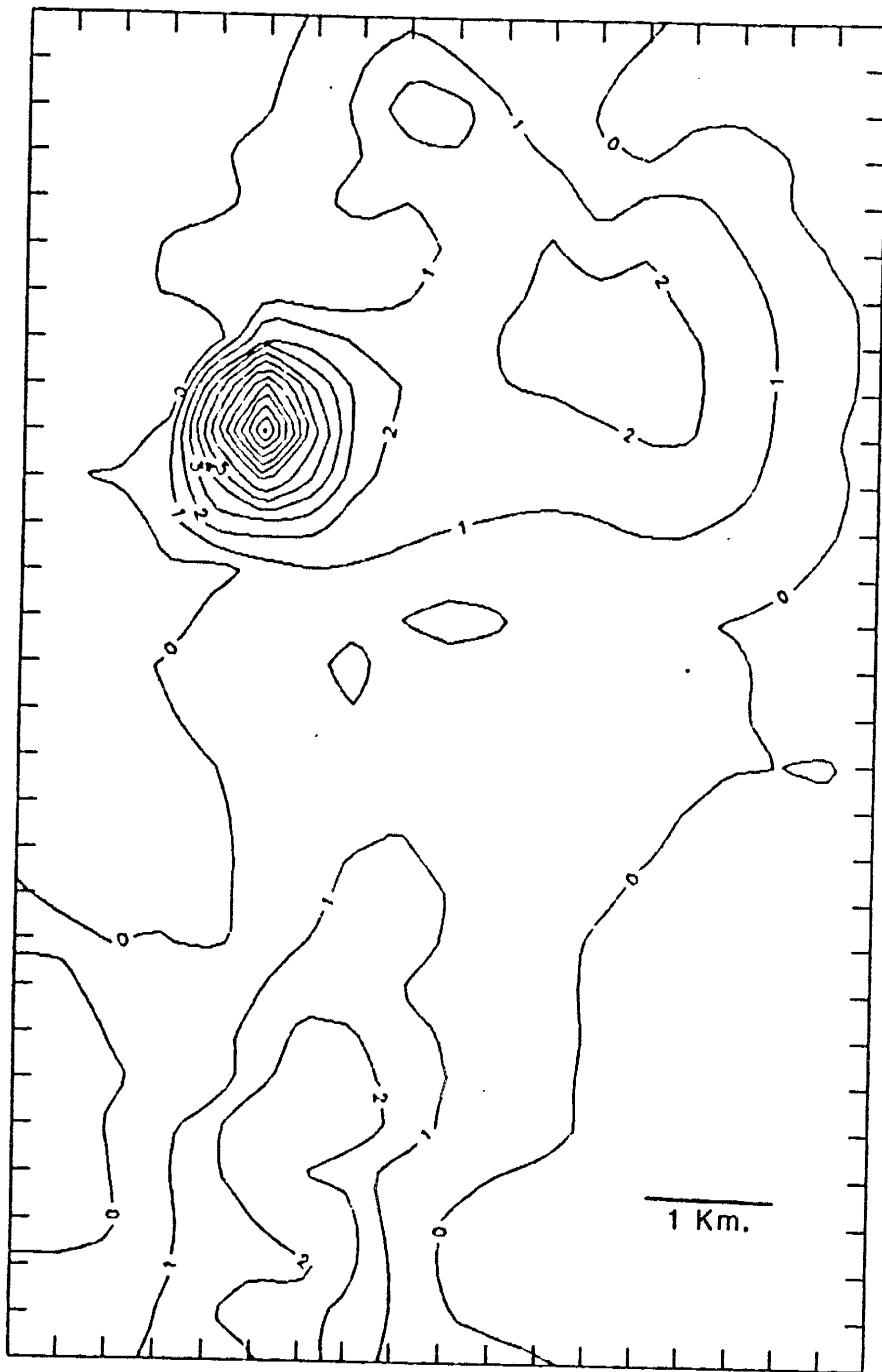


Bull Frog fault. The eastward dip of the fault may have prevented the flow of saline fluids to the west side of the district. Another explanation for this separation of low and high salinity fluids is that more than one fluid, with different salinities, existed in the hydrothermal system. Roedder (1972) and Henley (1986) noted that hydrothermal fluids with different salinities and temperatures may move in a system without mixing. Two or more fluids with different densities and composition will result in different mineral assemblages in epithermal systems. The second explanation is favored to explain the relatively sharp separation line between the low and high salinity fluids in the district. Ore mineralogy also supports this explanation because silver and base metal occurrences are associated with the high salinity fluids and gold occurrences are associated with the low salinity fluids. Because high salinity fluids are heavier, they move more slowly and travel less distance than lighter, low salinity fluids. The dip of the Bull Frog fault may have influenced the movement of the high salinity fluids in the district.

Gold, silver, and lead assay values of samples from the district were plotted. Gold occurrences in the district are shown in Figure 53. Not surprisingly, these occurrences correlate fairly well with high-temperature centers of the system. As in active geothermal systems throughout the world, gold in the Hermosa district has been deposited from low salinity fluids in or close to, the hottest zones and at

Figure 53.

Gold assay value distribution (ppm) in the Hermosa mining district. Note the correlation between high gold value zones with the high-temperature centers in Figures 50 and 51.

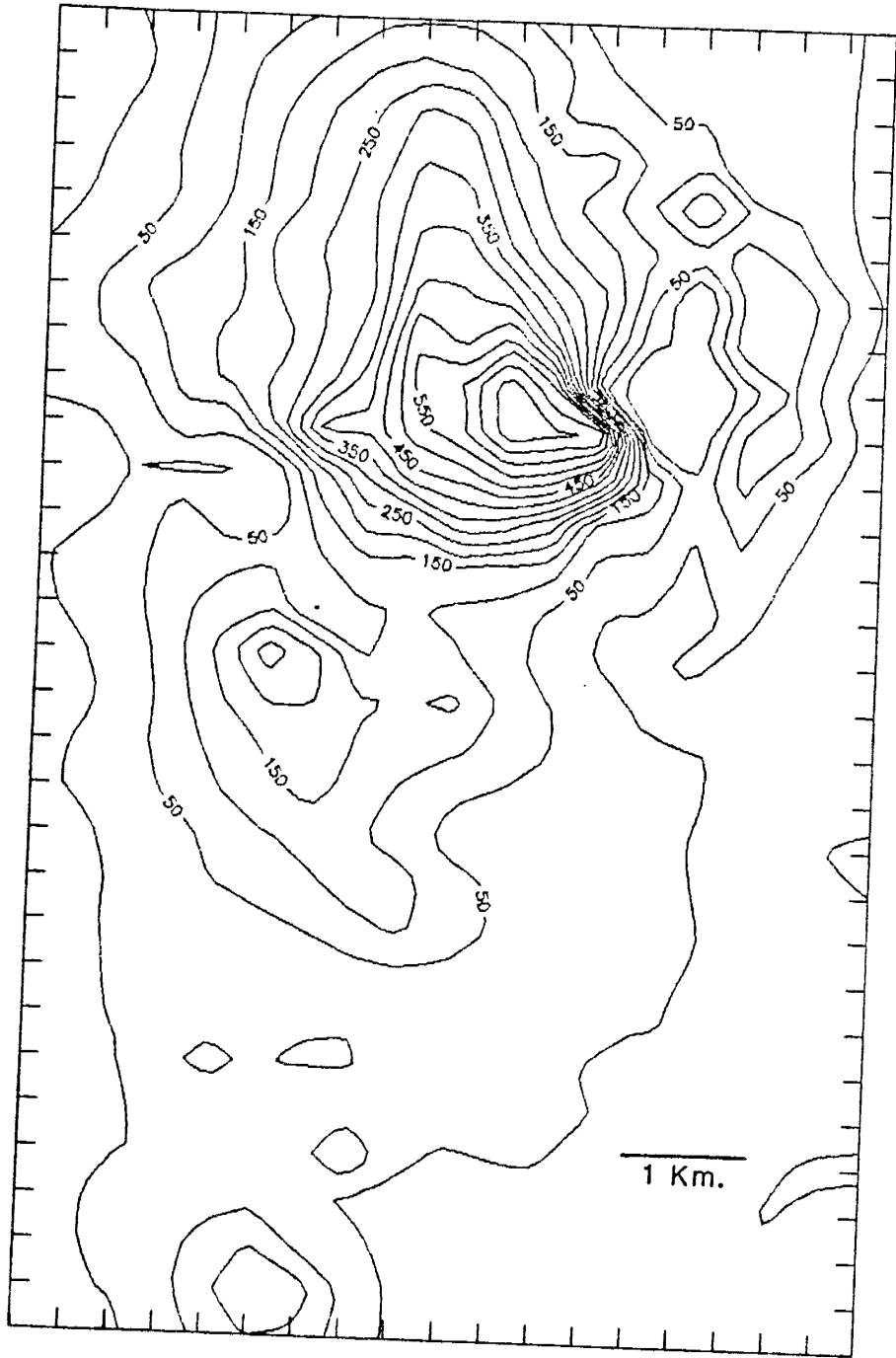


shallow depths. The gold values associated with the hot centers range from .5 to 3 ppm, except for one sample from the Antelope-Ocean Wave mines. In a sample from the Slater working of these mines up to 37 ppm gold and 24000 ppm silver were detected. Unconfirmed reports (Carlson, pers. comm.) indicate that samples with values up to 3 oz Au/ton have been encountered in this working. The mineralization temperature of gold samples in this working ranges from 270 to 290 C and the fluid salinity ranges from 0.5 to 2 eq. wt.% NaCl. The gold mineralization temperature in the district commonly ranges from 250 to 300 C and the salinity of gold depositing fluids ranges from 0.0 to 2.5 eq. wt.% NaCl (Figs. 50, 51 and 52).

The silver assay values for the district are plotted in Figure 54. The highest concentration of silver is associated with the high salinity fluids. This association suggests that in the high-grade silver zone, most of the silver was transported to the deposition site as silver chloride complex. Not all high salinity fluids deposited high-grade silver in the district. The comparison of the silver distribution map with temperature distribution maps reveals that high-grade silver occurrences in the district are positioned at the margins of the hot spots (except for the Palomas Camp area). These margins are about 10 to 30 C cooler. The same comparison between gold and silver occurrences indicates that, in and around the high-grade gold mineralization, silver grade decreases. Again this mineral zonation, with respect to

Figure 54.

Silver assay value (ppm) distribution in the Hermosa mining district. Note the correlation between high silver values and high salinity fluids.



temperature and salinity, agrees with present-day active geothermal behavior. The same mineral zonation in fossil geothermal systems has been noted by Buchanan (1981). The gold to silver ratios in the study area are very low (0.01 to 0.006, except for one which showed 0.75). These lower ratios of gold to silver place the deposits into Henley's (1986) category of the precious-base metal epithermal deposits. The precious-base metal epithermal deposits contain considerably less gold than the gold-silver epithermal deposits.

As discussed before, hydrothermal fluids with high temperature (240-300 C), low salinity (0.0-2 eq. wt.% NaCl) and high H₂S (>0.01 mole%) content deposit gold when the H₂S concentration decreases due to boiling or mixing. The H₂S concentration of the volatile phase of the analyzed samples is plotted in Figure 55. The contour lines represent mole percent H₂S in the fluid system in different parts of the district. The comparison between Figure 55 and gold assay values (Fig.53) shows very good correlation between these two maps. This correlation suggests that the gold was transported as bisulfide complexes to the site of deposition. Similar correlations exist between H₂S values and high temperature centers with low salinity fluids. Based on chemical composition and Th of the fluids, the gold solubility map of the district was developed (Fig.56). As expected, 100% correlation exists between H₂S values (Fig.55) and the gold solubility values (Fig.56). A comparison between gold solubility value and gold occurrences in the district (Fig.53)

Figure 55.

H₂S concentration distribution in the Hermosa mining district. The H₂S values are taken from gas analyses of fluid inclusions from the district. The contour lines represent mole% H₂S. Note the correlation between high H₂S values in this figure and the high gold values in Figure 60.

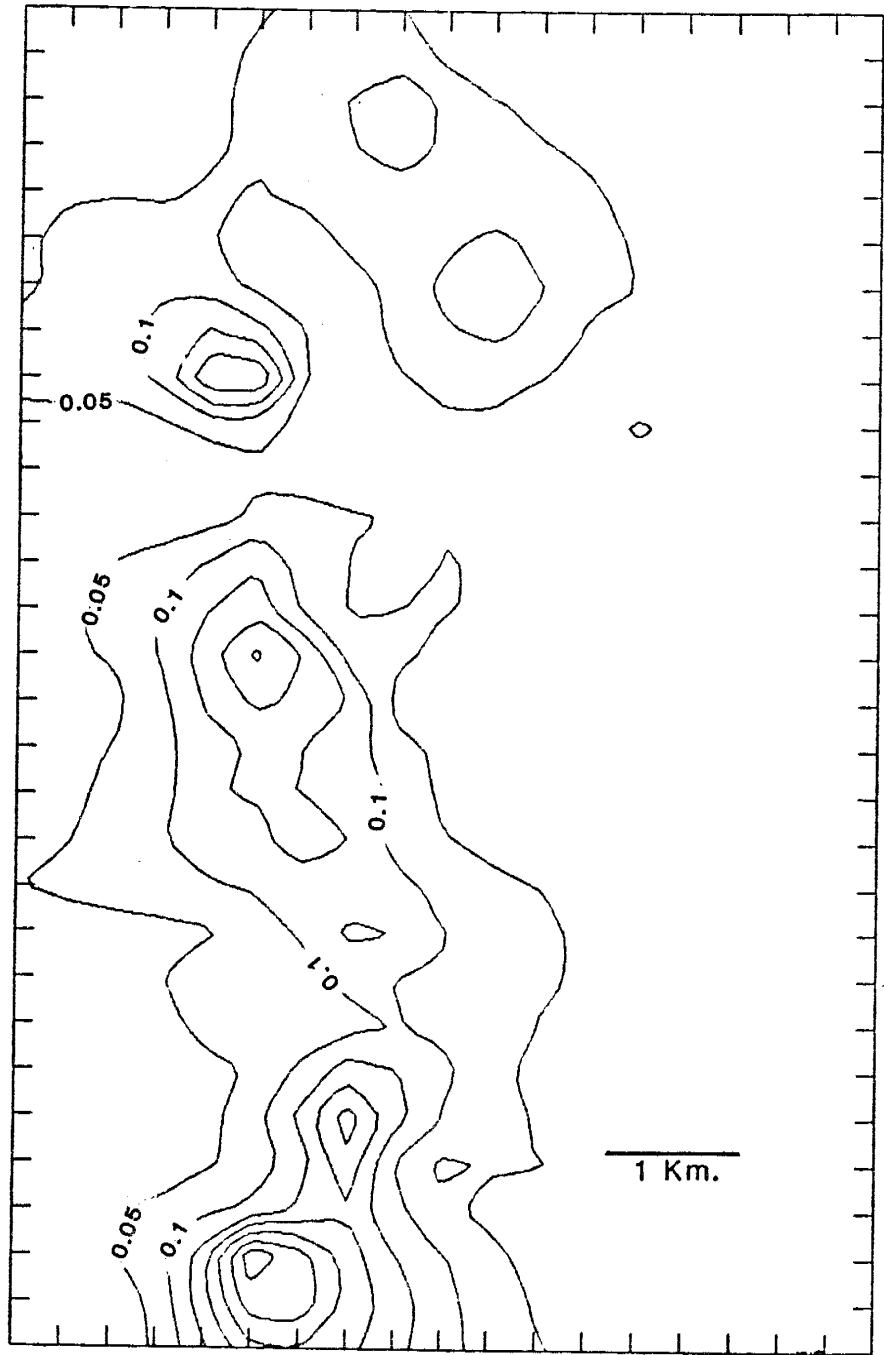


Figure 56.

Gold solubility map (ppm) of the Hermosa mining district. This figure is constructed using the H₂S values obtained from the gas analyses. Note the strong correlation between this figure and the gold assay values of the district (Fig. 53).



indicates strong correlation. Where inconsistencies exist, these can be explained as follows: (1) Although the fluid system was capable of carrying higher amounts of gold, there was not enough gold available in the fluid system to form higher ore grades. Or (2) the chemical composition of the transporting fluids did not change enough or fast enough to deposit all the gold content, and the fluids carried away the remaining gold (and other metals) forming non-ore grade deposits over a larger area. Or finally (3) a sampling error may exist or sufficient samples have not been analyzed for gold values. The H₂S (Fig. 55), temperature (Fig.51) and salinity (Fig.52) maps indicate favorable locations for gold deposition which have not been explored or sampled.

Since, in geothermal systems (active and fossil), the concentration of CO₂ and H₂S follow each other (Henley, 1986; 1989), a map of CO₂ concentration in the volatile phase of the analyzed samples was developed in order to see any correlation between these two components (Fig.57). The contour lines in this figure represent mole percent CO₂ in the gas phase of the hydrothermal system. For most parts of the district, CO₂ and H₂S values are similar to those of active geothermal systems. But high concentrations of CO₂ and little or no H₂S in the northeast part of the district (Palomas Camp area) does not show this correlation. The high CO₂ value for this location is attributed to the fact that most of the samples were calcite. It is quite possible that during the decrepitation of the inclusions around 400 C, some of the samples partially

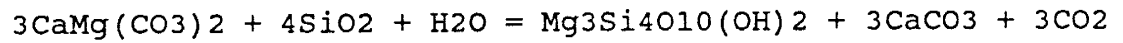
Figure 57.

Map of CO₂ concentration (mole%) in the fluid system in the Hermosa mining district. See the text for explanation.



decomposed and produced CO₂.

The main gangue mineral in the Palomas Camp is talc. During the formation of talc CO₂ is produced according to the following reaction:



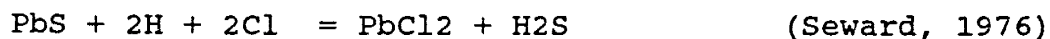
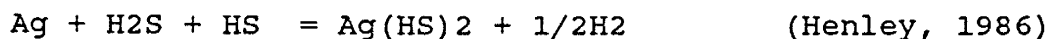
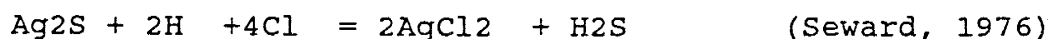
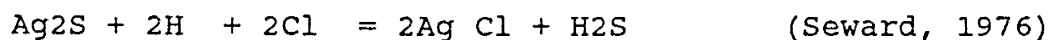
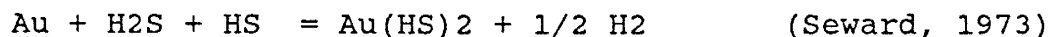
Excess CO₂ in the gas phase of the fluid system could be the result of this reaction.

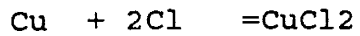
The gangue mineral distribution or zonation in the district follows the temperature, fluid composition, and related ore mineral distribution. In the high-temperature zones of the district the common gangue minerals are quartz, talc, and calcite in the order of decreasing abundance while in the lower temperature zones we observe talc, calcite and quartz.

MODELING FOR METAL TRANSPORTATION AND DEPOSITION BY THE
HYDROTHERMAL FLUIDS IN THE HERMOSA MINING DISTRICT

INTRODUCTION

Studies by Henley (1973, 1985, 1989), Seward (1973, 1976, 1984) and many others show that many factors control the solubility and deposition of minerals in a hydrothermal system. Geochemical data show the solubility of minerals increasing with higher temperature. Oxygen and sulfur fugacities and the pH of the fluid system also control the solubility of minerals. The common metal complexing ligands in hydrothermal fluids are Cl, HS or H₂S, F and water. The amount and type of complexing in these fluids depend on total Cl activity, sulfur concentration, oxidation state, pH value and the metal. Any change of these parameters disturbs the equilibrium of the fluid system and causes the deposition of one or more minerals depending on the nature of the changes. The following equations show the dominant metal complexing for different metals in a hydrothermal system:





(Crerar, 1976)

DEPOSITIONAL MECHANISMS (MODELS)

Present understanding of mineral deposition in epithermal systems is that boiling, mixing, cooling, or a combination of two or more of these mechanisms, disturbs the equilibrium of the epithermal system and causes the precipitation of the ore and gangue minerals. In the interpretation of the freezing and heating data, it was concluded that boiling and mixing were mechanisms of ore deposition in the study area. In Figure 39, are illustrated changes that the hydrothermal fluids could undergo. Figure 58 shows which mechanisms were responsible for individual deposits in the study area. This figure also shows the temperature and salinity ranges of different types of fluids in the system. The connecting lines show interactions between different fluid types in each mineralized area in the district. These lines are labeled to show the inferred mechanism (boiling or mixing) of mineralization in each deposit. Although the boiling mechanism for mineralization has been recognized only in two of the deposits, it is possible that unrecognized boiling was responsible for ore mineralization in some other mineralized zones. In the Antelope-Ocean Wave mines, indications of boiling (in the form of a high number of gas-rich fluid inclusions) are abundant, but the fluid salinity does not demonstrate this characteristic. It is possible that, some of the key samples

or inclusions have been overlooked.

Based on the results of gas analyses, microthermometric analyses and mineralogical studies, it is concluded that boiling and mixing were the mechanisms of ore deposition in the Hermosa mining district. Although the data show the presence of six types of fluids in the district, it is quite reasonable to conclude that there were only three types of fluids (F I, F II, and F V) present in the initial stage of hydrothermal system activity. The intermediate fluids (F III, F IV, and F VI) were the result of the interactions among the three initial fluids (Fig.58). Figure 59 shows the distribution of each type of fluid and their relationships to each other and to structures in the district. The F I fluid was the dominant fluid in the northern half and the F IV fluid was dominant in the southern half of the district. From this figure it could be concluded that the Bull Frog fault and related fractures were the main structures that controlled the fluid flow and ore mineralization in the district. The presence of F VI fluid in both north and south ends of the district indicates the importance and influence of this fault on the mineralizing events. The similarity of gold (1-3 ppm) and silver (200-400 ppm) values in these two areas of the Hermosa district supports this conclusion and, in the meantime, suggests there was possibly only one source for this ore-forming fluid.

To apply the boiling or mixing model for different deposits in the Hermosa mining district, the GEOMOD computer modeling

Figure 58.

Diagrammatic presentation of different types of fluids and their interaction with each other in the Hermosa mining district. The connecting lines show the mechanisms (boiling, mixing, or cooling, see Fig. 39) of mineralization for each deposit in the district. The lines also indicate which fluid or fluids were involved in the ore mineralization in each mineralized zone.

Fluid typ	Th (C)	Salinity (eq. wt.% NaCl)
F I	260-320	0.7-2.0
F II	250-310	6.5-9.0
F III	120-190	0.3-2.0
F IV	260-320	0.3-1.2
F V	20-40	0.0-0.7
F VI	290-330	2.5-4.5

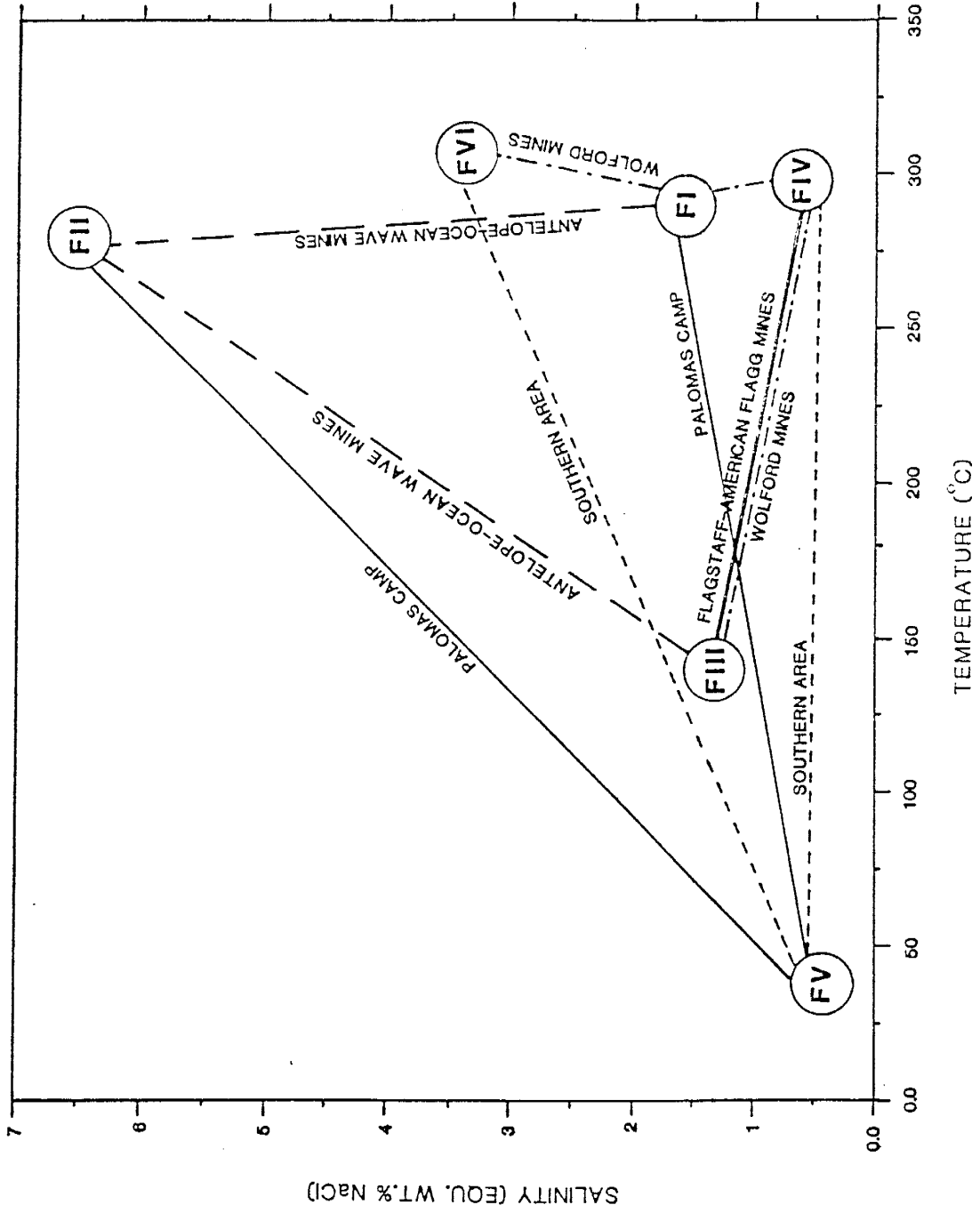


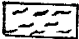


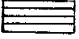
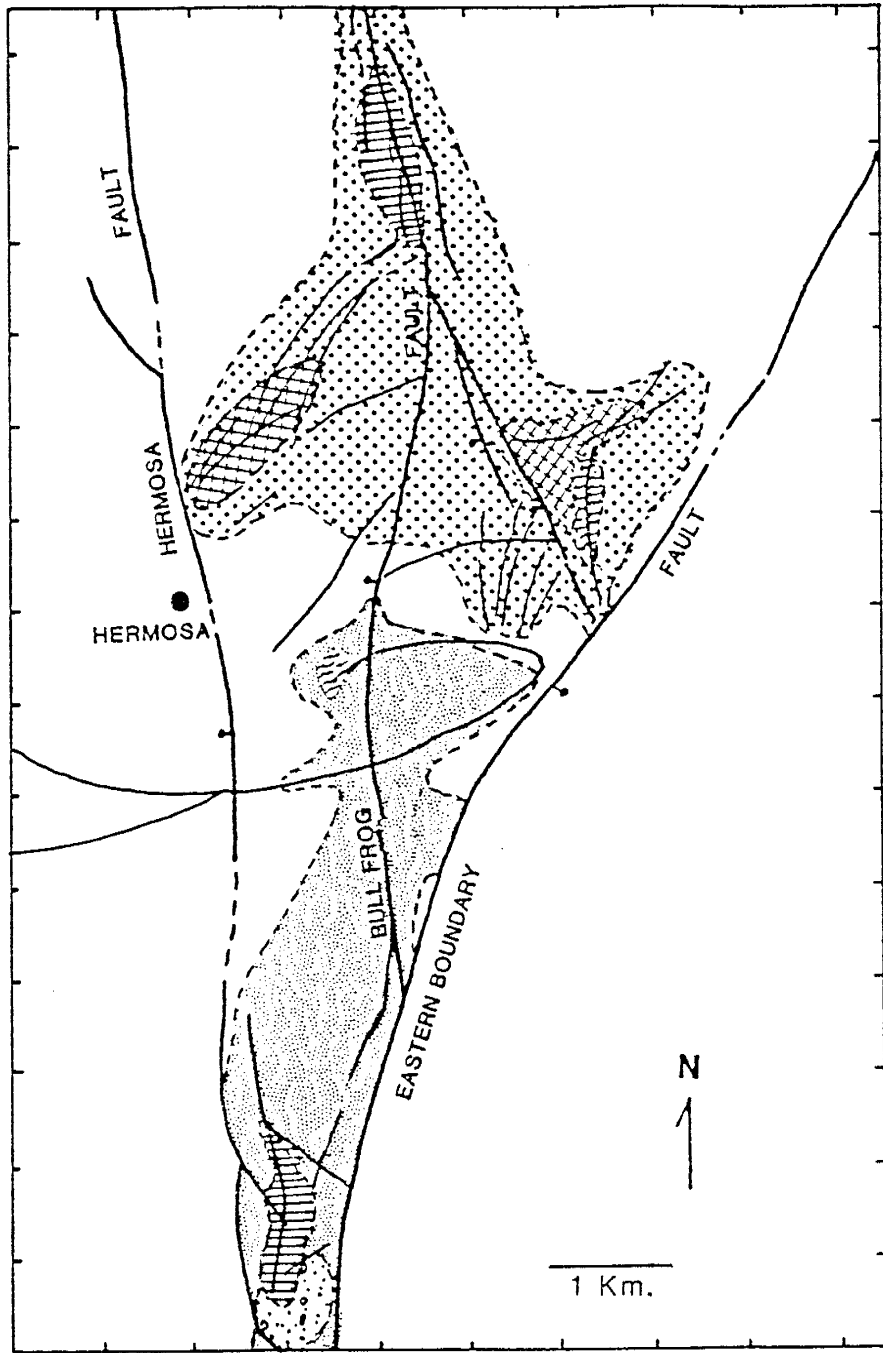


Figure 59.

Diagrammatic presentation of the distribution of different types of fluids in the Hermosa district. Note the influence of the Bull Frog fault and related fractures on fluid flow. This diagram also shows that ore is deposited when two or more fluids are present or interact with each other.

-  F I (260-320 C, 0.7-2% NaCl)
-  F II (250-310 C, 6.5-9% NaCl)
-  F III (120-190 C, 0.3-2% NaCl)
-  F IV (260-320 C, 0.3-1.2% NaCl)
-  F V (40 C, 0.0-0.5% NaCl)
-  F VI (240-300, 2.5-4.5% NaCl)



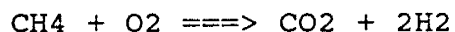
program (Norman, 1988) was used. Based on the microthermometric and gas analyses data, GEOMOD calculates the concentrations of ore minerals in the hydrothermal system. The program contains two calculation options, one for metal solubility at specified fluid conditions, the second for metal solubility and precipitation of specified fluid during boiling. The boiling program could be run under three different conditions: a closed system with a single-step gas separation for the fluid system; an open system with multistep gas separation; and an open system with continuous gas separations. Based on mineralogic and microthermometric analyses it is concluded that the mineralization in the Hermosa mining district was a continuous process and, as a result, the third option of the boiling model was used for calculation of ore deposition in the district.

BOILING MODEL

Boiling occurs when the pressure on the hydrothermal system is decreased. The decrease could be due to faulting or rise of the fluid to shallower depths. During boiling, dissolved gases (CO₂, H₂S, CH₄, and H₂) are rapidly fractionated to the vapor phase. This phase separation results in the increase of pH. Boiling also causes a decrease of temperature and an increase of salinity in the fluid system. These changes disturb the equilibrium of the hydrothermal system and reduce the solubility of dissolved minerals, which results in

precipitation.

The boiling model was used for the Wolford mines, the Flagstaff-American Flag mines and the Antelope-Ocean Wave mines in the district. The program is capable of calculating the solubility of Au, Ag, Cu, Pb, Zn, and Fe up to 350 C. Input parameters needed for solubility calculations are pH, temperature, salinity, oxygen fugacity, and gas concentrations. The pH of the ore-fluid was calculated by the model using the Na-K-Ca chemical geothermometer (Truesdell, 1974). The oxygen fugacity was calculated by the model using the following reaction:



The gas concentrations of CO₂, H₂S, CH₄, N₂, H₂, and H₂O entered as mole%. In the boiling model the concentrations of all metals are calculated in the ore-forming fluid for each specific temperature increment.

In each deposit a sample representative of the ore fluid was used to show the changes in metal solubility as the fluid boils. The boiling calculations were executed from 310 to 170 C for the Flagstaff-American Flag mines, 320 to 180 C for the Wolford mines and 300 to 160 C for the Antelope-Ocean Wave mines. The results of calculations are shown in Table 6 and Figure 60 A, B, and C. These calculations show increasing pH with decreasing temperature. They also show decreasing metal concentrations as the ore-fluid boils and cools down. As the

Table 6. Results of the boiling calculation.

Wolford Mines

Temperature (C)	pH	Zn (ppm)	Pb (ppm)	Ag (ppm)	Cu (ppm)	Au (ppm)	Fe (ppm)
320	5.17	12.7	1.3	0.3	0.3	0.65	1.07
310	5.41	8.00	0.63	0.14	0.2	0.54	0.25
300	5.67	4.51	0.28	0.07	0.15	0.36	0.06
290	5.94	2.09	0.10	0.04	0.11	0.16	0.01
280	6.19	0.75	0.03	0.02	0.09	0.04	0.003
270	6.36	0.19	0.01	0.01	0.10	0.004	0.001
260	6.44	0.04	0.003	0.01	0.15	0.000	0.000
250	6.46	0.07	0.01	0.02	0.24	0.000	0.000
240	6.45	0.92	0.15	0.05	0.42	0.000	0.000
230	6.45	34.45	5.09	0.23	0.75	0.000	0.000
220	6.44	4868.32	648.45	2.00	1.4	0.000	0.000
210	6.42	*****	*****	39.62	2.68	0.000	0.000
200	6.40	*****	*****	2572.6	5.34	0.000	0.000

***** = > 10000 ppm

Flagstaff Mines

Temperature (C)	pH	Zn (ppm)	Pb (ppm)	Ag (ppm)	Cu (ppm)	Au (ppm)	Fe (ppm)
310	5.35	33.25	2.6	0.26	0.17	5.507	0.03
300	5.55	20.41	1.26	1.91	0.14	3.74	0.007
290	5.80	10.52	0.52	0.12	0.12	2.01	0.001
280	6.11	4.29	0.17	0.07	0.08	0.80	0.000
270	6.48	1.27	0.04	0.025	0.06	0.18	0.000
260	6.78	0.25	0.006	0.005	0.04	0.016	0.000
250	6.89	0.028	0.001	0.002	0.06	0.000	0.000
240	6.90	0.007	0.001	0.003	0.10	0.000	0.000
230	6.89	0.15	0.025	0.012	0.18	0.000	0.000
220	6.88	14.18	2.000	0.080	0.34	0.000	0.000
210	6.87	6434.44	821.688	1.225	0.64	0.000	0.000
200	6.84	*****	*****	55.711	1.30	0.000	0.000

***** = > 10000 ppm

Table-6 continued

Antelope-Ocean Wave Mines
(Slater working)

Temperature (C)	pH	Zn (ppm)	Pb (ppm)	Ag (ppm)	Cu (ppm)	Au (ppm)	Fe (ppm)
300	5.28	12.27	0.76	0.13	0.57	1.67	0.018
290	5.66	7.00	0.35	0.07	0.35	1.48	0.004
280	6.08	3.23	0.13	0.05	0.20	0.95	0.001
270	6.44	1.11	0.04	0.02	0.14	0.30	0.000
260	6.71	0.26	0.006	0.006	0.12	0.035	0.000
250	6.82	0.04	0.001	0.003	0.16	0.001	0.000
240	6.84	0.009	0.001	0.005	0.26	0.000	0.000
230	6.84	0.116	0.017	0.014	0.46	0.000	0.000
220	6.83	6.605	0.86	0.08	0.86	0.000	0.000
210	6.82	1675.3	199.26	0.91	1.64	0.000	0.000
200	6.82	*****	*****	29.27	3.24	0.000	0.000

***** = > 10000 ppm

Figure 60.

Concentration of Zn, Pb, Cu, Fe, Ag and Au in the ore-forming fluids, from the open system boiling calculation. Note the solubility decrease of the metals as fluids boil and volatiles (H₂S, CO₂,...) are released from the fluid phase. The temperatures (240-290 C) of gold deposition are in good agreement with those determined from the microthermometric analyses.

A: Wolford mines

B: Flagstaff-American Flag mines

C: Antelope-Ocean Wave mines

Au *

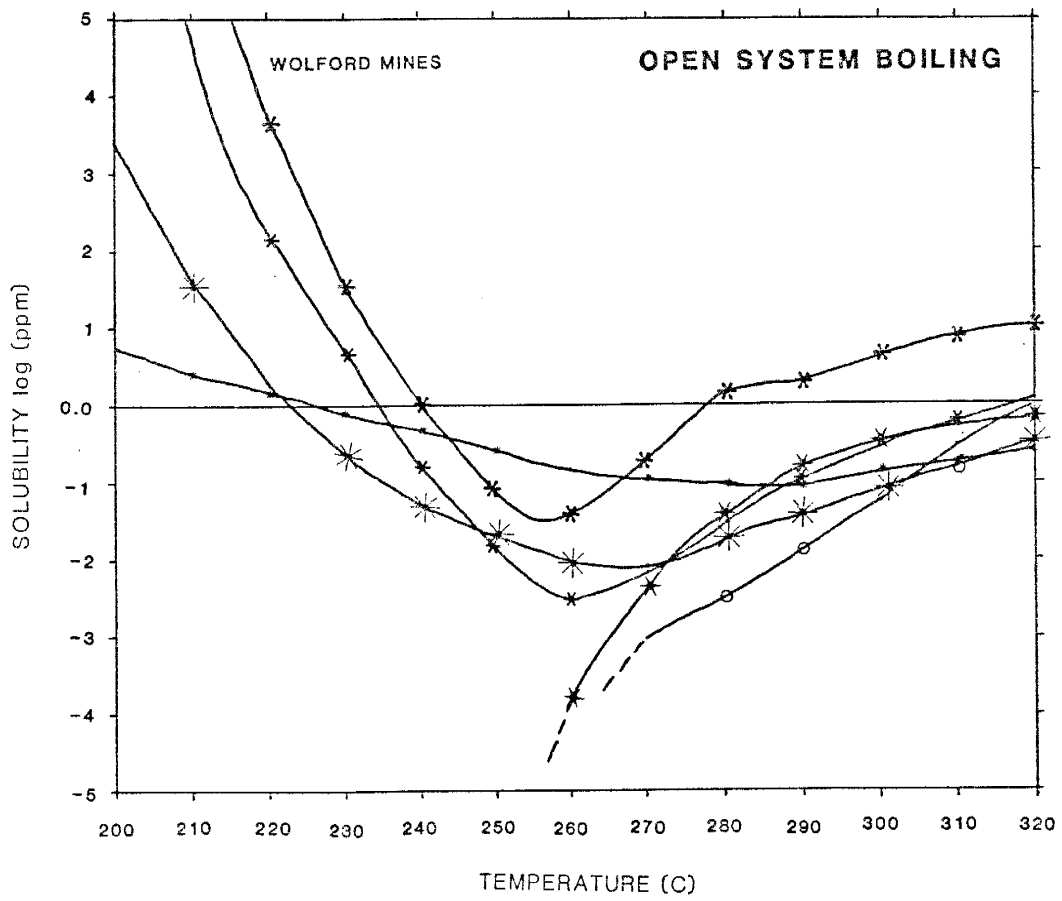
Ag *

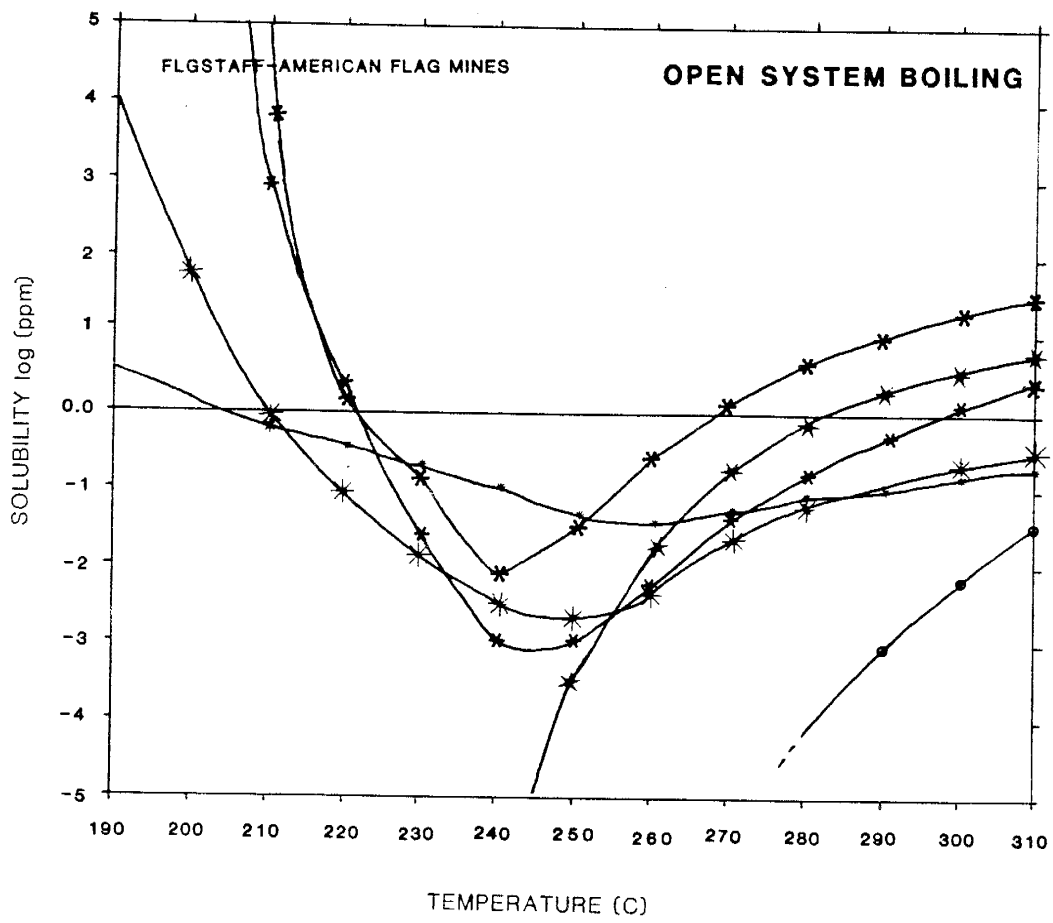
Pb *

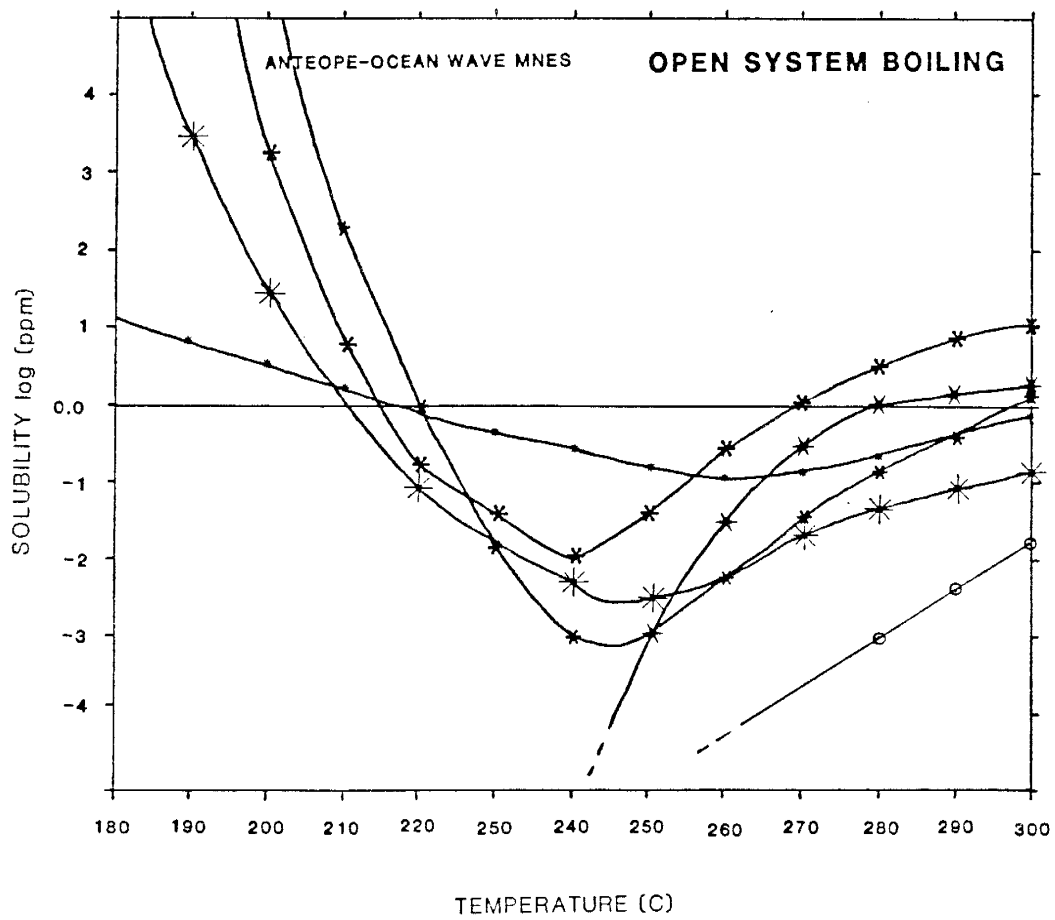
Zn *

Cu *

Fe o







fluid boils gold solubility decreases due to exsolution of CO₂ and H₂S. Experimental data have shown that, in the first few percent of boiling at or below the fluid temperature, most of the metals from a saturated solution will precipitate (Drummond and Ohmoto, 1985). Figures 60 A, B, and C show this rapid precipitation of metals from the ore-forming fluids in the district. The ore mineralization temperatures determined by microthermometric analysis are consistent with the rapid decrease of solubilities of gold, silver, lead, and zinc in the temperature range of 260 to 300 C as predicted by the boiling model. Copper is the exception in this model. The calculations show that copper solubility increases with decreasing temperature.

MIXING MODEL

The mixing (dilution) model involves the interaction of two or more fluids with different compositions and temperatures. The increase of pH and decrease of temperature of the ore-forming fluids are the main factors affecting mineral solubility during the mixing process. The solubility option of GEOMOD was used to evaluate the changes in metal solubility during the mixing of an ore-forming fluid with meteoric water. The data for the southern area of the district were used to develop a mixing model because the data indicate that mixing was the mechanism of ore deposition in the southern area. The

mixing calculations used 11 different proportions of each fluid, starting with 100% ore-fluid and ending with 100% meteoric water in increments of 10%. The physicochemical characteristics of the two fluids used in the mixing calculations and the results are listed in Table 7. Figure 61 shows the results of the mixing model graphically. In the mixing model, two possible processes could occur: 1) The gas concentration of the ore-forming fluids (in particular CO₂ and H₂S) is reduced, which results in the increase of pH and solubility reduction of precious metals. 2) In more saline systems the mixing causes the dilution of chloride ions and decreases the temperature, which results in the precipitation of base metals as sulfides. The result of this sulfide mineralization is the removal of H₂S, which lowers the solubility of gold. The second mechanism of mixing explains the association of the high-grade gold with the high salinity fluid in the Antelope-Ocean Wave mines. In this location, the F II fluid interacts with F III and F I fluids (Fig.58). The mixing of these fluids leads to the precipitation of high-grade gold (37 ppm), silver (23780 ppm), lead (15.6%) and zinc (23.1%). In the Palomas Camp area F II, F I and F V fluids interacted and high-grade silver, lead, and zinc ores were deposited. Little or no gold was encountered in this area. Analysis of volatiles (mostly in calcite) shows very low (0.0001 mol%) H₂S concentration.

Table 7. Results of the mixing calculations.

Temperature (C)	Zn (ppm)	Pb (ppm)	Ag (ppm)	Cu (ppm)	Au (ppm)	Fe (ppm)
290	12.94	0.65	0.127	0.60	0.127	0.018
278	2.14	0.10	0.08	0.70	0.04	0.079
265	0.75	0.04	0.042	0.92	0.006	0.673
252	0.25	0.03	0.033	1.33	0.0002	0.270
238	0.15	0.02	0.017	2.04	0.000	0.263
224	0.05	0.005	0.005	3.10	0.000	0.042
210	0.02	0.001	0.001	4.60	0.000	0.003
195	0.009	0.0008	0.0006	6.88	0.000	0.005
180	0.003	0.0001	0.0001	9.69	0.000	0.000

Figure 61.

Concentration of ore-metals from the mixing calculations. The irregular curves indicate problems during mixing of different proportions of ore-fluids and meteoric water. A rapid oxidation of H₂S in the mixture can result in rapid deposition of gold in a small temperature interval.

Au *

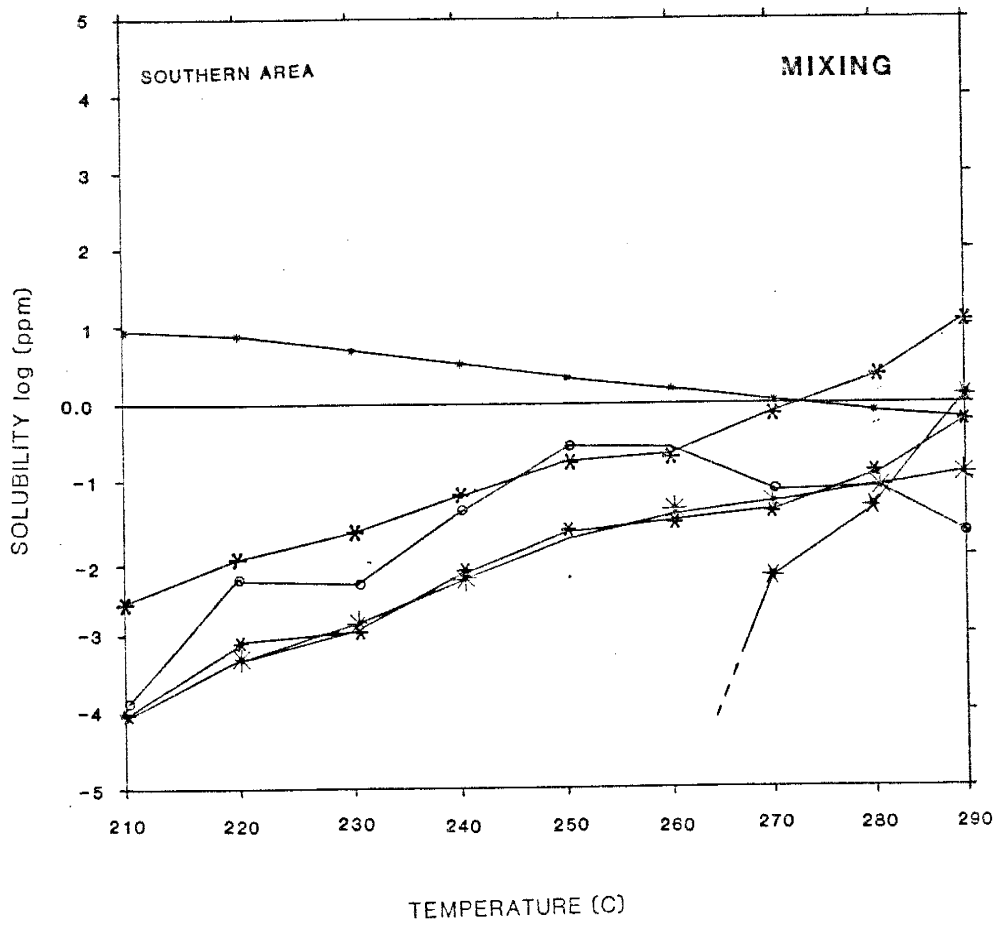
Ag *

Pb *

Zn *

Cu *

Fe o



2-76

SUMMARY AND CONCLUSIONS

The geologic and geochemical data presented have been used to develop a model that reconstructs the processes responsible for the ore deposits of the Hermosa mining district.

The ore bodies in the district formed in small pods, pipes and veins in fissure veins near steep faults in carbonate rocks. Low-grade replacement deposits are also present near ore-controlling faults. Stratigraphic ore control is limited to the Percha Shale in the Palomas Camp area. Mineral paragenesis indicates a continuous mineralizing process in the district.

The microthermometric analyses of ore and non-ore samples indicate that there were several upwelling zones of hydrothermal fluids along the Bull Frog fault and related fractures in the district during the time of mineralization. Ore mineralization temperatures ranged from 240 to 300 C. The salinity of the hydrothermal fluids ranged from 0.0 to 9 eq. wt.% NaCl.

Gold was deposited at shallow depths and high temperatures (260-290 C), and silver-base metals were deposited in deeper and cooler (240-270 C) environments. Microthermometric and gas analyses show boiling and mixing were the mechanisms of ore deposition in different parts of the district. The high H₂S values of the volatile phase of gold-bearing samples suggest that the gold was transported as bisulfide complexes in the hydrothermal fluids and was deposited due to the loss of H₂S

through boiling, dilution or oxidation. The high salinity fluids associated with the silver-base metal deposits suggest that most of these metals were transported in the fluid system as chloride complexes, and deposited due to dilution (mixing) or boiling.

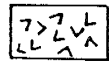
The limited oxygen and hydrogen isotope data suggests the possible contribution of magmatic components to the dominantly meteoric waters of the hydrothermal system. The helium isotope ratio of the volatile phase also suggests possible magmatic components in the fluid system.

All the geologic and geochemical data indicate that there are strong similarities between precious-base metal deposits of the Hermosa mining district and present-day active geothermal systems. Based on these similarities, these deposits could be placed in the epithermal class of ore deposits and in any future exploration for new discovery, they should be treated as such. Based on this realization and the obtained geologic and geochemical data, it is recommended that the WOLFORD mines area, the Flagstaff-American Flag area, and, in particular, the southern part of the district be explored for new gold and silver deposits.

Figure 62 is a generalized cross section showing gross structural relations and the inferred hydrothermal system for ore deposition in the Hermosa mining district. Based on geologic and geochemical data for the district the following conclusions have been reached. A hydrothermal system was initiated by heat emanating from intrusives of late Oligocene

Figure 62.

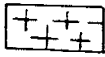
Highly generalized east-west cross section of the mineralized areas in the Hermosa mining district. The inferred hydrothermal system and fluid paths (arrows) are diagrammatically shown.



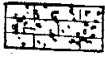
Palomas Gravels



Tertiary volcanic rocks



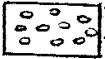
Tertiary rhyolite dome



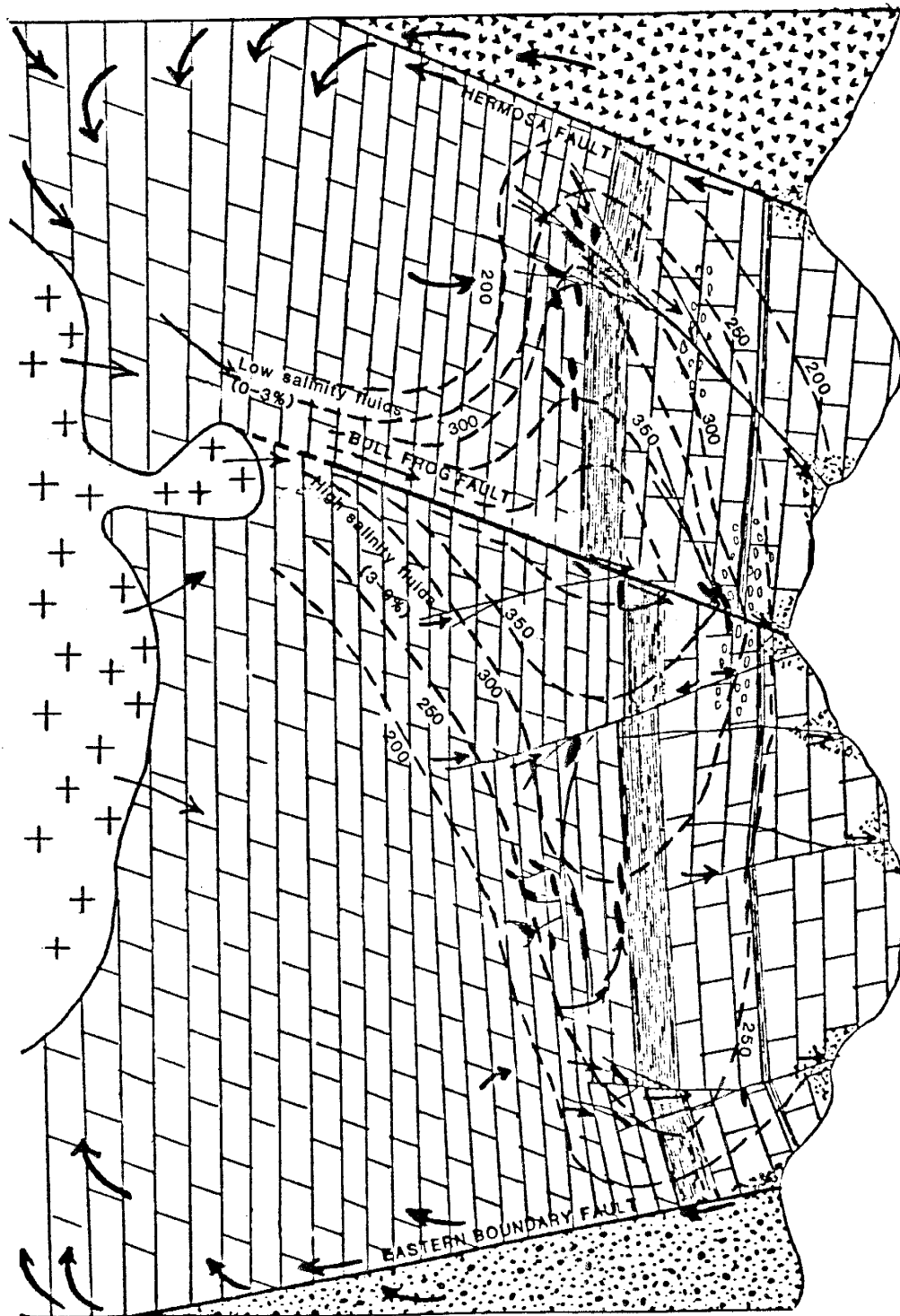
Jasperoid



Paleozoic sediments



Boiling zone



age. Dominantly meteoric waters received heat and volatile components from these igneous bodies. The heated fluid reacted with the source rocks at depth, extracting metal and gangue components. These fluids moved upward through faults and fractures into shallower, cooler and more permeable environments, started to boil or mix with fluids of different composition and temperature, and deposited the metal and gangue components, according to their physiochemical characteristics, in the changing fluids.

SUGGESTIONS FOR FUTURE INVESTGATIONS

Past mining activities and geologic-geochemical studies by this investigator and earlier works in the Hermosa mining district indicate that high-grade ore occurrences are small in size and limited to strongly fractured zones. Up to present, no development or investigation has focused on low-grade/low-tonnage deposits. Exploration program and geologic-geochemical studies similar to those in the other parts of the western U.S. for low-grade precious metal deposits are recomended. The high-temperature centers in the Wolford mines and southern area should be given a spicial attention for precious metal anomallies. For additional high-grade ores a drillig program is recomended to sample Silurian and Devonian rocks in the Wolford mines and Flagstaff-American Flag mines areas. In the past the Hermosa district was known for silver-

base metal deposits, but this study reveals that there is a potential for low-grade gold occurrences in the district. All jasperoids in the district should be sampled for gold and trace elements (Hg, Sb and As) anomalies.

Stable isotope study will be helpful for better understanding of the source of ore-fluids. Age determination of the ores should resolve any uncertainty about the timing of mineralization and related tectonic activity.

REFERENCES

- Abitz, R.J., 1986, Geology of Mid-Tertiary volcanic rocks of the east-central Black Range, Sierra County, New Mexico: Implication for a double-cauldron complex in the Emory Cauldron: New Mexico Geological Society 37th Guidebook, p. 161-166.
- Abitz, R.J., 1984, Volcanic geology and geochemistry of the northeastern Black Range Primitive Area and vicinity, Sierra County, New Mexico (M.S. thesis) University of New Mexico, Albuquerque, New Mexico, 121 p.
- Ahmad, N., and Rose, A.W., 1980, Fluid inclusions in porphyry and skarn ore at Santa Rita, New Mexico: Econ. Geol. V. 75, P. 220-250.
- Bagbay, W. C., and Berger, B. R., 1985, Geologic characteristics of sediment-hosted, disseminated precious-metal deposits in the western United States, in Berger, B. R. and Bethke, P. M., eds., Geology and geochemistry of epithermal systems: Reviews in Econ. Geol., V. 2 P. 169-202.

- Bazrafshan, K. and Norman, D.I., 1989, Location of gold-bearing centers in an epithermal district by fluid inclusion analysis. (in press)
- Barton, P.B. Jr., Bethke, P.M. and Roedder, E., 1977, Environment of ore deposition in the Creed Mining District, San Juan Mountains, Colorado: Part III. Progress toward interpretation of the chemistry of the ore-forming fluid for the OH vein: Econ. Geol. V. 72, P. 1-24.
- Brown, K.L., 1986, Gold deposition from geothermal discharges in New Zealand: Econ. Geol., V. 81, P. 979-983.
- Buchanan, L.J., 1980, Precious metal deposits associated with volcanic environments in the southwest. In: Relations of tectonic to ore deposits in the southern Cordillera, Dickenson, W.R., and Payne, W.D., (eds.), Arizona Geological Society Digest, V. 14, P. 237-262.
- Burruss, R.C., 1981, Analysis of phase equilibria in C-O-H-S fluid inclusions: in Hollister, L.S., and Crawford, M.L., eds. Fluid Inclusions: Applications to Petrology., Min. Assoc. Canada short course Handbook, V. 6, P. 39-74.
- Chapin, C.E. and Seager, W.R., 1975, Evolution of the Rio Grande rift in the Socorro and Las Cruces areas: New Mexico Geological Society 26th Guidebook, p. 299-321.

- Chapin, C.E. and Cather S.M., 1981, Eocene tectonics and sedimentation in the Colorado Plateau-Rocky Mountain area: Arizona Geological Society Digest V. 14, p. 173-198.
- Clayton, R.N., O'Neil, J.R., and Mayeda, T.K., 1972, Oxygen isotope exchange between quartz and water: Jour. Geophys. Res. V. 77, P. 3057-3067.
- Condie, K.C., 1982, Plate tectonics model for Proterozoic continental accretion in the southwestern United States: Geology, v. 10, p.37-42.
- Condie, K.C., and Budding, A.J., 1979, Geology and geochemistry of Precambrian rocks, central and south-central New Mexico: New Mexico Bureau of Mines and Mineral Resources, Mem. 35, 58 p.
- Christiansen, R.L. and Lipman, P.W., 1972, Cenozoic volcanism and plate tectonic evolution of the United State, II, late Cenozoic: Royal Society of London, Philosophical Transactions (A), 272: p. 249-284.
- Crawford, M.L., 1981, Phase equilibria in aqueous fluid inclusions: Hollister, L.S., and Crawford, M.L., (eds.); Fluid inclusions: Application to Petrology; Min. Soc. of Canada; Short course handbook V. 6, P. 75-100.

Crerar, D.A. and Barnes, H.L., 1976, Ore solution chemistry
V. Solubilities of chalcopyrite and chalcocite assemblages
in hydrothermal solution at 200 to 350 degrees C: Econ.
Geol., V. 71, P. 772-792.

Crerar, D., Wood, S., and Brantley, S., 1985, Chemical
controls on solubility of ore-forming minerals in
hydrothermal solutions: The Canadian Mineralogist, V. 23,
P. 333-352.

Cunningham, C. G., 1988, The Relationship Between some
Disseminated Gold Deposits, the Western Edge of the
Precambrian Craton, and Paleothermal Anomalies in Nevada;
in Bulk Mineable Precious Deposits of the Western United
States, Schefer, Cooper, and Vilkre (eds.): Symposium
Proceedings, The Geological Society of Nevada, P 35-48.

Dreier, J., 1984, Regional tectonic control of epithermal veins
in the western United States and Mexico. In: Gold and
silver deposits of the Basin and Range Province western
U.S.A., Wilkins, J, Jr., (ed.); Arizona Geological Society
Digest, V. XV, P. 28-50.

Drummond, S.E., 1981, Boiling and mixing of hydrothermal fluids: chemical effects on mineral precipitation: unpublished Ph.D. Thesis, The Pennsylvania State University, 380 P.

Drummond, S.E. and Ohmoto, H. 1985, Chemical evolution and mineral deposition in boiling hydrothermal systems, Econ. Geol., V. 80, P. 126-147

Eggleston, T.L., and Norman, D.I., 1983, Taylor Creek tin district; Stratigraphy, structure, and timing of mineralization: New Mexico Geology, 5 (1), P. 1-4.

Elston, W.E., 1957, Geology and mineral resources of Dwyer quadrangle, Grant, Luna, and Sierra counties, New Mexico: New Mexico Bureau of Mines and Mineral Resources, Bull. 38, 86 p.

Elston, W.E., 1978, Mid-Tertiary cauldrons and their relationship to mineral resources, southwestern New Mexico: a brief review: in Field Guide to Selected Cauldrons and Mining Districts of the Datil-Mogollon Volcanic Field: New Mexico Geological Society, Special Publ. No. 7, p. 107-113.

Elston, W.E., Rhodes, R.C., Coney, P.J., and Deal, E.G., 1976, Progress report on the Mogollon Plateau volcanic field, southwestern New Mexico, No. 3-surface expression of a pluton: in Cenozoic Volcanism in Southwestern New Mexico: New Mexico Geological Society Special Publ. No. 5. 3-28.

Elston, W.E., Rhodes, R.C., and Erb, E.E., 1976, Control of mineralization by mid-Tertiary volcanic centers, Southwestern New Mexico: in Cenozoic Volcanism in Southwestern New Mexico: New Mexico Geological Society Special Publ. No. 5, p. 125-130.

Elston, W.E. Seager, W.R., and Clemons, R.E., 1975, Emory cauldron, Black Range, New Mexico: Source of the Kneeling Nun Tuff: New Mexico Geological Society, Guidebook 26th field conference, p. 283-292.

Ericksen, G.E., Wedow, H. Jr., Eaton, G.P., and Leland, G.R., 1970, Mineral resources of the Black Range primitive area, Grant, Sierra, and Catron counties, New Mexico: U.S. Geol. Surv., Bull. 1319-E, 162 p.

Ewers, J. R., and Keays, R. R., 1977, Volatile and precious metal zoning in the Broadlands geothermal field, New Zealand: Econ. Geol. V. 72, P. 1337-13354.

- Giggenbach, W.F., 1984, Mass transfer in hydrothermal alteration system: *Geochemica et Cosmochimica Acta*, V. 48 P. 2693-2711.
- Giggenbach, W.F., 1980, Geothermal gas equilibria: *Geochimica et Cosmochimica Acta*, V. 44, P. 2021-2032.
- Gordon, C.H., 1907, Notes on the Pennsylvanian formations in the Rio Grande Valley, New Mexico: *Journal of Geology*, V. 15, P. 805-816.
- Harley, G.T., 1934, The geology and ore deposits of Sierra County, New Mexico: New Mexico Bureau of Mines and Mineral Resources, Bull. 10, 220 P.
- Harrison, R.W., 1988, A regional study of precious metal mineralization: Chloride mining district, New Mexico, (in press).
- Harrison, R.W., 1987, Cenozoic structure of north-central Black Range, New Mexico : Geological Society of America, Abstracts with programs, PP. 694-695.
- Harrison, R.W., 1986, General geology of Chloride mining district, Sierra and Catron Counties, New Mexico: New Mexico Geological Society, Guidebook 37th field conference, PP. 265- 272.

Hass, J.L., Jr., 1970a, An equation for the density of vapor-saturated NaCl-H₂O solutions from 75 to 325 C: Am. Jour. Sci., V. 266, P. 489-493.

Hass, J.L., Jr., 1971, The effect of salinity on the maximum thermal gradient of a hydrothermal system at hydrostatic pressure: Econ. Geol. V. 66, PP. 940-946.

Hayba, D.O., Bethke, P.M., Heald, D., and Foley, N.K., 1985, Geologic, mineralogic, and geochemical characteristics of volcanic-hosted, epithermal precious-metal deposits. In: Geology and Geochemistry of Epithermal Systems, Berger, B.R., and Bethke, P.M. (eds.), Soc. Econ. Geol., Rev. in Econ. Geol., V. 2, P. 249-272.

Hedenquist, J. W., and Henley, R. W., 1985a, The importance of CO₂ on freezing point measurements of fluid inclusions: Evidence from active geothermal systems and implications for epithermal ore deposition: Econ. Geol. V. 80, P. 1379-1406.

Hedenquist, J. W., and Henley, R. W., 1985b, Hydrothermal eruptions in the Waiotapu geothermal system, New Zealand: Their origin, associated breccias, and relation to precious metal mineralization: Econ. Geol. V. 80, P. 1640-1668.

- Henley, R. W., 1985, The geothermal framework for epithermal deposits, in Berger, B. R. and Bethke, P. M., eds., Geology and Geochemistry of Epithermal Systems: Society of Economic Geologists, Reviews in Economic Geology, V. 2, P. 1-24.
- Henley, R.W., 1986, Ore transport and deposition in epithermal environments, in Hubert, H. and Goldina, S., Stable Isotopes and Fluid Processes in Mineralisation: Geol. Soc. of Australia Special Issue, in press.
- Henley, R.W., 1989, Epithermal gold deposits in volcanic terranes, Foster, R.P. (ed.), Metallogeny and Exploration of Gold: Blackie in press.
- Henley, R.W. and Ellis, A.J., 1983, Geothermal systems ancient and modern: A geochemical review: Earth-Science Reviews, V. 19, P. 1-50.
- Henley, R.W. and Brown, K.L., 1985, A practical guide to the chemistry of geothermal and epithermal systems. In: Geology and Geochemistry of Epithermal systems., Berger, B.R., and Bethke, P.M. (eds.), Soc. Econ. Geol., Rev. in Econ Geol., V. 2, P. 25-45.
- Henley, R.W. and McNabb, Alex, 1978, Magmatic vapour plumes and ground-water interaction in porphyry copper emplacement: Econ. Geol. V. 73, P 1-20.

- Henley, R.W., Truesdell, A.H. and Barton, P.B., 1984, Fluid-Mineral Equilibria in Hydrothermal Systems: Soc. Econ. Geol., Rev. in Econ. Geol., V. 1 267 P.
- Hedlund, D.C., 1977 Geologic map of the Hillsboro and San Lorenzo quadrangles, Sierra and Grant counties, New Mexico: U.S. Geol. Surv. Misc. Field Studies Map MF 900-A.
- Hollister, L.S., 1981, Information intrinsically available from fluid inclusions: in Hollister, L.S., and Crawford, M.L., eds. Fluid Inclusions: Applications to Petrology., Min. Assoc. Canada short course Handbook, V. 6, P.1-12.
- Jahns, R.H., 1955a, Geology of the Sierra Cuchillo: New Mexico Geological Society, Guidebook 6th field conference, P. 158-174.
- Jahns, R.H. 1955b, Possibilities for discovery of additional lead-silver ore in the Palomas Camp area of the Palomas (Hermosa) mining district, Sierra County, New Mexico: New Mexico Bureau of Mines and Mineral Resources, Circ. 33, 14 P.
- Jahns, R.H., 1957, The Pelican area, Palomas (Hermosa) district, Sierra County, New Mexico: New Mexico Bureau of Mines and Mineral Resources, Bull. 55, 5 P.

Jahns, R.H., 1974, Ore deposits of the Palomas (Hermosa) district, Sierra County, New Mexico (abs.): New Mexico Geological Society, Guidebook 25th field conference, P. 381.

Jicha, H.L., Jr., 1954a, Geology and mineral resources of Lake Valley quadrangle, Grant, Luna, and Sierra Counties, New Mexico: New Mexico Bureau of Mines and Mineral Resources, Bull. 37, 93 P.

Jicha, H.L., Jr., 1954b, Paragenesis of the ores of the Palomas (Hermosa) district, southwestern New Mexico: New Mexico Bureau of Mines and Mineral Resources, Circ. 27, 20 P.

Johansing, R.J., 1982, Physical-chemical controls of dolomites hosted Sherman Type mineralization, Lake and Park Counties, Colorado: unpublished Colorado State Univ. M.S. thesis, 158 P.

Jones, F.A., 1922, A report on the properties of the Hermosa Silver Mines Company, New Mexico: Unpublished private report, 35 P.

Kamilli, R.J. and Ohmoto, H., 1977, Paragenesis, zoning, fluid inclusion, and isotopic studies of the Finlandia Vein, Colqui District, central Peru: Econ. Geol., V. 72, P. 950-982.

Kelley, V.C., 1955, Regional tectonics of south-central New Mexico: New Mexico Geological Society Guidebook, 6th field conference, P. 96-104.

Kelley, V.C., and Silver, Caswell, 1952, Geology of the Caballo Mountains: University of New Mexico: Publications in Geology, no. 4, 286 P.

Kelley, W.C., and Turneaure, F.S., 1970, Mineralogy, paragenesis and geothermometry of the tin and tungsten deposits of the eastern Andes, Bolivia: Econ. Geol., V. 65, PP. 609-680.

Kottowski, F.E., 1963, Paleozoic and Mesozoic strata of southwestern and south-central New Mexico: New Mexico Bureau of Mines and Mineral Resources, Bull. 79, 93 P.

Kuellmer, F. J., 1954, Geologic section of the Black Range at Kingston, New Mexico: New Mexico Bureau of Mines and Mineral Resources, Bull. 33, 100 P.

Lovering, T. G., 1972, Jasperoid in the United State - Its characteristics, origin, and economic significance: U. S. Geol. Surv., Prof. Paper 710, 164 P.

Marvin, R.F., and Cole, J.C., 1978, Radiometric ages: compilation A, U.S. Geol. Surv.: Isochron West, no. 22, P. 3-14.

Maxwell, C.H., and Heyl, A.V., 1976, Geology of the Winston quadrangle, New Mexico: U.S. Geol. Surv., Open-file Map 76- 858.

McDowell, F.W., 1971, K-Ar ages of igneous rocks from the western United States: Isochron West, no. 2, P. 2-16.

McNeil Canby, V. and Evatt, R.L., 1985, Geology, character, and controls of epithermal silver mineralization in the Carbonate Creek area, Kingston, New Mexico: New Mexico Bureau of Mines and Mineral Resources, Circular 199, P. 25-31.

Norman, D.I., 1977, Geology and geochemistry of the Tribag breccia pipes, Batchawana Bay, Ontario. Ph.D. thesis, University of Minnesota, Minneapolis, Minn. (unpublished)

Norman, D.I. and Sawkins, F.J., 1987, Analysis of volatiles in fluid inclusions by mass spectrometry, Chem. Geol. V. 61, P. 1-10

Norman, D.I., Apodaca, L.E., Bazrafshan, K., and Behr, C., 1987, The fluid inclusions for the exploration of epithermal Au-Ag fluids: IX symposium on fluid inclusions; European current research on fluid inclusions, University of Opatro, P. 93-94.

Piperov, N.B. and Penchev, N.P., 1973, A study of gas inclusions in mineral: Analyses of gases from micro-inclusions in allinite. Geochm. Cosmochim. Acta, V. 37, P. 2075-2097.

Potter, R. W., 1977, Pressure corrections for fluid inclusion homogenization temperatures based on the volumetric properties of the system NaCl-H₂O: Journal of Research of the U.S. Geol. Surv. V. 5, P. 603-607.

Potter, R. W., Clynne, M. A., and Brown, D. L., 1978, Freezing point depression of aqueous sodium chloride solutions: Econ. Geol., V. 73, P. 284-285.

Radtke, A.S., Rye, R.O., and Dickson, F.W., 1980, Geology and stable isotope studies of the Carlin gold deposit, Nevada: Econ. Geol. V. 75, P. 642-672.

- Renault, J., 1970, Major-element variations in the Potrillo, Carrizozo, and McCarty Basalt Field, New Mexico: New Mexico Bureau of Mines and Mineral Resources, Circular 113, P. 22.
- Richardson, G.B., 1908, Paleozoic formations of Trans-Pecos, Texas: American Journal of Science, 4th ser., V. 25, P. 474- 484.
- Roedder, E., 1962a, Studies of fluid inclusions I: Low temperature application of a dual-purpose freezing and heating stage: Econ. Geol., V. 57, 1045-1061.
- Roedder, E., 1972, Composition of fluid inclusions. U. S. Geol. Surv. Prof. Paper 440-jj.
- Roedder, E., 1977, Fluid inclusion studies of ore deposition in the Viburnum Trend, southwest Missouri: Econ. Geol. V. 72, P. 474-479.
- Roedder, E., 1984, Fluid Inclusions: Min. Soc. of Amer., Rev. in Min. V. 12, 644 P.
- 15

Roedder, E., Heyl, A.V., and Creel, J.P., 1968, Environment of ore deposition at the Mex-Tex deposits, Hansonburg district, New Mexico, from studies of fluid inclusions: Econ. Geol. V. 63, P. 336-348.

Roedder, E. and Skinner, B.J., 1968, Experimental evidence that fluid inclusions do not leak: Econ. Geol., V. 63, P. 715-730.

Roedder, E. and Bondar, R.J., 1980, Geologic pressure determinations from fluid inclusion studies: Ann. Rev. Earth Planet. Sci. V. 8, P. 263-301.

Romberger, S.B., 1986, Ore deposits No. 9, Disseminated gold deposits: Geoscience Canada, V. 13. no. 1, P. 23-31.

Rye, R.O. and Sawkins, F.J., 1974, Fluid inclusions and stable isotope studies on the Casapalca Ag-Pb-Zn-Cu deposits, Central Andes, Peru: Econ. Geol. V. 69, P. 181-295.

Sanders, P.A. and Girordano, T.H., 1986, Geology and mineralization of the Kingston mining district, New Mexico: New Mexico Geological Society, 37th Guidebook, P. 287-292.

- Sawkins, F.J., 1964, Lead-zinc deposition in the light of fluid inclusion studies, Providencia Mine, Zacatecas, Mexico: *Econ. Geol.*, V. 59, P. 883-919.
- Sawkins, F.J., 1966, Ore genesis in the north Pennine orofield, in the light of fluid inclusion studies: *Econ. Geol.* V. 61, P. 385-401.
- Seager, W.R., Shafiqullah, M., Hawley, J.W. and Margin, R.F., 1984, New K-Ar dates from basalts and the evolution of the southern Rio Grande rift: *Geol. Soc. of Amer. Bull.*, 95, P. 87-99.
- Seward, T.M., 1973, Thiocomplexes of gold and the transport of gold in hydrothermal ore solutions: *Geochimica et Cosmochimica Acta*, V. 37, P. 379-399.
- Seward, T.M., 1976, The stability of chloride complexes of silver in hydrothermal solutions up to 350 C: *Geochimica Cosmochimica Acta*, V. 40, P. 1329-1341.
- Seward, T.M., 1981, Metal complex formation in aqueous solutions at elevated temperatures and pressures: in Wickman, F. and Rickard, D., eds., *Physics and Chemistry of the Earth*, 13-14, P. 113-129.

- Shepard, M.D., 1983, Geology and ore deposits of the Hermosa mining district, Sierra County, New Mexico: M.S. thesis, The University of Texas at El Paso. (unpublished)
- Shepherd, T.J., 1981, Temperature-programmable heating-freezing stage for microthermometric analysis of fluid inclusions: Econ. Geol. V. 76, P.1244-1247.
- Shepherd, T. M., Rankin, A. H. and Alderton, D. H. M., 1985, A Practical Guide to Fluid Inclusion Studies: Blackie and Son Limited, London, 239 P.
- Stacey, J. S., and Hedlund, D. C., 1983, Lead isotopic composition of diverse igneous rocks and ore deposits from southwestern New Mexico and their implications for early Proterozoic crustal evolution in the western United States: Geol. Soc. of Amer., Bull., V. 94, P.43-57.
- Taylor, H. P. Jr., 1974, The application of oxygen and hydrogen isotope studies to problems of hydrothermal alteration and ore deposition: Econ. Geol. V. 69, P. 843-883.
- Thompson, T.B., Arehardt, G.B., Johansing, R.J., Osborne, L.W. Jr., and Landis, G.P., 1983, Geology and geochemistry of the Leadville district, Colorado:

- Tilley, C. E., 1948, Earlier stages in the metamorphism of siliceous dolomite: *Mineralogical Magazine*, V. 28, P. 272-276.
- Titley, S. R. and Megaw, P. K. M., 1985, Carbonate-hosted ores of the western Cordillera an overview: *Society of Mining Engineers of AIME*, 85-115.
- Truesdell, A. H., 1974, Oxygen Isotope Activities and Concentrations in Aqueous Salt Solutions at Elevated Temperatures: Consequences for Isotope Geochemistry: *Earth and Planetary Science Letters*, V. 23, P. 387-396.
- Weissberg, B. G., 1969, Gold-silver ore-grade precipitates from New Zealand thermal waters: *Econ. Geol.* V. 64, P. 95-108.
- Weissberg, B. G., Browne, P. R. L., and Seward, T. M., 1979, Ore metals in active geothermal systems, in Barnes, H. L., ed., *Geochemistry of hydrothermal ore deposits*, 2nd ed.: Wiley Interscience, P. 99-154.
- White, D.E., 1957, Thermal waters of volcanic origin: *Geol. Soc. of Amer. Bull.* V. 68, P. 1637-1658.

White, D. E., 1981, Active geothermal systems and hydrothermal ore deposits; in Skinner, B. J. (ed.), Economic Geology 75th Anniversary Volume, P. 392-423.

Winkler, Helmut G. F., 1979, Petrogenesis of metamorphic rocks: New York, Springer-Verlag, 348 P.

Woodard, T. W., 1982, Geology of the Lookout Mountain area, northern Black Range, Sierra County, New Mexico: M.S. thesis, University of New Mexico, 95 P.